

#### Editorial

My Approach to the Echocardiographic Evaluation of Mitral Valve Regurgitation

#### Original Article

Echocardiographic Correlation Between Right Ventricular Diastolic Function and Age and Gender in Subjects With Preserved Systolic Function

Left Atrial Reserve Function in Assessing Indeterminate Diastolic Function

#### Case Reports

Cardiac Amyloidosis: Infiltrative Cardiomyopathy with Restrictive Hemodynamic Behavior – Case Report

Amplatzer™ Prosthesis Embolization After Percutaneous Atrial Septal Defect Closure: A Case Report

Left Ventricular Pseudoaneurysm in a Diabetic Patient without Clinical Acute Coronary Syndrome

Mucopolysaccharidoses IV and VI: Aspects in Two-dimensional Speckle-tracking Strain Echocardiogram Imaging in a Case Series

Left Atrial Appendage Pseudo-Thrombus

Use of Color Doppler of Carotids in the Diagnosis of a Patient with Direct Carotid-Cavernous Fistula

#### Images

Large Lymphoma Involving the Aortic Arch and its Branches: Demonstration by Echocardiography and Contribution to the Assessment of Hemodynamic Repercussions

Ebstein's Anomaly, Noncompaction Cardiomyopathy, and Mitral Valve Stenosis

Spontaneous Pneumomediastinum

Cardioverter-Defibrillator Implantation Through Persistent Left Superior Vena Cava

Late Diagnosis of Anomalous Left Coronary Artery from Pulmonary Artery in Oligosymptomatic Women

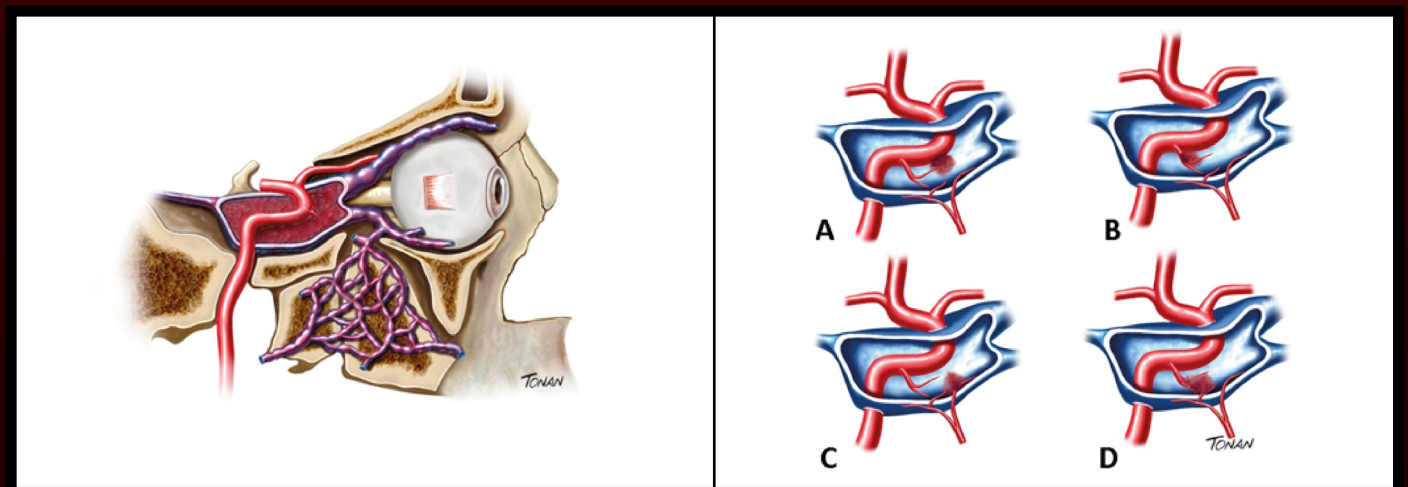


**Figure 1** – Direct carotid-cavernous (Barrow type A) fistula. **Figure 3** – Barrow classification of carotid-cavernous fistulae. Type A fistulae are characterized by a direct connection between the internal carotid artery and the cavernous sinus. Type B fistulae involve meningeal branches of the internal carotid artery. Type C fistulae involve external carotid branches. Type D fistulae include meningeal branches of the internal and external carotid arteries.



# ABC Imagem Cardiovascular

## Department of Cardiovascular Imaging

### Diretor Presidente

Dr. Carlos Eduardo Rochitte - SP

### Diretor Vice-Presidente Ecocardiografia

Dr. André Luiz Cerqueira de Almeida - BA

### Diretor Vice-Presidente Cardiologia Nuclear

Dr. Ronaldo de Souza Leão Lima - RJ

### Diretor Vice-Presidente Ecografia Vascular

Dr. Ana Cristina Lopes Albricker - MG

### Diretor Vice-Presidente de Ressonância Magnética

Dr. Marly Maria Uellendahl Lopes - SP

### Diretor Vice-Presidente de Tomografia Computorizada

Dr. Rodrigo Julio Cerci - PR

### Diretor Administrativo

Dr. David Costa de Souza Le Bihan - SP

### Diretora Financeiro

Dr. Jeane Mike Tsutsui - SP

### Diretor da Revista

Dr. Silvio Henrique Barberato - PR

### Conselho Deliberativo

#### Presidente

Dr. Arnaldo Rabischoffsky - RJ

#### Membros

Dr. José Luiz Barros Pena - MG  
Dra. Ana Cristina de Almeida Camarozano - PR  
Dr. Antonio Carlos Sobral Sousa - SE  
Dr. Ibraim Masciarelli Francisco Pinto - SP  
Dr. Luis Claudio Lemos Correia - BA  
Dr. Armando Luis Cantisano - RJ  
Dr. João Vicente Vitola - PR

#### Comissão Científica Coordenadores

Dra. Ana Clara Tude Rodrigues - SP  
Dra. Andrea de Andrade Vilela - SP  
Dr. Rodrigo Bellio de Mattos Barretto - SP

#### Membros

Dra. Viviane Tiemi Hotta

#### Comissão de Habilitação Coordenador

Dr. Marco Stephan Lofrano Alves - PR

#### Membros

Dra. Cecília Beatriz Bittencourt Viana Cruz - SP  
Dra. Claudia Cosentino Gallafrio - SP

Dr. Edgar Daminello - SP

Dr. Márcio Miranda Brito - TO

Dra. Minna Moreira Dias Romano - SP

Dra. Sandra Nívea dos Reis Saraiva Falcão - CE

#### Seniors

Dr. David Costa de Souza Le Bihan - SP

Dr. Fabio Villaga Guimarães Filho - SP

Dra. Mirian Magalhães Pardi - SP

Dra. Samira Saady Morhy - SP

#### Comissão de Informação, Internet Coordenador

Dr. Marcelo Souza Hadlich - RJ

#### Membros

Dra. Ana Paula dos Reis Velloso Siciliano - RJ

Dr. Alex dos Santos Félix - RJ

#### Comissão de Honorários e Defesa dos Profissionais Coordenador

Dr. Marcelo Haertel Miglioranza - RS

#### Membros

Dr. Wagner Pires de Oliveira Junior - DF

#### Comissão do Programa de Educação Continuada Coordenador

Dr. Mohamed Hassan Saleh - SP

#### Comissão de Ensino e Acreditação Coordenadores

Dr. Edgar Bezerra de Lira Filho - SP

Dr. David Costa de Souza Le Bihan - SP

Dra. Samira Saady Morhy - SP

#### Comissão de Eventos Coordenador

Dr. Rodrigo Bellio de Mattos Barretto - SP

#### Comissão de Inter-Societária Coordenadora

Dra. Marcia de Melo Barbosa - MG

#### Comissão de Relacionamento e Imagem Coordenadores

Dr. Wilson Mathias Júnior - SP

Dr. Juliano de Lara Fernandes - SP

#### Comissão de Temas Especiais e Eco Interoperatório/ Procedimentos Estruturais Coordenadores

Dr. Cláudio Henrique Fischer - SP

Dr. Marcelo Haertel Miglioranza - RS

Dr. David Costa de Souza Le Bihan - SP

#### Comissão de Cardiopediatria

##### Coordenadora

Dra. Cláudia Regina Pinheiro de Castro Grau - SP

##### Membros

Dra. Adriana Mello Rodrigues dos Santos - MG

Dra. Gláucia Maria Penha Tavares - SP

Dra. Renata de Sá Cassar - SP

#### Comissão Dic Jovem Coordenador

Dra. Eliza de Almeida Gripp - RJ

##### Membros

Dr. Rafael Rabischoffsky - RJ

Dra. Cecília Beatriz Bittencourt Viana Cruz - SP

Dra. Amanda Rocha Diniz Kimura - SP

Dra. Manuela Baima Costa Cabral - DF

Dra. Isabela Bispo Santos da Silva Costa - SP

#### Conselho de Ex Presidentes Coordenador

Dr. José Luiz Barros Pena - MG

##### Membros

Dr. Arnaldo Rabischoffsky - RJ

Dr. Carlos Eduardo Suaide Silva - SP

Dr. Djair Brindeiro Filho - PE

Dr. Jorge Eduardo Assef - SP

Dra. Marcia de Melo Barbosa - MG

Dra. Samira Saady Morhy - SP

Dr. Marcelo Luiz Campos Vieira - SP

#### Editor-chefe

Dr. Silvio Henrique Barberato

#### Editora anterior

Dra. Viviane Tiemi Hotta - SP

#### Editores Associados

Dra. Ana Cristina Lopes Albricker - MG (Vascular)

Dra. Bruna Morhy Borges Leal Assunção - SP

(Ecocardiografia Adulto)

Dr. José de Arimatéia Batista Araujo-Filho - EUA

(Inovação e Inteligência Artificial)

Dr. Marcelo Haertel Miglioranza - RS (Defesa

profissional e Formação do Ecocardiografista)

Dra. Marcia Ferreira Alves Barberato - PR

(Ecocardiografia Pediátrica)

Dr. Otavio Rizzi Coelho Filho - SP (Ressonância)

Dr. Rodrigo Julio Cerci - PR (Tomografia)

Dra. Simone Cristina Soares Brandão - PE

(Medicina Nuclear)

## SBC Directors

### Presidente

Dr. Marcelo Queiroga

### Vice-Presidente

Dr. Celso Amodeo

### Diretor Financeiro

Dr. Ricardo Mourilhe Rocha

### Diretor Científico

Dr. Fernando Bacal

### Diretora Administrativa

Dra. Olga Souza

### Diretor de Comunicação

Dr. Harry Corrêa Filho

### Diretor de Qualidade Assistencial

Dr. Silvio Henrique Barberato

### Diretor de Tecnologias da Informação

Dr. Leandro Ioschpe Zimerman

### Diretor de Relações Governamentais

Dr. Nasser Sarkis Simão

### Diretor de Relações com Estaduais e Regionais

Dr. João David de Souza Neto

### Diretora de Departamentos Especializados

Dra. Andréa de Araújo Brandão

### Diretor de Promoção de Saúde Cardiovascular - SBC/Funcor

Dr. José Francisco Kerr Saraiva

### Diretor de Pesquisa

Dr. David de Pádua Brasil

### Editor-Chefe Arquivos Brasileiros de Cardiologia

Dr. Carlos Eduardo Rochitte

## National Editorial Board

Adelino Parro Junior (SP)  
Adenalva Lima de Souza Beck (DF)  
Adriana Pereira Glavam (RJ)  
Afonso Akio Shiozaki (PR)  
Afonso Yoshihiro Matsumoto (RJ)  
Alessandro Cavalcanti Lianza (SP)  
Ana Clara Tude Rodrigues (SP)  
Ana Cláudia Gomes Pereira Petisco (SP)  
Ana Cristina Camarozano Wermelinger (PR)  
Ana Gardenia Liberato Ponte Farias (CE)  
Ana Lúcia Martins Arruda (SP)  
André Luiz Cerqueira de Almeida (BA)  
Andrea de Andrade Vilela (SP)  
Andrea Falcao (SP)  
Andressa Mussi Soares (ES)  
Aristarco Gonçalves de Siqueira Filho (RJ)  
Armando Luis Cantisano (RJ)  
Benedito Carlos Maciel (SP)  
Brivaldo Markman Filho (PE)  
Caio Cesar Jorge Medeiros (SP)  
Carlos Eduardo Rochitte (SP)  
Carlos Eduardo Suaide Silva (SP)  
Carlos Eduardo Tizziani Oliveira Lima (SP)  
Claudia Gianini Monaco (SP)  
Cláudio Henrique Fischer (SP)  
Cláudio Leinig Pereira da Cunha (PR)  
Claudio Tinoco Mesquita (RJ)  
Clerio Francisco de Azevedo Filho (RJ)  
David Costa de Souza Le Bihan (SP)  
Djair Brindeiro Filho (PE)  
Edgar Bezerra Lira Filho (SP)

Eliza de Almeida Gripp (RJ)  
Eliza Kaori Uenishi (SP)  
Estela Suzana Kleiman Horowitz (RS)  
Gabriel Leo Blacher Grossman (RS)  
Gabriela Nunes Leal (SP)  
Gláucia Maria Penha Tavares (SP)  
Henry Abensur (SP)  
Ibrahim Masciarelli Francisco Pinto (SP)  
Ilan Gottlieb (RJ)  
Iran de Castro (RS)  
Isabel Cristina Britto Guimaraes (BA)  
Ivan Romero Rivera (AL)  
Jaime Santos Portugal (RJ)  
Jeane Mike Tsutsui (SP)  
José Lázaro de Andrade (SP)  
José Luiz Barros Pena (MG)  
José Maria Del Castillo (PE)  
José Olímpio Dias Júnior (MG)  
José Sebastião de Abreu (CE)  
Joselina Luzia Menezes Oliveira (SE)  
Laise Antonia Bonfim Guimaraes (SP)  
Leonardo Sara da Silva (GO)  
Lilian Maria Lopes (SP)  
Luciano Aguiar Filho (SP)  
Luciano Herman Juaçaba Belém (RJ)  
Luiz Darcy Cortez Ferreira (SP)  
Luiz Felipe P. Moreira (SP)  
Manuel Adán Gil (SP)  
Marcelo Luiz Campos Vieira (SP)  
Marcelo Souza Hadlich (RJ)  
Marcia de Melo Barbosa (MG)

Márcio Vinícius Lins de Barros (MG)  
Maria do Carmo Pereira Nunes (MG)  
Maria Eduarda Menezes de Siqueira (SP)  
Marly Uellendahl (SP)  
Nathan Herszkowicz (SP)  
Orlando Campos Filho (SP)  
Oscar Francisco Sanchez Osella (DF)  
Oswaldo Cesar de Almeida Filho (SP)  
Paulo Zielinsky (RS)  
Reginaldo de Almeida Barros (SP)  
Roberto Caldeira Cury (SP)  
Roberto Pereira (PE)  
Rodrigo Alves Barreto (SP)  
Samira Saady Morhy (SP)  
Sandra da Silva Mattos (PE)  
Sandra Nivea dos Reis Saraiva Falcão (CE)  
Sérgio Cunha Pontes Júnior (SP)  
Silvio Henrique Barberato (PR)  
Simone Nascimento dos Santos (DF)  
Simone Rolim F. Fontes Pedra (SP)  
Tamara Cortez Martins (SP)  
Valdir Ambrósio Moisés (SP)  
Valeria De Melo Moreira (SP)  
Vera Márcia Lopes Gimenes (SP)  
Vera Maria Cury Salemi (SP)  
Viviane Tiemi Hotta (SP)  
Washington Barbosa de Araújo (RJ)  
Wercules Oliveira (SP)  
William Azem Chalela (SP)  
Wilson Mathias Júnior (SP)

## International Editorial Board

Anton E. Becker – Holanda  
Daniel Piñeiro – Argentina  
Eduardo Escudero – Argentina  
Eduardo Guevara – Argentina  
Fernando Bosch – Venezuela  
Gustavo Restrepo – Colombia  
Harry Acquatella – Venezuela

João A.C.Lima – Estados Unidos  
Jorge Lowenstein – Argentina  
Joseph Kisslo – Estados Unidos  
Leopoldo Pérez De Isla – Espanha  
Mani A. Vannan – Estados Unidos  
Laura Mercer-Rosa - Estados Unidos  
Natesa Pandian – Estados Unidos

Navin C. Nanda – Estados Unidos  
Nuno Cardim - Portugal  
Raffaele De Simone – Alemanha  
Ricardo Ronderos – Argentina  
Vera Rigolin – Estados Unidos  
Vitor Coimbra Guerra - Canada

**Volume 34, Nº 2, April/May/June 2021**


Indexing source: LILACS - Literatura Latino-Americana e do Caribe em Ciências da Saúde - [www.bireme.br](http://www.bireme.br), LATINDEX - Sistema Regional de Información en Línea para Revistas Científicas de América Latina, El Caribe, España y Portugal - [www.latindex.unam.mx](http://www.latindex.unam.mx)

**Department of Cardiovascular Imaging/ Brazilian Society of Cardiology**

Rua Barata Ribeiro nº 380 cj.54  
01308-000 - São Paulo - SP - Brasil  
Fone/Fax: +55 (11) 3259-2988  
Fones: +55 (11) 3120-3363  
+55 (11) 3259-2988 / +55 (11) 2589-4168



**Editorial Coordination**

 Atha Comunicação e Editora

Rua Machado Bittencourt, 190 - conj. 410  
São Paulo, SP, Brasil  
Tel.: (11) 50879502

**Editorial Support**

[revista@dicsbc.com](mailto:revista@dicsbc.com)

*The journal Arquivos Brasileiros de Cardiologia — Imagem Cardiovascular is the official body of the Department of Cardiovascular Imaging of the Brazilian Society of Cardiology.*

*The articles published here may only be reproduced upon express authorization given by the authors. Paid publications will not be accepted. Reprints of articles must be requested to the Editorial Department and will cost as much as the number of copies requested.*

## Contents - Sumário



Click on the title to read the article

### Editorial - Editorial

#### **My Approach to the Echocardiographic Evaluation of Mitral Valve Regurgitation**

*Como Eu Faço Avaliação Ecocardiográfica na Regurgitação Valvar Mitral*

Ana Cristina Camarozano, Luisa Maria Camarozano

DOI: 10.47593/2675-312X/20213402ecom12

### Original Article - Artigo Original

#### **Echocardiographic Correlation Between Right Ventricular Diastolic Function and Age and Gender in Subjects With Preserved Systolic Function**

*Correlação Ecocardiográfica da Função Diastólica do Ventrículo Direito com Idade e Gênero em Indivíduos com Função Sistólica Preservada*

Leonardo Lasari Melo, Ana Cristina Camarozano, Daniela de Castro Carmo, Jerônimo Antonio Fortunato, Rubens Zenóbio Darwich, Cintia Rocha Fortes de Sá, Liz Andréa Villela Baroncini

DOI: 10.47593/2675-312X/20213402eabc126

#### **Left Atrial Reserve Function in Assessing Indeterminate Diastolic Function**

*Função de Reserva do Átrio Esquerdo na Avaliação da Função Diastólica Indeterminada*

Silvio Henrique Barberato, Rafael Borsoi

DOI: 10.47593/2675-312X/20213402eabc196

### Case Reports - Relatos de Caso

#### **Cardiac Amyloidosis: Infiltrative Cardiomyopathy with Restrictive Hemodynamic Behavior – Case Report**

*Amiloidose Cardíaca: Cardiomiopatia Infiltrativa com Comportamento Hemodinâmico Restritivo – Relato de Caso*

José Leonardo Gomes Rocha Júnior, Ivan Lucas Rocha Liberato, Larissa Ferreira Lopes, Letícia Maria Queiroz Rocha, Christiane Bezerra Rocha Liberato

DOI: 10.47593/2675-312X/20213402eabc162

#### **Amplatzer™ Prosthesis Embolization After Percutaneous Atrial Septal Defect Closure: A Case Report**

*Embolização de Prótese de Amplatzer™ após Fechamento Percutâneo de Comunicação Interatrial: Relato de Caso*

Raul Serra Valério, Alfredo Augusto Eyer Rodrigues, Artur José da Silva Raoul, Marly Maria Uellendahl, Carlos Eduardo Suaide Silva, Luciana Braz Peixoto

DOI: 10.47593/2675-312X/20213402eabc135

#### **Left Ventricular Pseudoaneurysm in a Diabetic Patient without Clinical Acute Coronary Syndrome**

*Pseudoaneurisma Ventricular Esquerdo em Paciente Diabético sem Clínica de Síndrome Coronariana Aguda*

Alice Mirane Malta Carrijo, Marcela Gomes de Souza, Marina Vitória Silva Costa, João Lucas O'Connell

DOI: 10.47593/2675-312X/20213402eabc136



# ABC Imagem Cardiovascular

## **Mucopolysaccharidoses IV and VI: Aspects in Two-dimensional Speckle-tracking Strain Echocardiogram Imaging in a Case Series**

*Mucopolissacaridoses IV e VI: Aspectos ao Ecocardiograma Bidimensional com Strain pelo Speckle Tracking em uma Série de Casos*

João Vitor Tiveron Teodoro, Lavínia Ayumi Borges Ribeiro, José Marques Ferreira Neto, Vinícius Marques Ferreira, Carlos Henrique Paiva Grangeiro, Adriana de Nazaré Miziara Oliveira

DOI: 10.47593/2675-312X/20213402eabc159

## **Left Atrial Appendage Pseudo-Thrombus**

*Pseudotrombo em Apêndice Atrial Esquerdo*

Marcio Augusto Silva, Marcelo Pazolini, José Guilherme Cazelli, Daniel Escobar Bueno Peixoto, Rafael Soares Rua, Rodolpho Jacques de Melo Farinazzo

DOI: 10.47593/2675-312X/20213402eabc168

## **Use of Color Doppler of Carotids in the Diagnosis of a Patient with Direct Carotid-Cavernous Fistula**

*Uso do Doppler Colorido das Carótidas no Diagnóstico de um Paciente com Fístula Carotideocavernosa Direta*

Mauro de Deus Passos, Isabella Godoy-Gomes, Mariana de Gregório Faria

DOI: 10.47593/2675-312X/20213402eabc178

## **Images - Imagens**

## **Large Lymphoma Involving the Aortic Arch and its Branches: Demonstration by Echocardiography and Contribution to the Assessment of Hemodynamic Repercussions**

*Grande Linfoma Envolvendo o Arco Aórtico e seus Ramos: Demonstração pela Ecocardiografia e Contribuição na Avaliação de Repercussão Hemodinâmica*

Israel Nilton de Almeida Feitosa, Maísa Carneiro Wanderley

DOI: 10.47593/2675-312X/20213402eabc138

## **Ebstein's Anomaly, Noncompaction Cardiomyopathy, and Mitral Valve Stenosis**

*Anomalia de Ebstein, não Compactação Miocárdica e Estenose Valvar Mitral*

Anderson da Costa Armstrong, Gustavo Volpe, Tiago Augusto Magalhães, Dinani Armstrong, Marcelo Nacif

DOI: 10.47593/2675-312X/20213402eabc158

## **Spontaneous Pneumomediastinum**

*Pneumomediastino Espontâneo*

Luísa Gonçalves, Inês Pires, João Santos, Joana Correia, Davide Moreira

DOI: 10.47593/2675-312X/20213402eabc170

## **Cardioverter-Defibrillator Implantation Through Persistent Left Superior Vena Cava**

*Implante de Cardioversor-Desfibrilador Através da Veia Cava Superior Esquerda Persistente*

Luísa Gonçalves, Inês Pires, João Santos, Joana Correia, António Costa

DOI: 10.47593/2675-312X/20213402eabc172

## **Late Diagnosis of Anomalous Left Coronary Artery from Pulmonary Artery in Oligosymptomatic Women**

*Diagnóstico Tardio de Origem Anômala da Artéria Coronária Esquerda a Partir da Artéria Pulmonar em Mulher Oligossintomática*

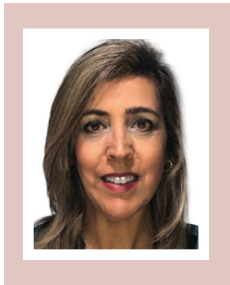
Carolina de Souza Galvão, Sterffeson Lamare Lucena de Abreu, Magda Luciene de Sousa Carvalho, José Eduardo da Cruz Sales, Ana Bárbara Silva dos Santos Leite

DOI: 10.47593/2675-312X/20213402eabc179

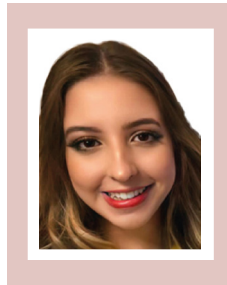
## My Approach to the Echocardiographic Evaluation of Mitral Valve Regurgitation

*Como Eu Faço Avaliação Ecocardiográfica na Regurgitação Valvar Mitral*

<sup>1</sup>Federal University of Paraná, Curitiba, PR, Brazil. Pontifícia University Católica (PUC),<sup>2</sup> Curitiba, PR, Brazil.



Ana Cristina Camarozano<sup>1</sup>



Luisa Maria Camarozano<sup>2</sup>

### Introduction

Chronic mitral valve regurgitation is a very common disease that must be differentiated into primary (structural mitral valve disease) and secondary (left ventricular [LV] disease) types to ensure appropriate management and treatment. Echocardiography is an essential exam in the etiological diagnosis to quantify a valve lesion and its repercussion as well as being decisive for defining the best surgical timing. Intraoperative echocardiography, such as MitraClip<sup>®</sup> placement, is a Class I indication in mitral valve repair and interventional treatment.<sup>1</sup>

Untreated mitral regurgitation (MR) is associated with worse outcomes due to the adverse consequences of volume overload on the cardiac chambers, whereas early intervention has shown excellent results for primary MR. However, what is the mechanism of MR?

This answer and its quantification decisively influence the choice of mitral valve intervention.

### My approach to mitral valve evaluation

The first step of mitral valve evaluations is to determine the presence of any structural mitral valve changes. In Brazil, the most common cause of primary MR cases is rheumatic disease, followed by mitral valve prolapse. Mitral annulus calcification is a common cause in older patients, while radiation can occasionally affect the mitral valve in patients undergoing radiotherapy.

### Keywords

Diagnosis; Echocardiography; Mitral Valve Insufficiency.

Mailing Address: Ana Cristina Camarozano •

E-mail: a.camarozano@yahoo.com.br

Manuscript received 4/6/2020; revised 5/10/2020; accepted 1/27/2021

DOI: 10.47593/2675-312X/20213402ecom12

When rheumatic involvement of the mitral valve is identified (the so-called dome opening), it is important to determine the presence or absence of associated mitral stenosis or other valve lesions. In cases of mitral valve prolapse, fibroelastic disease (with thin cusps and generally localized prolapse) must be differentiated from Barlow's disease, in which the cusps are redundant and well thickened and the prolapse is diffuse. Prolapse syndrome is present in the latter case, and some studies have shown a correlation with sudden death from cardiac arrhythmia.<sup>2</sup>

The association between mitral valve prolapse, aortic ectasia and Marfan syndrome should be investigated. Senile calcification presents a clear scenario, with mitral annulus calcification and the possibility of associated mitral stenosis. In such cases, lesions are rarely severe. Mitral valve thickening induced by radiation is associated with a history of neoplasia and chest radiotherapy.<sup>3</sup>

These pathologies define most primary MR cases. Cases without structural mitral annular changes but with LV dilatation and dysfunction, as occurs in dilated cardiomyopathy with annular dilatation and secondary mitral reflux, or contractile changes in the inferior or inferolateral wall due to myocardial infarction with impaired posterior mitral cusp coaptation, are defined as secondary MR, with the valve problem being a consequence rather than the cause.

After discerning of the valve lesion mechanism, it is important to quantify the mitral damage and its hemodynamic repercussions.<sup>5</sup> MR can be quantified by qualitative (Color Doppler evaluation of the regurgitant jet), semi-quantitative (vena contracta [VC] evaluation), and quantitative (evaluation of the effective regurgitant orifice [ERO], regurgitant volume [RV], and regurgitant fraction [RF]) analyses. These parameters can be analyzed using the proximal isovelocity surface area method or flow analysis.

Quantitative parameters currently have the greatest diagnostic value, in the mitral valve regurgitation important (Table 1).

**Table 1 – Reference values for important mitral valve regurgitation<sup>5</sup>**

Parameter	Value
<b>Central regurgitant jet or eccentric jet</b>	<b>Occupies &gt; 40% of the LA Holosystolic</b>
Vena contracta	≥ 0,7 cm
Regurgitant volume	> 60 mL
Regurgitant fraction	> 50%
ERO	≥ 0.40cm <sup>2</sup>

AE: átrio esquerdo; ERO: orifício regurgitante.

Two-dimensional echocardiography and Doppler are able to quantify the MR degree and evaluate these parameters, but three-dimensional echocardiography more accurately evaluates ERO and VC. Yosefy et al. used real-time three-dimensional echocardiography to show that, in most cases, the region of proximal convergence of the regurgitant flow (proximal isovelocity surface area method) is hemielliptic, not hemispheric, and more accurate for this quantification.<sup>6</sup>

Two-dimensional transesophageal echocardiography, and particularly three-dimensional echocardiography, provides more accurate anatomical detailing of the mitral valve and an etiological definition when necessary, but the quantification of the degree of valve regurgitation using this information remains inaccurate.

Once mitral valve regurgitation is defined as important, the results depend on the presence of symptoms and the presence or absence of LV dysfunction, with the need for surgery being well defined. Non-surgical patients in New York Heart Association functional classes I and II present a mortality rate of about 4.1% per year compared to those in functional classes III and IV, whose mortality rate is 34% per year. However, the results are not so promising if the ejection fraction (EF) is lower than 60% or the LV systolic diameter (LVSD) is greater than 40 mm, as these parameters are predictors of LV dysfunction in the postoperative period and worse prognosis.<sup>7</sup> Ideally, patients should undergo surgery before the onset of such a condition, and the use of echocardiography is fundamental for their monitoring.

The next step after defining MR as primary or secondary and quantifying it is to consider the disease stages.<sup>8</sup>

## Stages of primary MR

### MR risk

Primary MR involves discreet mitral prolapse with normal coaptation, the absence of MR or mild central MR, and a VC < 0.3 cm.

### Progressive MR with evident prolapse but normal cusp coaptation

This stage involves a central MR jet occupying 20–40% of the left atrium in which the VC is <0.7 cm, RV is <60 mL, RF is <50%, and ERO is <0.40 cm<sup>2</sup>. No increased LV or pulmonary arterial hypertension are noted.

### Asymptomatic with severe MR

This stage involves prolapse with a loss of cusp coaptation or flail; MR with a central jet occupying > 40% of the left atrium or eccentric holosystolic jet; and a VC ≥ 0.7 cm, RV ≥ 60 mL, RF ≥ 50%, and ERO ≥ 0.40 cm<sup>2</sup>. It also features enlarged left chambers and pulmonary arterial hypertension at rest or on exertion. Stage C1 is defined as LVEF > 60% and LVSD < 40 mm, while stage C2 is defined as LVEF ≤ 60% and LVSD ≥ 40 mm.

### Symptomatic severe MR

This stage involves important prolapse and cusp coaptation failure or flail; a central jet > 40% of the left atrium or eccentric holosystolic jet; and a VC ≥ 0.7 cm, RV ≥ 60 mL, RF ≥ 50%, and ERO ≥ 0.40 cm<sup>2</sup>. It also features enlarged left chambers, pulmonary arterial hypertension, dyspnea on exertion, and reduced exercise tolerance.

## Stages of secondary MR

### MR risk

Secondary MR involves normal cords, cusps, and mitral annulus in a patient with coronary artery disease or dilated cardiomyopathy. No mitral or mild central MR is seen, while the VC is <0.3 cm. The LV is normal or with infarction or dilatation due to primary myocardial disease. Symptoms of ischemia or heart failure may be present.

### Progressive MR with parietal abnormality and LV dysfunction

This stage involves possible annular dilatation and loss of coaptation. The RV is <60 mL, while the RF is <50%. No increased LV or pulmonary arterial hypertension is noted. Symptoms of ischemia or heart failure may be present.

### Asymptomatic severe MR

This stage involves a parietal abnormality and/or LV dilatation as well as annular dilatation and cusp coaptation failure. The RV is ≥60 mL, RF ≥50%, and ERO ≥0.40 cm<sup>2</sup>, with an ERO ≥ 0.2 cm<sup>2</sup> being more sensitive. Contractile changes with LV dysfunction or cardiomyopathy-induced dysfunction are evident, and symptoms of ischemia or heart failure may be present.

### Symptomatic severe MR

This stage involves a parietal abnormality and/or LV dilatation. It also features annular dilatation with an RV ≥ 60 mL, RF ≥ 50%, and ERO ≥ 0.40 cm<sup>2</sup> as well as contractile changes in LV dysfunction or cardiomyopathy-induced dysfunction. Symptoms of ischemia or heart failure may be present in addition to dyspnea on exertion with reduced exercise tolerance.

In cases of significant MR, it is important to mention the basic Carpentier's classification used to choose the surgical mitral approach (Table 2 and Figure 1).

Type I classification refers to a mitral annulus without



structural changes but with annular dilatation that causes cusp coaptation failure with consequent valve reflux. This is caused by involvement of the LV due to chamber dilatation and/or dysfunction induced by dilated cardiomyopathy (secondary MR).

Type II classification refers to cord prolapse, elongation, or rupture with annular prolapse as the main finding. In this situation, fibroelastic disease must be differentiated from Barlow's disease, for which echocardiography is very useful. In the first entity, the degree of degeneration is mild and the prolapse is generally more localized (in the P2 and/or A2 segments) without calcification points and with mild to moderate annular dilatation. In this situation, surgical intervention is highly successful. In Barlow's disease, the annular degeneration is more severe and affects more segments. (When the prolapse involves more than three segments with extension to the posterior commissure, annulus calcification and moderate annular dilatation, valve repair is possible but not simple; when the prolapse involves more than three valve segments and extends to the anterior commissure with significant calcification (annulus and cusps) and large annular dilatation, valve repair is unlikely due to technical difficulty).<sup>10</sup>

The use of intraoperative transesophageal echocardiography is essential during mitral valve repair surgery, and some criteria must be observed to evaluate its success. The distance from the P2 stump must be up to 20 mm, the coaptation A2–P2 zone must be smaller than 10 mm, the posterolateral angle must be lower than 45°, and the LA/LV gradient must not indicate LV inflow tract stenosis. The LV outflow tract gradient should be analyzed since it should present a small cavity,

septal hypertrophy (>15 mm), smaller mitral-aortic angulation (<120°), narrow mitral annulus, shorter distance from the septum to the anterior mitral cusp (<25 mm), and a distance from the P2 stump > 20 mm, as these factors increase the propensity of mitral valve anterior systolic motion (Figure 2).<sup>11</sup>

The diameter of the tricuspid annulus should be analyzed before mitral repair since a tricuspid annulus  $\geq 40$  mm or  $\geq 21$  mm/m<sup>2</sup> is an indication for tricuspid surgery regardless of the degree of regurgitation through this valve.<sup>5,12</sup>

Carpentier's type III classification refers to restricted cusp motion, which can be seen in rheumatic (primary) and ischemic (secondary) disease cases. In these cases, restricted cusp motion is recognized either by commissure fusing, as in rheumatic disease, or by the lack of ventricular wall support, as in ischemic disease, leading to valve coaptation failure.<sup>9</sup> In both situations, surgical repair is unfavorable, even when performed by an experienced surgeon.

There have been great advances in mitral valve repair in cases of primary valve regurgitation since valve repair is associated with low operative mortality, good survival, increased quality of life, and low bleeding rates compared to valve replacement. Surgical repair has excellent success rates in patients with preserved ventricular function. These findings have encouraged early surgery in asymptomatic patients with severe MR, even those with an EF > 60% or LVSD < 40 mm, as long as the valve repair probability is >95% with low operative risk (<1%) as defined in the 2017 update on valve disease of the American Heart Association/American College of Cardiology (AHA/ACC).<sup>12</sup>

Tables 3 and 4 show the AHA/ACC recommendations,<sup>12</sup> highlighting any differences versus the 2014 guideline,<sup>5</sup> and Figure 3 shows a conduct guideline for chronic mitral valve regurgitation.

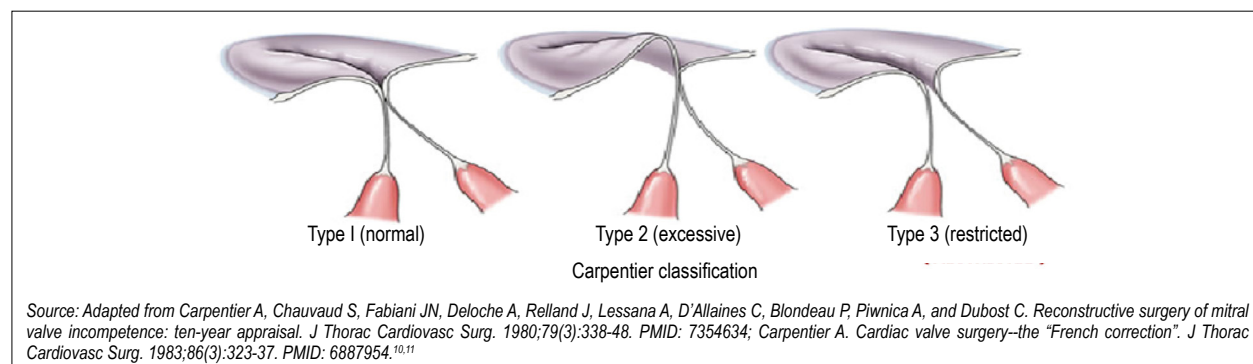
**Tabela 2 – Classificação de Carpentier sobre o movimento das cúspides mitrais para planejamento e abordagem cirúrgica.<sup>9</sup>**

Type	Motion
I	Normal cusp motion (e.g., mitral annular dilatation)
II	Excessive cusp motion (e.g., mitral cord prolapse and rupture or elongation)
III	Restricted cusp motion (e.g., commissural fusion and myocardial infarction)

## Complementary evaluation of chronic MR

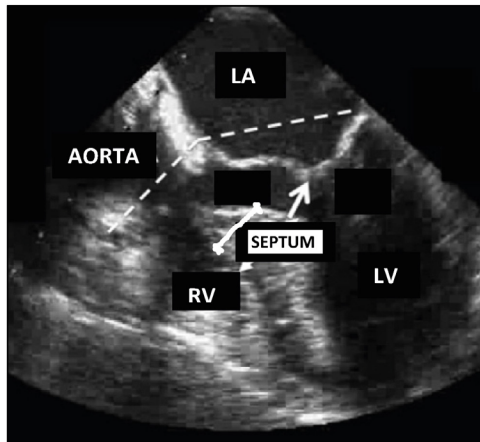
### Stress echocardiography

Stress echocardiography findings predict latent ventricular dysfunction before surgical intervention in patients with mitral valve prolapse using the mean global longitudinal strain (GLS). Patients with a mild GLS change (<2%) have no contractile reserve.<sup>13</sup>



Source: Adapted from Carpentier A, Chauvaud S, Fabiani JN, Deloche A, Relland J, Lessana A, D'Allaines C, Blondeau P, Piwnica A, and Dubost C. Reconstructive surgery of mitral valve incompetence: ten-year appraisal. *J Thorac Cardiovasc Surg.* 1980;79(3):338-48. PMID: 7354634; Carpentier A. Cardiac valve surgery—the "French correction". *J Thorac Cardiovasc Surg.* 1983;86(3):323-37. PMID: 6887954.<sup>10,11</sup>

**Figure 1 – Classificação de Carpentier.**



Source: Adapted from Varghese R, Itagaki S, Anyanwu AC, Trigo P, Fischer G, Adams DH. Predicting systolic anterior motion after mitral valve reconstruction: using intraoperative transesophageal echocardiography to identify those at greatest risk. *Eur J Cardiothorac Surg.* 2014;45(1):132-7; discussion 137-8. doi: 10.1093/ejcts/ezt234.<sup>13</sup> LA, left atrium; LV, left ventricle; RV, right ventricle.

Figure 2 – Schematic model of the mid-esophageal five-chamber cross-section considering the points that should be analyzed for predisposing dynamic LVOT gradient.

Table 3 – Recommendations for chronic primary mitral regurgitation intervention.

COR	LOE	Recomendações	Comentários
I	B	Mitral valve surgery is recommended for asymptomatic patients with chronic severe MR (stage D) and an LVEF > 30%	The 2014 recommendation currently remains
I	B	Mitral valve surgery is recommended for asymptomatic patients with chronic severe primary MR and left ventricular dysfunction (LVEF = 30–60% and/or LVSD ≥ 40 mm, stage C2)	The 2014 recommendation currently remains
I	B	Mitral valve repair is more commonly recommended than valve replacement when the surgical treatment is indicated for patients with chronic severe primary MR limited to the posterior cusp	The 2014 recommendation currently remains
I	B	Mitral valve repair is more commonly recommended than valve replacement when the surgical treatment is indicated for patients with chronic severe primary MR involving the anterior cusp when a successful and durable repair can be performed	The 2014 recommendation currently remains
I	B	Concomitant mitral valve repair (or replacement) is indicated in patients with chronic severe primary MR undergoing cardiac surgery for other reasons	A recomendação de 2014 permanece atualmente
Ila	B	Mitral valve surgery is acceptable for asymptomatic patients with chronic severe primary mitral regurgitation (stage C1) and preserved left ventricular function (LVEF > 60% and LVSD < 40 mm) when the likelihood of repair success and durability without residual MR exceeds 95% with an expected mortality rate of less than 1% when performed in a referral hospital (center)	The 2014 recommendation currently remains
Ila	C	Mitral valve surgery is acceptable for asymptomatic patients with chronic severe primary mitral regurgitation (stage C1) and preserved left ventricular function (LVEF > 60% and LVSD < 40 mm) with progressively increased left ventricular size or consistent EF decreases in imaging studies	New: Severe MR patients with an EF ≤ 60% or LVSD ≥ 40 mm have already developed left ventricular systolic dysfunction; thus, operating them before reaching these parameters was considered rational in several studies, particularly when the left ventricular size is progressively increasing or EF is decreasing
Ila	B	Mitral valve repair is acceptable for asymptomatic patients with chronic non-rheumatic severe primary MR (stage C1) and preserved LV function (LVEF > 60% and LVSD < 40 mm) with a high probability of successful and durable repair, especially in cases of new-onset atrial fibrillation or pulmonary hypertension at rest (systolic pulmonary artery pressure > 50 mmHg)	The 2014 recommendation currently remains

MR progressively leads to severe MR (“mitral regurgitation generates mitral regurgitation”). The concept is that the initial MR level causes LV dilatation, which increases stress in the mitral tract, causing additional valve damage, more severe MR, and additional LV dilatation, thus starting a perpetual cycle of LV volume increases and MR progression. This volume causes LV overload and leads to irreversible LV dysfunction, worsening the prognosis. Patients with severe MR and an EF ≤ 60% or LVSD ≥ 40 mm already present with LV systolic dysfunction. A study suggested that to normalize LV function and size after mitral repair, LVEF should be >64% and LVSD < 37 mm. It is reasonable to consider intervention when longitudinal follow-up shows a progressively decreased EF near 60% or a progressive LVSD increase near 40 mm. Nevertheless, asymptomatic patients with stable dimensions and excellent exercise capacity can be safely observed.

Source: Adapted from Nishimura RA, Otto CM, Bonow RO, Carabello BA, Erwin JP 3rd, Fleisher LA, et al. 2017 AHA/ACC Focused Update of the 2014 AHA/ACC Guideline for the Management of Patients With Valvular Heart Disease: A Report of the American College of Cardiology/American Heart Association Task Force on Clinical Practice Guidelines. *Circulation.* 2017;135(25):e1159-e1195. doi: 10.1161/CIR.0000000000000503.<sup>14</sup> COLOR, recommendation; EF, ejection fraction; LOE, level of evidence; LVEF, left ventricle ejection fraction; LVSD, left ventricle systolic diameter.

**Table 4 – Recommendations for secondary mitral regurgitation intervention.**

Class	Recommendations for secondary MR intervention	Comments
IIa	Mitral valve surgery is reasonable for patients with severe secondary MR (stages C and D) undergoing cardiac surgery	The 2014 recommendation currently remains
IIa	It is reasonable to preserve the mitral valve cords and annuloplasty in a symptomatic severe patient (NYHA III-IV) with ischemic MR (stage D) and persistent symptoms	New: Valve repair has been associated with a greater chance of moderate and severe MR than mitral valve replacement in patients with severe ischemic and symptomatic MR and no mortality difference in a 2-year follow-up.
IIb	Mitral valve repair or replacement can be considered for stage D symptomatic severe patients (NYHA III-IV) with chronic severe MR and persistent symptoms despite optimized therapy	The 2014 recommendation currently remains
IIb	The mitral repair indication is uncertain for a patient with moderate chronic ischemic MR (stage B) who underwent myocardial revascularization surgery	No clinical benefit was demonstrated for mitral valve repair in this population, with an increased risk of postoperative complications (neurological events and supraventricular arrhythmia)

Source: Adapted from Nishimura RA, Otto CM, Bonow RO, Carabello BA, Erwin JP 3rd, Fleisher LA, et al. 2017 AHA/ACC Focused Update of the 2014 AHA/ACC Guideline for the Management of Patients With Valvular Heart Disease: A Report of the American College of Cardiology/American Heart Association Task Force on Clinical Practice Guidelines. *Circulation*. 2017;135(25):e1159-e1195. doi: 10.1161/CIR.000000000000503.<sup>12</sup> MR, mitral regurgitation; NYHA, New York Heart Association.

The presence of stress-induced MR or stress MR worsening increases the morbidity rate and pulmonary artery systolic pressure > 60 mmHg of patients, decreasing their functional capacity, which allows the identification of patients at higher risk. Although patients with severely increased MR and pulmonary arterial hypertension on exertion benefit from early elective mitral valve surgery, the presence of pulmonary hypertension is considered a IIb class indication for mitral valve repair in asymptomatic patients without LV dysfunction or dilation in the European Society of Cardiology and ACC guidelines.<sup>14,15</sup>

## Intervention criteria based on symptoms and the LV

### Referral for surgical intervention

Unless surgery is contraindicated, all patients with severe and symptomatic MR should be considered for surgery. Whether the valve is repaired or replaced, surgery usually improves patients' symptoms. However, while awaiting the onset of symptoms, these patients present worse long-term outcomes since many develop incipient or latent LV dysfunction.

The AHA/ACC guidelines recommend surgery for asymptomatic patients with evidenced LV dysfunction<sup>5</sup> due to adequate conditions for cardiac performance (increased preload and decreased afterload). The normal EF in severe primary MR must be greater than the truly normal EF. Therefore, when the EF decreases to <60% (or 64%), LV systolic dysfunction is possible. If the EF decreases to < 60%, valve repair should be performed in asymptomatic patients; in this context, a gradually decreased EF should also be considered. An LVSD > 40 mm is another sign of systolic dysfunction; however, if repair success is very probable, surgery should be considered. Surgery is associated with high risk and myocardial recovery uncertainty in patients with advanced systolic dysfunction (EF < 30%) and chronic primary MR; thus, each case must be evaluated individually.

In the past, due to high surgical mortality and adverse consequences of mitral valve replacement, these patients were followed up until the onset of LV symptoms or

dysfunction. With advanced technology and valve repair techniques, consideration of the earliest approach is currently recommended. However, in cases of a low possibility of repair, close follow-up should be the chosen strategy, as the premature placement of valve prostheses essentially substitutes one disease for another, with risks of thromboembolism, bleeding, and need for future interventions.

Reference center studies have shown a postoperative success rate greater than 98% and low surgical mortality in posterior cusp prolapse repair. The success rate of anterior cusp prolapse repair is 90–95% and surgical mortality is lower than 1%, with excellent 20-year durability.<sup>16,17</sup>

There are several types of repair, the most commonly used being posterior prolapse with triangular or quadrangular resection, anterior prolapse with artificial cords, and commissure prolapse with commissuroplasty. Almost all techniques include annuloplasty rings for greater support and durability. The mitral valve can be replaced using a mechanical or biological prosthesis with effort made to preserve the mitral cords.

### Referral for percutaneous intervention

#### MitraClip®

The MitraClip® device is placed using the tip-to-tip technique in the presence of a catheter. This new method has been studied and approved for clinical use. It simulates the surgical repair technique by Alfieri.<sup>20</sup> The EVEREST study reported that the original MitraClip® strategy can significantly improve symptoms in patients with severe symptomatic primary MR and a higher surgical risk. This strategy must be safe and present no difference in long-term mortality.<sup>19</sup>

The MitraClip® intervention depends on prolapse type, with the prolapse involving the P2–A2 segments being the most appropriate for this intervention. This device can be used to treat severe symptoms caused by primary MR, although it does not promote better results than surgery. The MitraClip® is approved for patients with primary MR, severe symptoms, and a high surgical risk. Other catheter-based methods used to treat MR include percutaneous valve replacement and ring placement.<sup>19</sup>

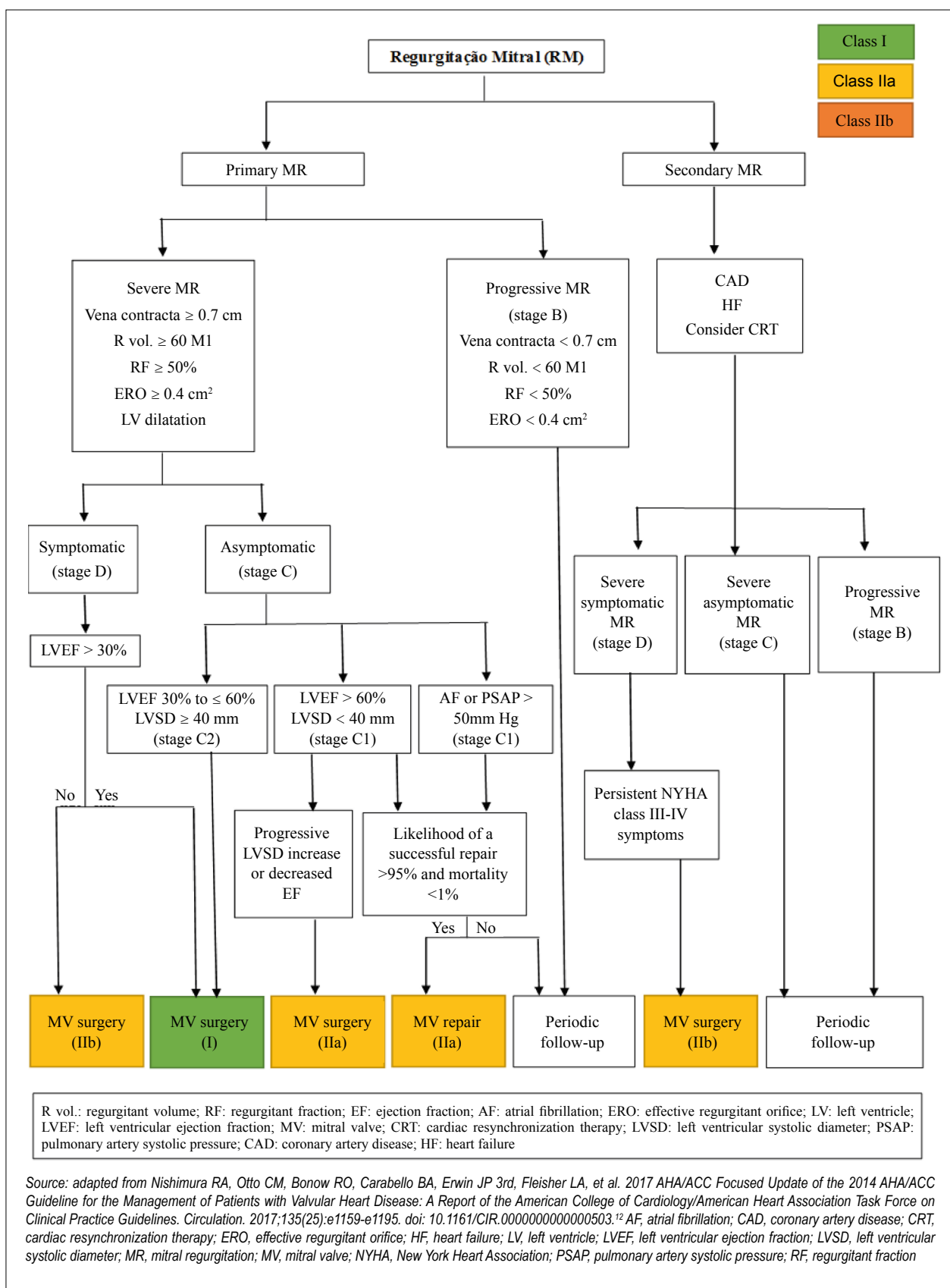


Figure 3 – Practical conduct guide for chronic mitral valve regurgitation.

### Percutaneous annuloplasty

The percutaneous procedure aims to correct functional MR (secondary to LV dilatation) through catheterization. Percutaneous mitral valve repair is most commonly used for posterior cusp prolapse. Annuloplasty is performed indirectly or directly.<sup>20</sup> In the indirect technique, the internal jugular vein is pulsed and the catheter is inserted into the coronary sinus. This involves approximately two-thirds of the mitral valve annulus' circumference. The prosthetic ring tightens the mitral valve annulus in the coronary sinus, reducing its diameter and consequently reducing the degree of mitral valve regurgitation. The problem with this method is that it can compress the circumflex artery. Therefore, it is important to perform left catheterization after device placement to evaluate arterial patency.

An arterial puncture is performed in direct annuloplasty, and the catheter is retrogradely inserted into the LV with a series of anchors placed around the mitral valve annulus. These anchors are fixed and place tension on the mitral valve annulus, reducing its diameter. The advantage of this method is that it does not compress the coronary artery.

### Transcatheter mitral valve procedure

The transcatheter mitral valve procedure is still in its initial phase. Although the MitraClip® is already a transcatheter surgery option approved by the United States Food and Drug Administration, catheter implantation is used to place surgical bioprostheses. The purpose of this approach is to place the heart valve in the mitral valve position using a catheter.<sup>21</sup>

### Secondary MR considerations

Both forms of secondary MR result from enlarged ventricles and lateral displacement of the papillary muscles or a parietal abnormality that impairs posterior mitral cusp coaptation.

If the myocardium is viable, myocardial revascularization or percutaneous coronary intervention should be considered for patients with severe secondary MR and secondary LV systolic dysfunction induced by ischemia.<sup>22</sup> Although the effect on ischemic MR varies, revascularization in patients with a low EF can improve their long-term prognosis. Mitral valve repair in ischemic

MR during myocardial revascularization is controversial, with possible beneficial results but a higher rate of complications. One study showed that, in a period of 2 years, 68% of patients undergoing mitral valve repair experienced reduced MR severity only if treated with myocardial revascularization.<sup>23</sup>

Another randomized study supported the use of mitral valve replacement in patients with severe ischemic MR. According to the authors, mitral valve repair was associated with an unacceptable recurrence rate, with moderate or severe MR within 2 years (58.8% vs 3.8%), a decreased quality of life, and heart failure-related hospitalizations.<sup>24</sup>

It remains unclear whether the treatment of secondary MR will benefit these patients, but the COAPT study demonstrated that the use of a MitraClip® associated with drug therapy was superior at a 2-year interval with significantly reduced hospitalization and mortality rates compared to drug therapy alone.<sup>25</sup>

### Conclusion

Primary and secondary MR are two completely different diseases whose natural history, lesion mechanism, treatment strategy, and response to treatment differ. The origin of secondary MR should also be divided into ischemic or non-ischemic, as there are important approach differences between them. These MR phenotypes can be defined using echocardiography, which, in addition to guiding patient selection and conduct, is essential for the diagnosis and choice of therapeutic approaches.

### Authors' contributions

Research conception and design: Camarozano AC; data collection: Camarozano AC; data analysis and interpretation: Camarozano AC; manuscript writing: Camarozano AC, Camarozano LM; critical review of the manuscript for important intellectual content: Camarozano AC; table preparation: Camarozano LM.

### Conflict of interest

The authors have declared that they have no conflict of interest.

### References

- Hahn RT, Abraham T, Adams MS, Bruce CJ, Glas KE, Lang RM, et al. Guidelines for performing a comprehensive transesophageal echocardiographic examination: recommendations from the American Society of Echocardiography and the Society of Cardiovascular Anesthesiologists. *J Am Soc Echocardiogr.* 2013;26(9):921-64. doi: 10.1016/j.echo.2013.07.009
- Han HC, Ha FJ, Teh AW, Calafiore P, Jones EF, Johns J, et al. Mitral valve prolapse and sudden cardiac death: a systematic review. *J Am Heart Assoc.* 2018;7(23):e010584. doi: 10.1161/JAHA.118.010584
- Cozzarín A, Cianciulli TF, Saccheri MC, Lax JA, Simonetti ME, Zappi A, et al. Severe mitral regurgitation after radiotherapy. *Echocardiography.* 2014;31(2):E37-40. doi: 10.1111/echo.12409
- Chehab O, Roberts-Thomson R, Ng Yin Ling C, Marber M, Prendergast BD, Rajani R, et al. Secondary mitral regurgitation: pathophysiology, proportionality and prognosis. *Heart.* 2020;106(10):716-23. doi: 10.1136/heartjnl-2019-316238
- Nishimura RA, Otto CM, Bonow RO, Carabello BA, Erwin JP 3rd, Guyton RA, O'Gara PT, Ruiz CE, Skubas NJ, Sorajja P, Sundt TM 3rd, Thomas JD; ACC/AHA Task Force Members. 2014 AHA/ACC Guideline for the Management of Patients With Valvular Heart Disease: executive summary: a report of the American College of Cardiology/American Heart Association Task Force on Practice Guidelines. *Circulation.* 2014;129(23):2440-92. doi: 10.1161/CIR.0000000000000029
- Yosefy C, Levine RA, Solis J, Vaturi M, Handschumacher MD, Hung J. Proximal flow convergence region as assessed by real-time 3-dimensional echocardiography: challenging the hemispheric assumption. *J Am Soc Echocardiogr.* 2007;20(4):389-96. doi: 10.1016/j.echo.2006.09.006
- Grigioni F, Enriquez-Sarano M, Ling LH, Bailey KR, Seward JB, Tajik AJ, et al. Sudden death in mitral regurgitation due to flail leaflet. *J Am Coll Cardiol.* 1999;34(7):2078-85. doi: 10.1016/s0735-1097(99)00474-x
- Nishimura RA, Otto CM, Bonow RO, Carabello BA, Erwin JP 3rd, Guyton

- RA, O'Gara PT, Ruiz CE, Skubas NJ, Sorajja P, Sundt TM 3rd, Thomas JD; ACC/AHA Task Force Members. 2014 AHA/ACC Guideline for the Management of Patients With Valvular Heart Disease: a report of the American College of Cardiology/American Heart Association Task Force on Practice Guidelines. *Circulation*. 2014;129(23):e521-643. doi: 10.1161/CIR.0000000000000031. Erratum in: *Circulation*. 2014;129(23):e651. Erratum in: *Circulation*. 2014;130(13):e120. Dosage error in article text.
9. Carpentier A, Chauvaud S, Fabiani JN, Deloche A, Relland J, Lessana A, et al. Reconstructive surgery of mitral valve incompetence: ten-year appraisal. *J Thorac Cardiovasc Surg*. 1980;79(3):338-48. PMID: 7354634. AND Carpentier A: Cardiac Valve Surgery—the “French Correction”. *J Thorac Cardiovasc Surg*. 1983; 86:323-337
  10. Lancellotti P, Moura L, Pierard LA, Agricola E, Popescu BA, Tribouilloy C, Hagendorff A, Monin JL, Badano L, Zamorano JL; European Association of Echocardiography. European Association of Echocardiography recommendations for the assessment of valvular regurgitation. Part 2: mitral and tricuspid regurgitation (native valve disease). *Eur J Echocardiogr*. 2010;11(4):307-32. doi: 10.1093/ejchocard/jeq031
  11. Varghese R, Itagaki S, Anyanwu AC, Trigo P, Fischer G, Adams DH. Predicting systolic anterior motion after mitral valve reconstruction: using intraoperative transoesophageal echocardiography to identify those at greatest risk. *Eur J Cardiothorac Surg*. 2014;45(1):132-7; discussion 137-8. doi: 10.1093/ejcts/ezt234
  12. Nishimura RA, Otto CM, Bonow RO, Carabello BA, Erwin JP 3rd, Fleisher LA, et al. 2017 AHA/ACC Focused Update of the 2014 AHA/ACC Guideline for the Management of Patients With Valvular Heart Disease: A Report of the American College of Cardiology/American Heart Association Task Force on Clinical Practice Guidelines. *Circulation*. 2017;135(25):e1159-e1195. doi: 10.1161/CIR.0000000000000503
  13. Magne J, O'Connor K, Mahjoub H. Evaluation and impact on outcome of left ventricular contractile reserve in asymptomatic degenerative mitral regurgitation. *Eur Heart J*. 2011;32:(Suppl):170.
  14. Joint Task Force on the Management of Valvular Heart Disease of the European Society of Cardiology (ESC); European Association for Cardio-Thoracic Surgery (EACTS), Vahanian A, Alfieri O, Andreotti F, Antunes MJ, Barón-Esquivias G, Baumgartner H, et al. Guidelines on the management of valvular heart disease (version 2012). *Eur Heart J*. 2012;33(19):2451-96. doi: 10.1093/eurheartj/ehs109
  15. American College of Cardiology/American Heart Association Task Force on Practice Guidelines; Society of Cardiovascular Anesthesiologists; Society for Cardiovascular Angiography and Interventions; Society of Thoracic Surgeons, Bonow RO, Carabello BA, Kanu C, de Leon AC Jr, Faxon DP, Freed MD, et al. ACC/AHA 2006 guidelines for the management of patients with valvular heart disease: a report of the American College of Cardiology/American Heart Association Task Force on Practice Guidelines (writing committee to revise the 1998 Guidelines for the Management of Patients With Valvular Heart Disease): developed in collaboration with the Society of Cardiovascular Anesthesiologists: endorsed by the Society for Cardiovascular Angiography and Interventions and the Society of Thoracic Surgeons. *Circulation*. 2006;114(5):e84-231. doi: 10.1161/CIRCULATIONAHA.106.176857. Erratum in: *Circulation*. 2007;115(15):e409. Erratum in: *Circulation*. 2010;121(23):e443.
  16. Castillo JC, Anyanwu AC, El-Eshmawi A, Adams DH. All anterior and bileaflet mitral valve prolapses are repairable in the modern era of reconstructive surgery. *Eur J Cardiothorac Surg*. 2014;45(1):139-45; discussion 145. doi: 10.1093/ejcts/ezt196
  17. Suri RM, Schaff HV, Dearani JA, Sundt TM 3rd, Daly RC, Mullany CJ, et al. Survival advantage and improved durability of mitral repair for leaflet prolapse subsets in the current era. *Ann Thorac Surg*. 2006;82(3):819-26. doi: 10.1016/j.athoracsur.2006.03.091
  18. Alfieri O, Maisano F, De Bonis M, Stefan PL, Torracca L, Oppizzi M, et al. The double-orifice technique in mitral valve repair: a simple solution for complex problems. *J Thorac Cardiovasc Surg*. 2001;122(4):674-81. doi: 10.1067/mtc.2001.117277
  19. Feldman T, Foster E, Glower DD, Kar S, Rinaldi MJ, Fail PS, Smalling RW, Siegel R, Rose GA, Engeron E, Loghini C, Trento A, Skipper ER, Fudge T, Letsou GV, Massaro JM, Mauri L; EVEREST II Investigators. Percutaneous repair or surgery for mitral regurgitation. *N Engl J Med*. 2011;364(15):1395-406. doi: 10.1056/NEJMoa1009355. Erratum in: *N Engl J Med*. 2011;365(2):189. Glower, Donald G [corrected to Glower, Donald D].
  20. Feldman T, Cilingiroglu M. Percutaneous leaflet repair and annuloplasty for mitral regurgitation. *J Am Coll Cardiol*. 2011;57(5):529-37. doi: 10.1016/j.jacc.2010.10.012
  21. Guilherme F, Attizzania B. Tratamento transcatereter da insuficiência mitral grave no Brasil: uma novidade na área. *Rev Bras Cardiol Invasiva*. 2015 [citado 2021 abr 6];23(2):82-83. Disponível em: <https://www.elsevier.es/en-revista-revista-brasileira-cardiologia-invasiva-233-articulo-tratamento-transcatereter-da-insuficiencia-mitral-S0104184315000351>
  22. El Sabbagh A, Reddy YNV, Nishimura RA. Mitral Valve Regurgitation in the Contemporary Era: Insights Into Diagnosis, Management, and Future Directions. *JACC Cardiovasc Imaging*. 2018;11(4):628-43. doi: 10.1016/j.jcmg.2018.01.009
  23. Michler RE, Smith PK, Parides MK, Ailawadi G, Thourani V, Moskowicz AJ, Acker MA, Hung JW, Chang HL, Perrault LP, Gillinov AM, Argenziano M, Bagiella E, Overbey JR, Moquete EG, Gupta LN, Miller MA, Taddei-Peters WC, Jeffries N, Weisel RD, Rose EA, Gammie JS, DeRose JJ Jr, Puskas JD, Dagenais F, Burks SG, El-Hamamsy I, Milano CA, Atluri P, Voisine P, O'Gara PT, Gelijs AC; CTSN. Two-year outcomes of surgical treatment of moderate ischemic mitral regurgitation. *N Engl J Med*. 2016;374(20):1932-41. doi: 10.1056/NEJMoa1602003
  24. Goldstein D, Moskowicz AJ, Gelijs AC, Ailawadi G, Parides MK, Perrault LP, Hung JW, Voisine P, Dagenais F, Gillinov AM, Thourani V, Argenziano M, Gammie JS, Mack M, Demers P, Atluri P, Rose EA, O'Sullivan K, Williams DL, Bagiella E, Michler RE, Weisel RD, Miller MA, Geller NL, Taddei-Peters WC, Smith PK, Moquete E, Overbey JR, Kron IL, O'Gara PT, Acker MA; CTSN. Two-Year Outcomes of Surgical Treatment of Severe Ischemic Mitral Regurgitation. *N Engl J Med*. 2016;374(4):344-53. doi: 10.1056/NEJMoa1512913
  25. Baron S, Kumbhani DJ. Cardiovascular outcomes assessment of the mitraclip percutaneous therapy for heart failure patients with functional mitral regurgitation – COAPT. American College of Cardiology, 2020 [cited 2021 Apr 4]. Available from: <https://www.acc.org/latest-in-cardiology/clinical-trials/2018/09/21/20/12/coapt>

# Echocardiographic Correlation Between Right Ventricular Diastolic Function and Age and Gender in Subjects With Preserved Systolic Function

*Correlação Ecocardiográfica da Função Diastólica do Ventrículo Direito com Idade e Gênero em Indivíduos com Função Sistólica Preservada*

Leonardo Lasari Melo<sup>1</sup>, Ana Cristina Camarozano<sup>1</sup>, Daniela de Castro Carmo<sup>1</sup>, Jerônimo Antonio Fortunato<sup>1</sup>, Rubens Zenóbio Darwich<sup>1</sup>, Cintia Rocha Fortes de Sá<sup>1</sup>, Liz Andréa Villela Baroncini<sup>1</sup>

Hospital da Cruz Vermelha,<sup>1</sup> (PR), Brazil.

## Abstract

**Introduction:** Right ventricular (RV) systolic and diastolic functions influence the outcomes of cardiovascular diseases. However, right chamber size and function have not been uniformly assessed by age and sex.

**Objective:** To evaluate RV diastolic function by age and sex in an outpatient population with preserved left ventricular (LV) and RV systolic function using transthoracic echocardiography.

**Method:** This observational cross-sectional study included a total of 97 patients (56 women) aged  $61.5 \pm 12.5$  years. The assessed parameters included RV E/A ratio; peak E-wave and A-wave velocity, E-wave acceleration and deceleration time, and integral E-wave and A-wave velocity-time; and pulmonary artery systolic pressure (PASP), tricuspid reflux velocity, inferior vena cava diameter, and right atrial volume.

**Results:** A reduced E-wave was observed with increasing age (Pearson's correlation coefficient [PCC], -0.30;  $p = 0.003$ ). The same was observed for the E/A ratio (PCC, -0.21;  $p = 0.035$ ). There was a significant positive association between age and PASP results (PCC, 0.40;  $p = 0.004$ ) and tricuspid reflux velocity (PCC, 0.36;  $p = 0.008$ ). There was no significant intersex difference in echocardiography variables.

**Conclusion:** The present study showed the impact of age on RV diastolic function indices, which remained within the normal range, in subjects with preserved LV and RV function. The study did not evidence a significant difference between genders in relation to the diastolic function of the right ventricle.

**Keywords:** Right ventricle; Diastolic function; Echocardiography.

## Resumo

**Introdução:** As funções sistólica e diastólica do ventrículo direito influenciam no desfecho de doenças cardiovasculares. A avaliação sistemática das dimensões e da função das câmaras direitas, de acordo com sexo e idade, não é uniformemente realizada.

**Objetivo:** Avaliar, ao ecocardiograma transtorácico, a correlação da função diastólica do ventrículo direito com idade e sexo, em uma população ambulatorial variada, com função sistólica dos ventrículos esquerdo e direito preservada.

**Métodos:** Estudo observacional, transversal. Foram selecionados 97 pacientes,  $61,5 \pm 12,5$  anos, sendo 56 mulheres. Foram avaliadas as seguintes medidas da função diastólica do ventrículo direito: velocidade de pico das ondas E e A, relação E/A, tempos de aceleração e desaceleração de onda E, integral velocidade-tempo da onda E, integral velocidade-tempo da onda A, além da pressão sistólica de artéria pulmonar, velocidade do refluxo tricúspide, diâmetro da veia cava inferior e volume do átrio direito.

**Resultados:** Ocorreu redução da onda E com o aumento da idade (coeficiente de correlação de Pearson de -0,30;  $p=0,003$ ) e da relação E/A (coeficiente de correlação de Pearson de -0,21;  $p=0,035$ ). Houve associação positiva e significativa entre idade e os resultados das variáveis pressão sistólica de artéria pulmonar (coeficiente de correlação de Pearson de 0,40;  $p=0,004$ ) e velocidade do refluxo tricúspide (coeficiente de correlação de Pearson de 0,36;  $p=0,008$ ). Não houve diferença significativa na comparação entre os sexos em relação a variáveis ecocardiográficas.

**Conclusão:** O presente estudo mostrou impacto da idade nos índices de função diastólica do ventrículo direito, embora ainda com valores dentro da normalidade, em indivíduos com função sistólica dos ventrículos direito e esquerdo preservada, mas sem diferença significativa entre os sexos.

**Palavras-chave:** Ventrículo direito; Função diastólica; Ecocardiografia.

Mailing Address: Leonardo Lasari Melo •

E-mail: lmelo\_@hotmail.com

Manuscript received 7/20/2020; revised 11/20/2020; accepted 11/27/2020

DOI: 10.47593/2675-312X/20213402eabc126



## Introduction

Cardiovascular diseases are the main cause of death in Brazil and worldwide, being responsible for about 20% of all deaths in people aged over 30 years.<sup>1</sup> Some noninvasive methods for the diagnosis of cardiovascular diseases, including transthoracic echocardiography, provide morphological and functional information about the cardiac chambers.

Right ventricular (RV) function influences the outcomes of cardiac and pulmonary diseases such as heart failure, pulmonary hypertension, myocardial infarction, heart valve disease, and congenital heart disease regardless of left ventricular (LV) function.<sup>2</sup> Although standard echocardiography can reliably assess LV function, the ultrasound assessment of RV structure and function is generally suboptimal due to its anatomical location and specific geometric configuration.

RV function was neglected for a long time due to its complex detection and measurement. Several researchers recently started to implement transthoracic Doppler echocardiography to assess RV diastolic function in normal subjects versus those with a variety of cardiovascular disorders.<sup>3</sup> Evidence of the clinical importance of RV function has increased, partly due to improved imaging techniques. RV function impacts the outcomes of patients hospitalized with heart and lung disease.<sup>4</sup>

In recent years, transthoracic echocardiography using Doppler ultrasound has been increasingly used to assess RV diastolic function in several pathologies. Similarly to LV diastolic dysfunction, multiple etiologies have been associated with relaxation changes that lead to RV diastolic dysfunction.<sup>5</sup>

Thus, this study aimed to assess RV diastolic function in terms of age and sex in an outpatient population with preserved LV and RV systolic function undergoing routine echocardiographic examinations.

## Methods

### Study population

This was an observational cross-sectional study. A total of 115 patients of both sexes over 18 years of age (mean age,  $63.2 \pm 12.1$  years; 58 women) of any ethnicity who were referred by their attending physician for transthoracic echocardiography for any clinical indication were selected from the Cardiology outpatient clinic of the Red Cross Hospital of Curitiba, PR, Brazil. The patients were chosen by convenience using no statistical criteria according to their availability to participate in the research. A protocol form of clinical and echocardiographic parameters was filled out for each patient. The clinical data analyzed included age, sex, weight, height, body mass index (BMI), presence of systemic arterial hypertension (SAH), diabetes mellitus (DM), coronary artery disease (CAD), dyslipidemia, and smoking (current or previous). The diagnoses of SAH, DM, dyslipidemia, and smoking were retrieved from the patients' medical records and/or reported by the patients (referred information). The presence of CAD was confirmed by medical record data and by the patient, including non-fatal myocardial infarction and surgical or percutaneous myocardial revascularization. The regular use of drugs was also registered.

The exclusion criteria were significant valve diseases (moderate and severe), prosthetic valves, confirmed CAD and/or segmental changes in LV contraction due to ischemic heart disease or other cardiomyopathies,<sup>6</sup> pulmonary emphysema or chronic obstructive pulmonary disease, moderate to severe pulmonary arterial hypertension (PASP > 50 mmHg), LV contractile dysfunction (ejection fraction < 52% for men and < 54% for women), RV systolic dysfunction (tricuspid annular systolic excursion < 17 mm, tricuspid annulus peak systolic velocity < 9 cm/s, and RV fractional area < 35%), and atrial fibrillation or pacemaker rhythm.

The patients underwent complete two-dimensional transthoracic echocardiography using a Phillips IE 33, Phillips HD 11, Phillips Envisor, or ultrasound machine. Sonographic measurements were collected by two experienced echocardiographers licensed by the Department of Cardiovascular Imaging of the Brazilian Society of Cardiology.

All echocardiographic measurements of all standard acoustic windows were collected, including RV diastolic function measurements.

All patients signed two copies of the Informed Consent Form, one of which they kept. The study was approved by the local research ethics committee.

### Main echocardiographic parameters analyzed in this study

The indices for calculating RV diastolic function were assessed by apical four-chamber view by positioning of the sample volume at the tips of the tricuspid leaflets during diastole. RV diastolic function was initially assessed by pulsatile spectral Doppler of the tricuspid inflow. The Doppler bundle was aligned parallel to the blood flow vector. An electrocardiography tracing was included in all studies.

RV diastolic indices were calculated by tricuspid flow pulsed spectral Doppler, including E-wave peak velocity representing early filling, A-wave peak velocity representing late filling, peak ratio of early velocity at the late peak (E/A), E-wave acceleration time, E-wave deceleration time, E-wave velocity-time integral, and A-wave velocity-time integral (Figures 1 and 2). A tricuspid E/A ratio < 0.8 suggests a impaired relaxation, a tricuspid E/A ratio of 0.8–2.1 with a predominance of diastolic flow in the hepatic veins suggests a pseudo-normal filling pattern, and a tricuspid E/A ratio > 2.1 with E-wave deceleration time < 120 ms suggests a restrictive filling pattern.

The atrial filling fraction, which represents the percentage of RV filling due to atrial contraction, was calculated by the fraction of the A velocity integral compared to all tricuspid inflow.

PASP was estimated by tricuspid reflux continuous spectral Doppler in millimeters of mercury (Figure 3) using the maximum tricuspid regurgitation speed (m/s), when present, added to the diameter of the inferior vena cava (mm) to determine the right atrial (RA) pressure.<sup>6-7</sup>

Right atrium (RA) was analyzed in the apical transthoracic four-chamber window. The RA area was estimated from this window by planimetry considering a reference limit of 18 cm<sup>2</sup>. Indexed RA volume, the most accurate way to assess chamber size, was calculated as a reference value of 32 mL/m<sup>2</sup> for men and 27 mL/m<sup>2</sup> for women (Figure 4).



All quantifications and values considered in the present study were based on American Society of Echocardiography and of the European Association of Cardiovascular Imaging guidelines.<sup>8-12</sup>

**Statistical analysis**

The results of this study are described as mean, median, minimum and maximum values, or standard deviation for quantitative variables and as frequency and percentage for categorical variables. Student’s t-test for independent samples was used to compare the echocardiographic variables between the sexes. The association between age and echocardiographic variables was assessed by estimating Pearson’s correlation

coefficient (PCC). A univariate linear regression model was adjusted for each echocardiographic variable (response variable), including age, sex, BMI, SAH, DM, dyslipidemia, and smoking as explanatory variables. Subsequently, a multivariate linear regression model was adjusted for each echocardiographic variable of age and sex (as they are the main interest of the study) and the variables with values of  $p < 0.10$  in the univariate analysis (univariate model).

The normality of the quantitative variables was assessed by the Kolmogorov-Smirnov test. P values  $< 0.05$  were considered statistical significance. The data were analyzed using Stata/SE software v.14.1 (Statacorp LP, USA).

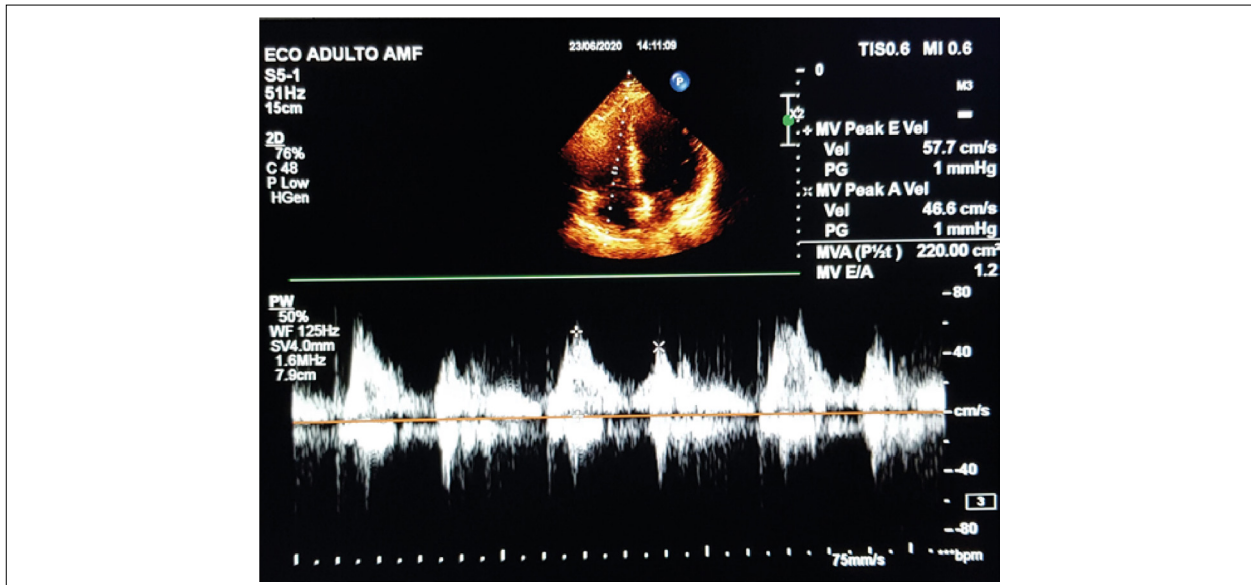


Figure 1 – Pulsatile spectral Doppler ultrasound image of the tricuspid flow used to assess right ventricular diastolic function.

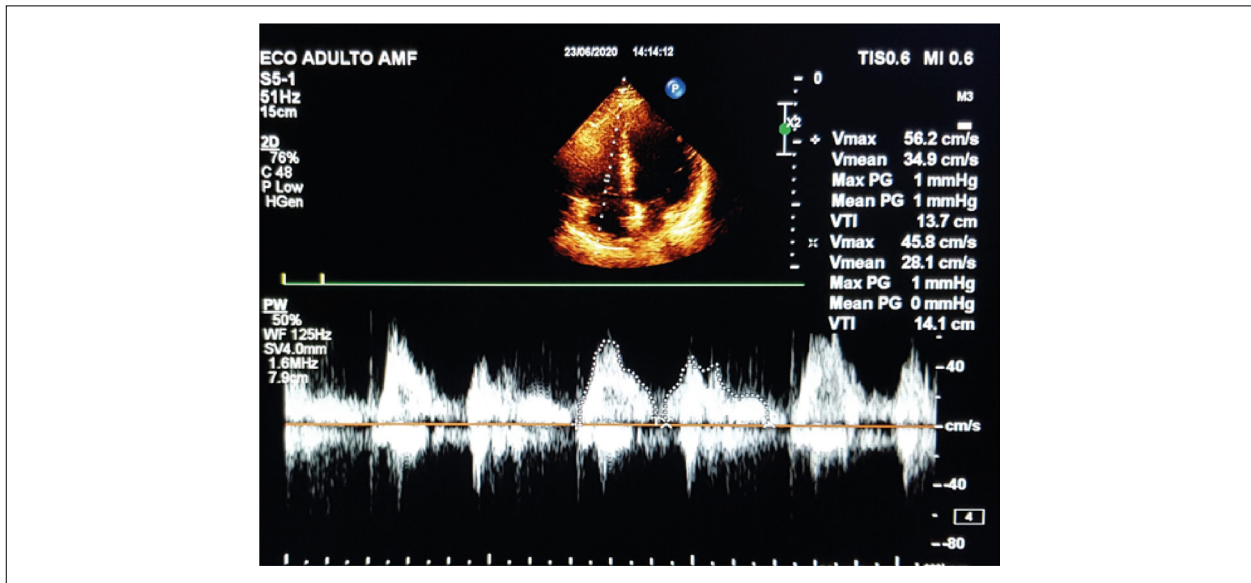


Figure 2 – Determination of right ventricular diastolic function.

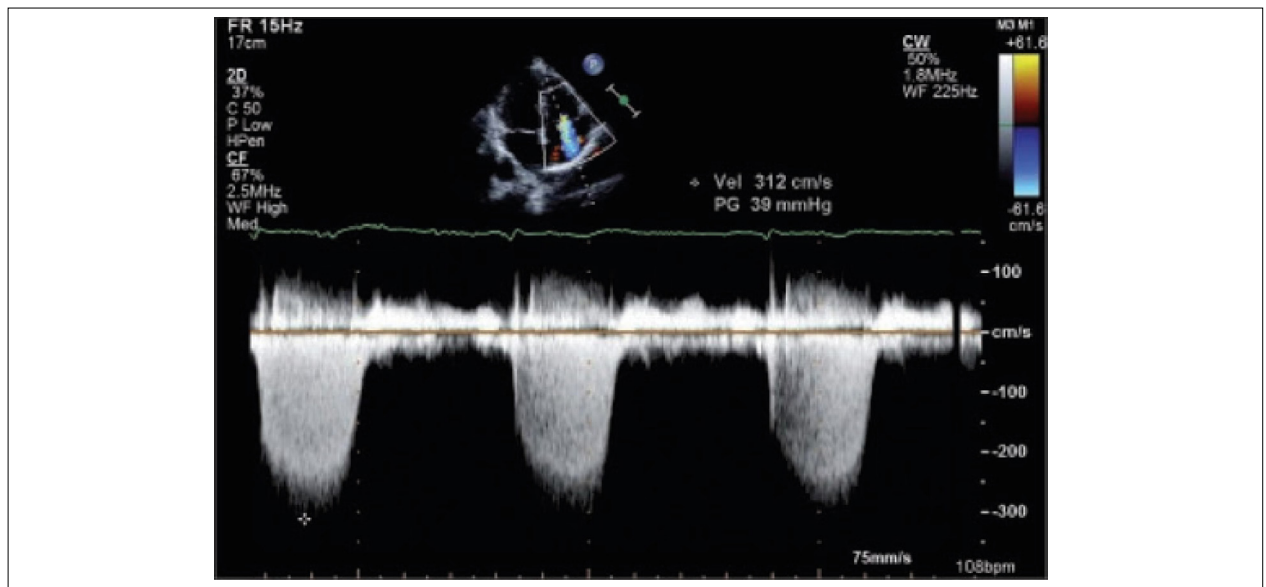


Figure 3 – Determination of estimated pulmonary artery systolic pressure using continuous spectral Doppler ultrasound of the tricuspid reflux (in mmHg).

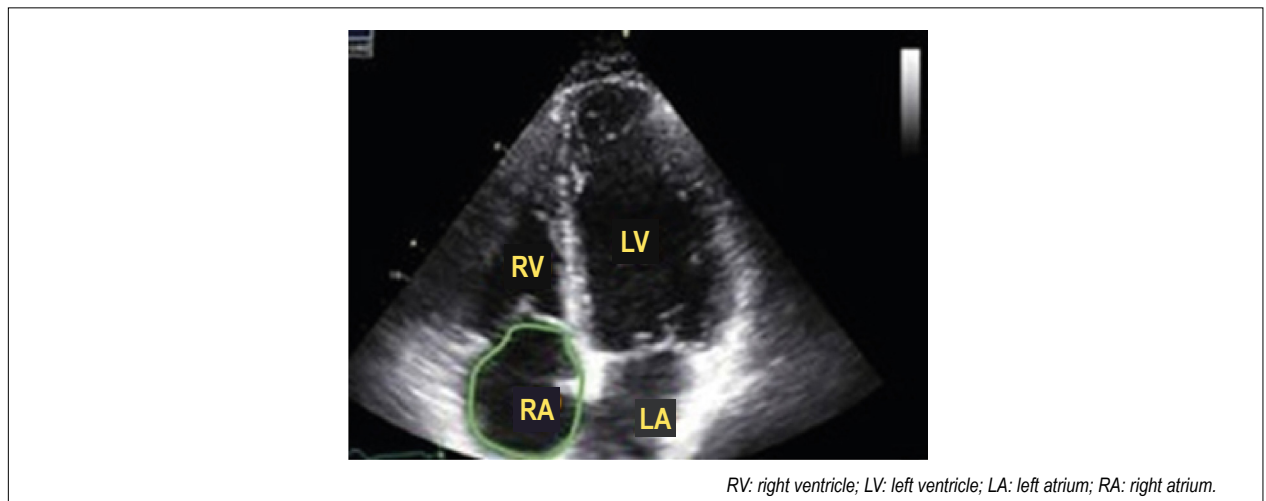


Figure 4 – Determination of right atrial volume.

## RESULTS

Eighteen patients were excluded from the study according to the selected parameters. The characteristics of the remaining 97 subjects are shown in Table 1. The mean participant age was  $61 \pm 12.5$  years; 56 (57%) were women. The echocardiographic variables found in the sample are shown in Table 2.

There was no significant intergroup difference in the echocardiographic variables (Table 3).

Tricuspid influx E/A ratio values were within the normal range, indicating preserved diastolic RV function. PASP was also within the normal range in all subjects. However, the echocardiographic E-wave peak velocity variables decreased with increasing age (PCC, -0.30;  $p = 0.003$ ). The same was

observed for the E/A ratio (PCC, -0.21;  $p = 0.035$ ). There was a significant positive association between age and PASP variables (PCC, 0.40;  $p = 0.004$ ) and tricuspid velocity (PCC, 0.36;  $p = 0.008$ ) (Figure 5). The other parameters showed no significant correlation with age. The presence of comorbidities did not influence the results (Table 4).

Uni- and multivariate analyses showed decreasing E-wave and E/A ratio values (coefficient, -0.003,  $p = 0.003$ ,  $R^2 = 7.1\%$ ; and coefficient, -0.005,  $p = 0.004$ ,  $R^2 = 3\%$ , respectively) and increasing PASP and tricuspid reflux velocity values (coefficient, 0.21,  $p = 0.004$ ,  $R^2 = 14.5\%$ ; and coefficient, 0.01,  $p = 0.009$ ,  $R^2 = 10\%$ , respectively) with increasing age. A-wave and A-wave integral values increased (coefficient, 0.009,  $p = 0.0001$ ; and coefficient, 0.112;  $p = 0.005$ , respectively) while the E/A ratio decreased

**Table 1 – General descriptive statistics of the study population.**

Classification	Men		Women	
	n	Mean (SD)	n	Mean (SD)
Age (years)	41	62.5 ± 10.9	56	60.8 ± 13.6
Body mass index (kg/m <sup>2</sup> )	41	27.1 ± 4.4	56	27.5 ± 4.2
Systemic arterial hypertension				
No	15	36.6	22	39.3
Yes	26	63.4	34	60.7
Diabetes mellitus				
No	33	80.6	45	80.4
Yes	8	19.4	11	19.6
Dyslipidemia				
No	24	58.5	43	76.8
Yes	17	41.5	13	23.2
Smoking				
No	25	61.0	48	85.7
Yes	16	39.0	8	14.3

SD, standard deviation.

**Table 2 – Baseline echocardiographic parameters in the study population.**

Variable	n	Mean	Standard deviation
E-wave (m/s)	97	0.48	0.12
A-wave (m/s)	97	0.43	0.12
E/A ratio	97	1.18	0.33
E-wave deceleration (ms)	97	178.1	61.6
E-wave integral	92	7.49	2.46
A-wave integral	92	4.85	1.60
Pulmonary artery systolic pressure (mmHg)	50	26.1	7.0
Vena cava (mm)	94	11.4	2.1
Right atrial volume (mL/m <sup>2</sup> )	97	19.5	6.1
Tricuspid velocity (m/s)	53	2.22	0.45
Right atrium area (cm <sup>2</sup> )	94	8.08	2.02
Atrial filling fraction (%)	92	39.5	9.6

(coefficient, -0.003,  $p < 0.001$ ) with increasing BMI. SAH, diabetes, dyslipidemia, and sex did not influence the analyzed variables (data not shown).

## Discussion

The present study found a significant correlation between RV diastolic function and age similar to what occurs with LV diastolic function. Innelli P et al.<sup>13</sup> demonstrated that the E/A ratio on spectral Doppler ultrasound of the tricuspid inflow decreases about 0.1 point per decade of life. That study<sup>13</sup> found a significant negative correlation between age and RV tricuspid inflow E-wave peak velocity and a positive correlation between age and A-wave peak velocity. The data presented here corroborate these results since the E-wave peak velocity progressively decreased with age but remained within the normal range,<sup>12</sup> indicating the influence of the aging process on relaxation of the RV base. Likewise, Lindqvist P et al.<sup>14</sup> reported a decreased tricuspid inflow E/A ratio on Doppler ultrasound with increasing age.

**Table 3 – Correlation between sex and echocardiographic variables.**

Variable	n	Mean	Standard deviation	p*
<b>E-wave (m/s)</b>				
Male	41	0.48	0.12	
Female	56	0.48	0.12	0.992
<b>A-wave (m/s)</b>				
Male	41	0.44	0.11	
Female	56	0.43	0.13	0.752
<b>E/A ratio</b>				
Male	41	1.15	0.30	
Female	56	1.20	0.34	0.451
<b>E-wave deceleration (ms)</b>				
Male	40	179.4	50.8	
Female	56	177.2	68.7	0.861
<b>E-wave integral (cm)</b>				
Male	37	7.26	2.49	
Female	55	7.64	2.45	0.467
<b>A-wave integral (cm)</b>				
Male	37	4.95	1.60	
Female	54	4.79	1.62	0.630
<b>PASP (mmHg)</b>				
Male	19	27.3	8.4	
Female	31	25.3	6.1	0.327
<b>Inferior vena cava (mm)</b>				
Male	40	11.9	2.0	
Female	54	11.1	2.2	0.063
<b>Right atrial volume (mL/m<sup>2</sup>)</b>				
Male	40	19.9	6.9	
Female	56	19.1	5.4	0.534
<b>Tricuspid reflux velocity (ms)</b>				
Male	19	2.3	0.5	
Female	34	2.2	0.4	0.522
<b>Right atrial area (cm<sup>2</sup>)</b>				
Male	38	8.2	2.4	
Female	56	8.0	1.7	0.714
<b>Atrial filling fraction (%)</b>				
Male	37	40.7	9.7	
Female	54	38.6	9.6	0.321

\*Student's t-test for independent samples,  $p < 0.05$ . PASP, pulmonary artery systolic pressure.

The RV may present relaxation changes due to collagen deposition with increased local fibrosis. In addition, calcium uptake from the cardiomyocytes leads to incomplete relaxation and worsening diastolic function in aged hearts.<sup>15</sup> This reduced RV diastolic function can decrease the heart's tolerance of structural diseases and functional conditions that affect RV filling.<sup>16-17</sup> However, the data presented here show no significant influence of comorbidities such as SAH, DM, dyslipidemia, and smoking on the evaluated parameters. It is worth mentioning that the American Society of Echocardiography<sup>12</sup> recommendations for echocardiographic evaluation of the right chambers did not establish reference values for normality based on body surface area and height since it was a compilation of several independent studies including those of patients with several systemic pathologies.

In the present study, an increased PASP was also correlated

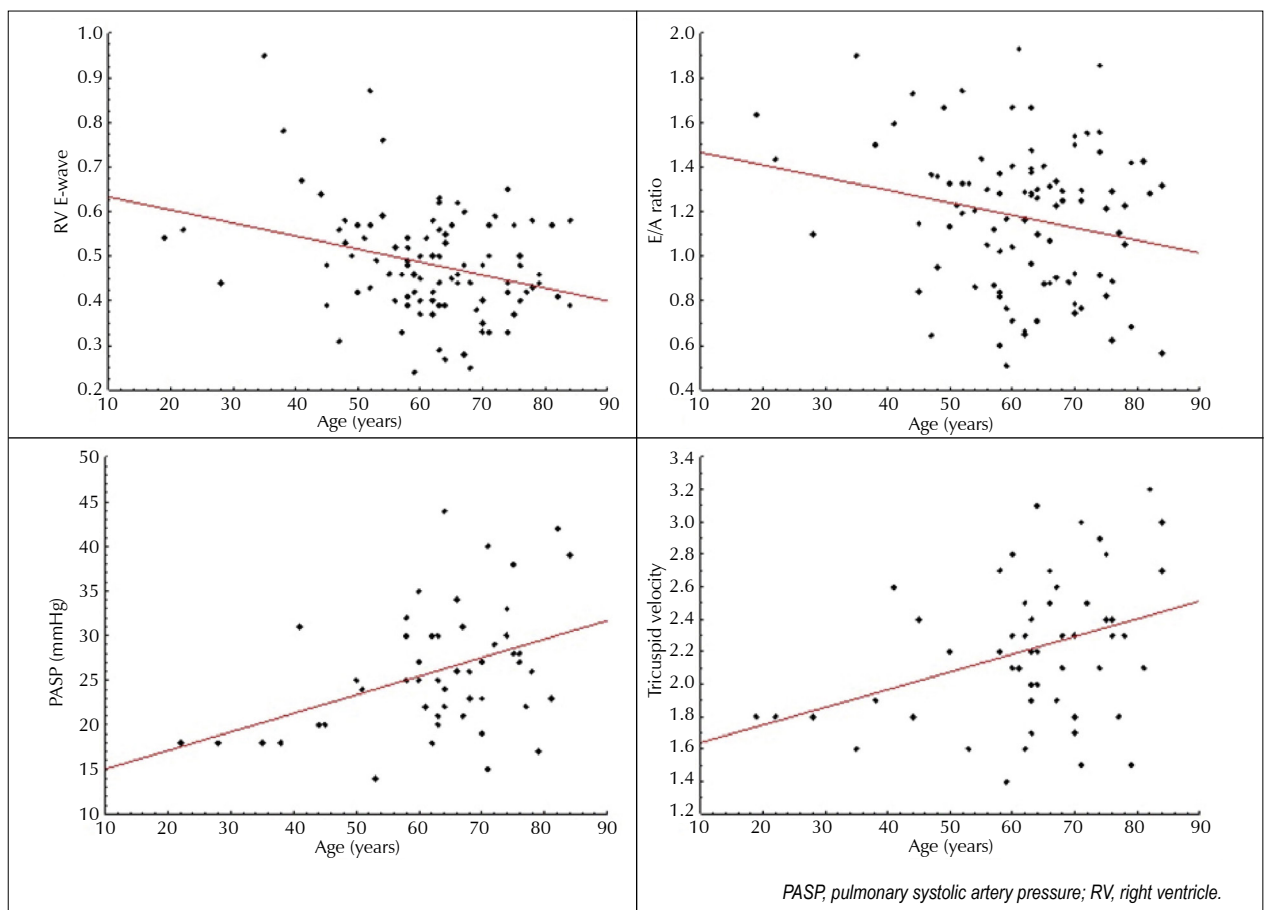


Figure 4 – Correlation between age and E-wave, E/A ratio, PASP, and tricuspid reflux.

Table 4 – Correlation between age (years) and echocardiographic variables.

Variable	n	PCC	p
Age × E-wave (m/s)	97	-0.30	0.003
Age × A-wave (m/s)	97	0.01	0.961
Age × E/A ratio	97	-0.21	0.035
Age × E-wave deceleration (ms)	96	0.15	0.148
Age × E-wave integral (cm)	92	-0.15	0.157
Age × A-wave integral (cm)	91	-0.02	0.859
Age × pulmonary artery systolic pressure (mmHg)	50	0.40	0.004
Age × inferior vena cava (mm)	94	0.15	0.147
Age × right atrial volume (mL/m <sup>2</sup> )	96	0.16	0.124
Age × tricuspid velocity (m/s)	53	0.36	0.008
Age × right atrial area (cm <sup>2</sup> )	94	0.12	0.260
Age × atrial filling fraction (%)	91	0.09	0.423

PCC, Pearson's correlation coefficient.

with age, although it remained within the normal range, due to increased arterial stiffness of the pulmonary vessels.<sup>18</sup> The pulmonary blood flow decreases with age, with increased mean pulmonary arterial pressure and pulmonary resistance, which is probably related to decreased lung compliance. Likewise, high left atrial pressures occur frequently in older people since LV stiffness increases, often leading to diastolic dysfunction.<sup>19-20</sup>

The data presented here showed no intersex differences in any of the analyzed parameters. Previous studies<sup>21-25</sup> demonstrated significant differences in both contractile and diastolic RV function in men versus women. These differences should be considered to avoid potential errors in the assessment of RV systolic and diastolic function.

Considering the above, the limitations of the present study must be clarified. First, the strict exclusion criteria resulted in no significant changes in the analyzed data; however, they enabled a homogeneous sample of relatively healthy subjects. The small number of participants (97) was also a determining factor in the results, for example, it limited the finding of a possible parameter difference between men and women. Another factor was the exclusion of subjects with any sign of RV contractile dysfunction AND ALSO having been excluded the data regarding the size and volume of the RV. A joint analysis of RV systolic-diastolic function could have added further interesting findings. It was also not computed whether heart rate (HR) variations would influence the findings presented here. In previous studies, Berman GO et al.<sup>26</sup> evaluated a population of only 41 people, reporting an influence of HR on RV diastolic function assessed by tricuspid influx spectral pulsed Doppler ultrasound; however, without clarifying which parameters were actually affected

by the HR variation. Yu CM et al.<sup>27</sup> studied 106 patients and determined that an increased HR influences the A-wave, therefore influencing the E/A ratio on mitral influx spectral Doppler ultrasound. However, RV velocity was analyzed with tricuspid annulus tissue Doppler ultrasound, which presented a small variation with HR. Similarly, Zoghbi et al.<sup>28</sup> studied 50 volunteers and presented no significant HR differences on spectral pulsed Doppler ultrasound of the mitral or tricuspid inflows. There are few studies to date on this topic.

We were unable to find a study with an older population and the same number of participants without cardiovascular comorbidities such as SAH, DM, dyslipidemia, and smoking as controls, which influences the echocardiographic variables used to assess LV and RV function.<sup>12</sup>

Therefore, no tissue Doppler ultrasound data were collected from the tricuspid annulus. The RV walls include superficial layers in which the fibers are arranged circumferentially in a direction parallel to the atrioventricular groove as well as deep layers where the fibers are aligned longitudinally.<sup>9</sup> Therefore, an echocardiographic evaluation using tissue Doppler ultrasound can be considered ideal for assessing RV diastolic function changes since it measures both longitudinal shortening and elongation of this chamber.

Studies worldwide have demonstrated changes in the population pattern. An increased incidence of heart failure and cardiovascular diseases, in which the RV plays an important

role, has been documented. Thus, the careful monitoring of RV changes is both necessary and relevant.

## Conclusions

The present study showed the significant impact of age on RV diastolic function indices in subjects with preserved LV and RV systolic function analyzed by transthoracic echocardiography. Although the values remained within the normal range, the observed changes suggest a progressive RV diastolic function deficit with aging; however, no significant intersex differences were noted.

## Authors' contributions

Data collection: Baroncini LAV, Melo LL, Camarozano AC, Carmo DC, Fortunato JA, Darwich RZ, Sá CRF; data analysis: Baroncini LAV, Melo LL, Camarozano AC, Carmo DC; data design: Baroncini LAV, Melo LL, Camarozano AC, Carmo DC; manuscript writing: Baroncini LAV, Melo LL, Camarozano AC, Carmo DC, Fortunato JA, Darwich RZ, Sá CRF; critical review of the manuscript for important intellectual content: Baroncini LAV, Melo LL, Camarozano AC.

## Conflict of interest

The authors have declared that they have no conflict of interest.

## References

1. Yusuf S, Reddy S, Ounpuu S, Anand S. Global burden of cardiovascular diseases: part I: general considerations, the epidemiologic transition, risk factors, and impact of urbanization. *Circulation*. 2001;104(22):2746-53. doi: 10.1161/hc4601.099487
2. Haddad F, Hunt SA, Rosenthal DN, Murphy DJ. Right ventricular function in cardiovascular disease, part I: Anatomy, physiology, aging, and functional assessment of the right ventricle. *Circulation*. 2008;117(11):1436-48. doi: 10.1161/CIRCULATIONAHA.107.653576
3. Scapellato F, Temporelli PL, Eleuteri E, Corrà U, Imparato A, Giannuzzi P. Accurate noninvasive estimation of pulmonary vascular resistance by Doppler echocardiography in patients with chronic failure heart failure. *J Am Coll Cardiol*. 2001;37(7):1813-9. doi: 10.1016/s0735-1097(01)01271-2
4. Bossone E, Rubenfire M, Bach DS, Ricciardi M, Armstrong WF. Range of tricuspid regurgitation velocity at rest and during exercise in normal adult men: implications for the diagnosis of pulmonary hypertension. *J Am Coll Cardiol*. 1999;33(6):1662-6. doi: 10.1016/s0735-1097(99)00055-8
5. Endo Y, Maddukuri PV, Vieira ML, Pandian NG, Patel AR. Quantification of right ventricular volumes and function by real time three-dimensional echocardiographic longitudinal axial plane method: validation in the clinical setting. *Echocardiography*. 2006;23(10):853-9. doi: 10.1111/j.1540-8175.2006.00327.x
6. Nagueh SF, Kopelen HA, Zoghbi WA. Relation of mean right atrial pressure to echocardiographic and Doppler parameters of right atrial and right ventricular function. *Circulation*. 1996;93(6):1160-9. doi: 10.1161/01.cir.93.6.1160
7. Kittipovanonh M, Bellavia D, Chandrasekaran K, Villarraga HR, Abraham TP, Pellikka PA. Doppler myocardial imaging for early detection of right ventricular dysfunction in patients with pulmonary hypertension. *J Am Soc Echocardiogr*. 2008;21(9):1035-41. doi: 10.1016/j.echo.2008.07.002
8. Lang RM, Badano LP, Mor-Avi V, Afilalo J, Armstrong A, Ernande L, et al. Recommendations for cardiac chamber quantification by echocardiography in adults: an update from the American Society of Echocardiography and the European Association of Cardiovascular Imaging. *J Am Soc Echocardiogr*. 2015;28(1):1-39.e14. doi: 10.1016/j.echo.2014.10.003
9. Grünig E, Biskupek J, D'Andrea A, Ehlken N, Egenlauf B, Weidenhammer J, et al. Reference ranges for and determinants of right ventricular area in healthy adults by two-dimensional echocardiography. *Respiration*. 2015;89(4):284-93. doi: 10.1159/000371472
10. Voelkel NF, Quaife RA, Leinwand LA, Barst RJ, McGoon MD, Meldrum DR, Dupuis J, Long CS, Rubin LJ, Smart FW, Suzuki YJ, Gladwin M, Denholm EM, Gail DB; National Heart, Lung, and Blood Institute Working Group on Cellular and Molecular Mechanisms of Right Heart Failure. Right ventricular function and failure: report of a National Heart, Lung, and Blood Institute working group on cellular and molecular mechanisms of right heart failure. *Circulation*. 2006;114(17):1883-91. doi: 10.1161/CIRCULATIONAHA.106.632208
11. Levine RA, Gibson TC, Aretz T, Gillam LD, Guyer DE, King ME, et al. Echocardiographic measurement of right ventricular volume. *Circulation*. 1984;69(3):497-505. doi: 10.1161/01.cir.69.3.497
12. Rudski LG, Lai WW, Afilalo J, Hua L, Handschumacher MD, Chandrasekaran K, et al. Guidelines for the echocardiographic assessment of the right heart in adults: a report from the American Society of Echocardiography endorsed by the European Association of Echocardiography, a registered branch of the European Society of Cardiology, and the Canadian Society of Echocardiography. *J Am Soc Echocardiogr*. 2010;23(7):685-713; quiz 786-8. doi: 10.1016/j.echo.2010.05.010
13. Innelli P, Esposito R, Olibet M, Nistri S, Galderisi M. The impact of ageing on right ventricular longitudinal function in healthy subjects: a pulsed tissue Doppler study. *Eur J Echocardiogr*. 2009;10(4):491-8. doi: 10.1093/ejehocard/jeu313

14. Lindqvist P, Waldenström A, Henein M, Mörner S, Kazzam E. Regional and global right ventricular function in healthy individuals aged 20-90 years: a pulsed Doppler tissue imaging study: Umeå General Population Heart Study. *Echocardiography*. 2005;22(4):305-14. doi: 10.1111/j.1540-8175.2005.04023.x
15. Alam M, Wardell J, Andersson E, Samad BA, Nordlander R. Characteristics of mitral and tricuspid annular velocities determined by pulsed wave Doppler tissue imaging in healthy subjects. *J Am Soc Echocardiogr*. 1999;12(8):618-28. doi: 10.1053/jje.1999.v12.a99246
16. Nikitin NP, Witte KK, Thackray SD, de Silva R, Clark AL, Cleland JG. Longitudinal ventricular function: normal values of atrioventricular annular and myocardial velocities measured with quantitative two-dimensional color Doppler tissue imaging. *J Am Soc Echocardiogr*. 2003;16(9):906-21. doi: 10.1016/S0894-7317(03)00279-7
17. Davidson WR Jr, Fee EC. Influence of aging on pulmonary hemodynamics in a population free of coronary artery disease. *Am J Cardiol*. 1990;65(22):1454-8. doi: 10.1016/0002-9149(90)91354-9
18. Dib JC, Abergel E, Rovani C, Raffoul H, Diebold B. The age of the patient should be taken into account when interpreting Doppler assessed pulmonary artery pressures. *J Am Soc Echocardiogr*. 1997;10(1):72-3. doi: 10.1016/S0894-7317(97)80035-1
19. Efthimiadis GK, Parharidis GE, Gemitzis KD, Nouskas IG, Karvounis HI, Styliadis IK, et al. Doppler echocardiographic evaluation of right ventricular diastolic function in isolated valvular aortic stenosis. *J Heart Valve Dis*. 1999;8(3):261-9
20. Yu CM, Sanderson JE. Right and left ventricular diastolic function in patients with and without heart failure: effect of age, sex, heart rate, and respiration on Doppler-derived measurements. *Am Heart J*. 1997;134(3):426-34. doi: 10.1016/S0002-8703(97)70077-2
21. Louie EK, Lin SS, Reynertson SI, Brundage BH, Levitsky S, Rich S. Pressure and volume loading of the right ventricle have opposite effects on left ventricular ejection fraction. *Circulation*. 1995;92(4):819-24. doi: 10.1161/01.cir.92.4.819
22. Davidson WR Jr, Fee EC. Influence of aging on pulmonary hemodynamics in a population free of coronary artery disease. *Am J Cardiol*. 1990;65(22):1454-8. doi: 10.1016/0002-9149(90)91354-9
23. Lakatta EG. Arterial and cardiac aging: major shareholders in cardiovascular disease enterprises: Part III: cellular and molecular clues to heart and arterial aging. *Circulation*. 2003;107(3):490-7. doi: 10.1161/01.cir.0000048894.99865.02
24. D'Andrea A, Vriz O, Carbone A, Ferrara F, Di Maio M, Cocchia R, et al. The impact of age and gender on right ventricular diastolic function among healthy adults. *J Cardiol*. 2017;70(4):387-395. doi: 10.1016/j.jjcc.2016.12.005
25. Kawut SM, Lima JA, Barr RG, Chahal H, Jain A, Tandri H, et al. Sex and race differences in right ventricular structure and function: the multi-ethnic study of atherosclerosis-right ventricle study. *Circulation*. 2011;123(22):2542-51. doi: 10.1161/CIRCULATIONAHA.110.985515
26. Berman GO, Reichek N, Brownson D, Douglas PS. Effects of sample volume location, imaging view, heart rate and age on tricuspid velocimetry in normal subjects. *Am J Cardiol*. 1990;65(15):1026-30. doi: 10.1016/0002-9149(90)91008-t
27. Yu CM, Lin H, Ho PC, Yang H. Assessment of left and right ventricular systolic and diastolic synchronicity in normal subjects by tissue Doppler echocardiography and the effects of age and heart rate. *Echocardiography*. 2003;20(1):19-27. doi: 10.1046/j.1540-8175.2003.00003.x
28. Zoghbi WA, Habib GB, Quinones MA. Doppler assessment of right ventricular filling in a normal population. Comparison with left ventricular filling dynamics. *Circulation*. 1990;82(4):1316-24. doi: 10.1161/01.cir.82.4.1316

# Left Atrial Reserve Function in Assessing Indeterminate Diastolic Function

*Função de Reserva do Átrio Esquerdo na Avaliação da Função Diastólica Indeterminada*

Silvio Henrique Barberato<sup>1,2</sup>, Rafael Borsoi<sup>1</sup>

<sup>1</sup>Quanta Diagnostic Imaging, Curitiba, PR; <sup>2</sup>CardioEco - Cardiovascular Diagnostic Center, Curitiba, PR, Brazil.

## Abstract

**Background:** Elevation of left ventricular filling pressures secondary to diastolic dysfunction plays a central role in the pathophysiology of heart failure. However, international guidelines still fail to diagnose diastolic dysfunction in some cases.

**Objective:** To evaluate left atrial reservoir function in indeterminate diastolic function

**Method:** Observational study with individuals in sinus rhythm and preserved left ventricular ejection fraction, submitted to echocardiogram and divided into three groups according to the combined analysis of E/e' ratio and indexed left atrium volume: Group 1, if normal left ventricular filling pressures; Group 2, if increased left ventricular filling pressures and Group 3, if indeterminate left ventricular filling pressures. Two-dimensional speckle tracking was used to measure peak left atrial strain (LAS). Analysis of variance, Student's t test and receiver-operator curve (ROC) were used in the statistical analysis.

**Results:** We included 58 patients who had  $61 \pm 14$  years old, 57% of whom were women, and had average left ventricular ejection fraction  $62 \pm 7\%$ . Groups 2 and 3 had lower LAS than Group 1 ( $20 \pm 5\%$  versus  $22 \pm 6\%$  versus  $30 \pm 8\%$ , respectively,  $p = 0.004$ ), but did not differ between them ( $p = 0.93$ ). LAS was a good predictor of elevated left ventricular filling pressures ( $p = 0.026$ ; area under the curve = 0.80), obtaining sensitivity of 60% and specificity of 80% with a cut-off value  $\leq 20\%$ .

**Conclusion:** The findings suggest that the left atrial reservoir function of individuals with indeterminate diastolic function is similar to that of individuals with advanced diastolic dysfunction, rendering LAS the potential to support the reclassification of indeterminate diastolic function.

**Keywords:** Diastolic function; Left atrium; Heart failure; Echocardiography.

## Resumo

**Fundamento:** A elevação das pressões de enchimento secundária à disfunção diastólica do ventrículo esquerdo ocupa papel central na fisiopatologia da insuficiência cardíaca. Mesmo assim, as diretrizes internacionais falham em detectar a disfunção diastólica em uma parte dos casos.

**Objetivo:** Avaliar a função de reserva do átrio esquerdo, estimada pelo strain longitudinal de pico do átrio esquerdo, nos casos de função diastólica indeterminada.

**Método:** Estudo observacional com indivíduos em ritmo sinusal e fração de ejeção do ventrículo esquerdo preservada, submetidos ao ecocardiograma e divididos em três grupos conforme a análise conjunta da relação E/e' e do volume de átrio esquerdo indexado: Grupo 1, se pressões de enchimento normais; Grupo 2, se pressões de enchimento elevadas e Grupo 3, se pressões de enchimento indeterminadas. Speckle tracking bidimensional foi empregado para medir o strain longitudinal de pico do átrio esquerdo. Análise de variância, teste t Student e curva receptor-operador (ROC) foram empregados na análise estatística.

**Resultado:** Foram incluídos 58 pacientes, com  $61 \pm 14$  anos, sendo 57% mulheres, com fração de ejeção do ventrículo esquerdo de  $62 \pm 7\%$ . Os Grupos 2 e 3 tiveram strain longitudinal de pico do átrio esquerdo menor que o Grupo 1 ( $20 \pm 5\%$  versus  $22 \pm 6\%$  versus  $30 \pm 8\%$ , respectivamente,  $p=0,004$ ), mas não diferiram entre si ( $p=0,93$ ). O strain longitudinal de pico do átrio esquerdo foi preditor de pressões de enchimento elevadas ( $p=0,026$ , área sob a curva=0,80), obtendo-se sensibilidade de 60% e especificidade de 80% com valor de corte  $\leq 20\%$ .

**Conclusão:** A função de reserva do átrio esquerdo dos indivíduos com função diastólica indeterminada é similar à dos indivíduos com disfunção diastólica avançada, conferindo ao strain longitudinal de pico do átrio esquerdo o potencial de auxiliar na reclassificação da função diastólica indeterminada.

**Palavras-chave:** Função Diastólica; Átrios do coração; Insuficiência cardíaca; Ecocardiografia.

Mailing Address: Silvio H. Barberato •

E-mail: silviohb@cardiol.br

Manuscript received 3/17/2021; revised 3/18/2021; accepted 4/9/2021

DOI: 10.47593/2675-312X/20213402eabc196



## Introduction

Increased filling pressures (FP) secondary to left ventricular (LV) diastolic dysfunction (DD) is the main hemodynamic determinant of the onset of heart failure (HF).<sup>1</sup> Thus, in cardiology practice, it is essential to determine whether there is underlying DD in patients with dyspnea of unknown origin and/or suspected HF, especially in those with a preserved ejection fraction (EF). Echocardiography provides essential noninvasive information about cardiac structure, function, and hemodynamics and should be performed on all patients with clinically suspected HF.

The American Society of Echocardiography/European Association of Cardiovascular Imaging (ASE/ EACVI) guideline recommends that the noninvasive analysis of increased FP adopt an integrated approach to the following echocardiographic parameters: E/e' ratio (ratio between early diastolic mitral inflow velocity on pulsed Doppler (E) and early diastolic mitral annular velocity on tissue Doppler [e']), tricuspid regurgitation velocity (TRV), and left atrial volume indexed (LAVI) for body surface area.<sup>2</sup> When more than half of the parameters are changed, FP is considered abnormal. However, the definitive criteria are not completely met in all cases; thus, DD presence and/or degree can be indeterminate.<sup>2</sup> This often occurs when it is impossible to determine the tricuspid regurgitation curve (due to the absence of regurgitation or inadequate tracing) and the other two parameters are conflicting.

The left atrium (LA) plays an important physiological role in LV filling dynamics, improving reserve function and atrial conduit and contraction. A decreased reserve function prior to chamber dilation can occur in the early stages of LVDD, when only the LV end-diastolic pressure is elevated and this increase is transmitted to the LA.<sup>3</sup> Two-dimensional speckle tracking echocardiography can measure LA deformation in the reserve phase, like the peak LA longitudinal strain (LAS), for example, which has the potential to be a subclinical DD marker.<sup>1,3</sup>

This study compared LAS in cases of indeterminate diastolic function versus cases with a normal or increased FP.

## Methods

This cross-sectional observational study included a random sample of patients in sinus rhythm with an LVEF  $\geq$  50% who were referred to the echocardiography service by their attending physician for testing. The exclusion criteria were significant valvular heart disease (moderate- or severe-degree regurgitation, stenosis degree [if any], and presence of prosthetic valve), congenital heart disease, or pericardiopathy. Basic demographic and clinical data were collected from a form completed by all patients before the test. All patients signed a consent form.

The participants underwent complete transthoracic echocardiography using a commercially available echocardiography machine (EPIQ7; Philips Medical Systems). LVEF was calculated of part of the sample by the two-dimensional Simpson's method in all patients and the three-dimensional method. Myocardial hypertrophy was

diagnosed when the LV mass index was  $>95$  g/m<sup>2</sup> in women or  $>115$  g/m<sup>2</sup> in men. Diastolic function analysis included the following parameters: mitral flow E and A waves on pulsatile Doppler, E/A ratio, e' velocity on tissue Doppler, E/e' ratio, TRV, and LAVI. The cutoff values used to distinguish the presence or absence of increased FP were E/e' ratio  $\geq$  15 (mean of the septal and lateral annulus) and LAVI  $>$  34 mL/m<sup>2</sup>.<sup>2</sup> The cases were then divided into three groups with FP defined according to the combined analysis of these two parameters. Group 1, normal FP with normal E/e' and LAVI ratios; Group 2, high FP with increased E/e' and LAVI ratios; and Group 3, indeterminate FP with one normal and one increased parameter.

Values of TRV  $>$  2.8 m/s were excluded from this analysis for often being unfeasible (absent or inadequate tricuspid regurgitation curve) in clinical practice and resulting in indeterminate diastolic function. Concomitantly, a traditional secondary LV diastolic function analysis was performed according to the specific algorithms recommended in the ASE/ EACVI guideline (including the E/e', LAVI, and TRV ratios).<sup>2</sup> DD was classified in ascending order of severity as: grade I, decreased ventricular relaxation without increased FP; grade II, decreased relaxation with increased FP; and grade III, highly increased FP with restrictive mitral flow pattern.

Two-dimensional speckle tracking echocardiography was used to measure the LAS using a zoomed-in apical four-chamber view LA image and analysis by a commercially available semi-automatic software (Cardiac Motion Quantification, QLAB 9.0; Philips Medical Systems). The start of the QRS complex was used as a zero-reference point and resulted in a positive strain by convention (Figure 1).<sup>4</sup> The frame rate used was 50–70 frames per second. The atrial endocardial border was identified manually by clicking on three points for the software to generate the region of interest. Subsequently, the images were manually optimized by exclusion of the pulmonary veins and the left atrial appendage. The region of interest was adjusted to include the atrial wall (generally 3 mm). Visual inspection of the moving image ensured myocardial tracking adequacy. The LA was divided into six segments, and the mean peak positive LAS (maximum) of the segments, which represents the reserve function, was recorded.<sup>4</sup> The LV LAS was calculated from the analysis of the three usual apical sections.

Continuous variables are expressed as mean and standard deviation and categorical variables as percentages and absolute numbers. The statistical analyses were performed using SPSS Statistics 22 software (IBM) and included analysis of variance, Student's t-test, chi-square test, receiver operating characteristic curve, and multivariate logistic regression analysis. Statistical significance was defined as values of  $p <$  0.05.

## Results

A total of 58 patients with a mean age of  $61 \pm 14$  years were included; 57% were women, 50% hypertensive, 22% diabetic, 12% smokers, and 36% dyslipidemic. Table 1 shows the main demographic and clinical characteristics of the study population. The mean two-dimensional EF was  $62 \pm 7\%$ . Myocardial hypertrophy was found in 21% of the sample (12 patients, of



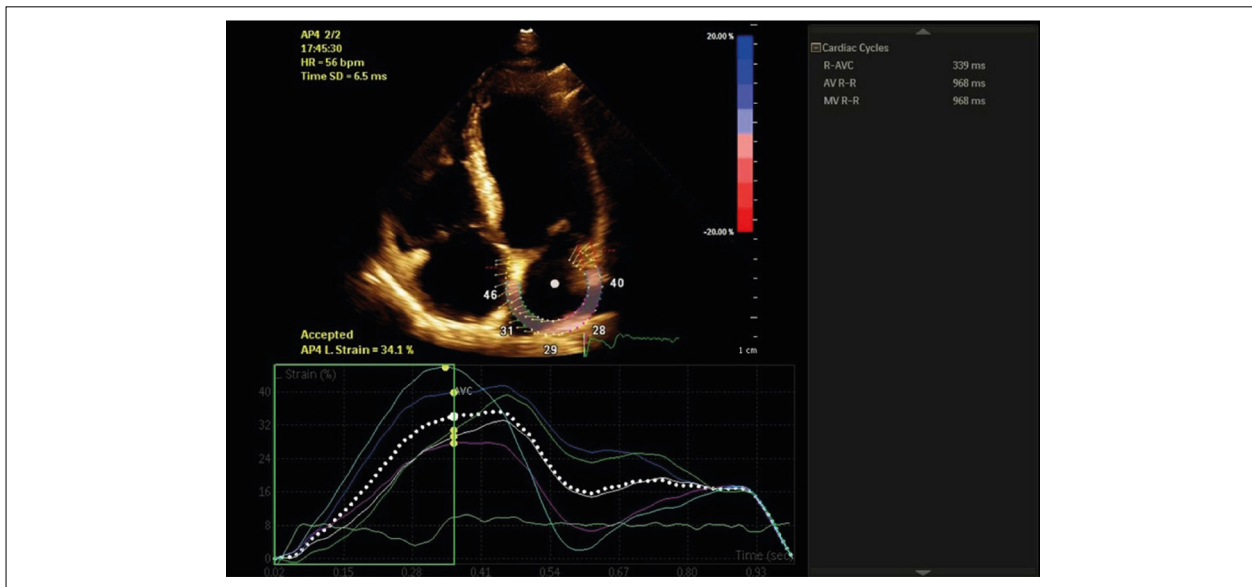


**Figure 1** – Left atrium in the apical four-chamber view with atrial deformation analysis performed by semi-automatic software. The beginning of the QRS complex was used as a zero-reference point by convention, resulting in a positive strain.

whom eight had concentric and four had eccentric hypertrophy). The mean LA dimension was  $34 \pm 5$  mm, while the mean LAVI was  $28 \pm 7$  mL/m<sup>2</sup>. Table 2 shows the main echocardiographic characteristics of the studied population. The patients with an increased FP were older ( $74 \pm 8$  vs.  $59 \pm 14$  years;  $p = 0.023$ ) and had a higher proportion of arterial hypertension (100% vs. 45%;  $p = 0.026$ ) than those with a normal FP. There were no differences in sex, body mass index, LVEF, or LV global LAS.

The combined analysis of the E/e' and LAVI ratios showed that the FP was normal in 66% (Group 1), increased in 5% (Group 2), and indeterminate in 29% (Group 3) of the studied population. Groups 2 and 3 had lower mean LAS strains than Group 1 ( $20 \pm 5\%$  vs.  $22 \pm 6\%$  vs.  $30 \pm 8\%$ , respectively;  $p = 0.004$ ), but the values did not differ from one another ( $p = 0.93$ ). Figure 2 compares the mean LAS between groups. LAS was a predictor of a high FP ( $p = 0.026$ , area under the curve [AUC], 0.80) with 60% sensitivity, 80% specificity, and a cutoff value of  $\leq 20\%$  (Figure 3). Age-adjusted multivariate logistic regression analysis and LAVI showed that LAS was an independent predictor of an increased FP according to the criteria.

According to the ASE/EACVI guideline, DD was diagnosed in 55% of the patients (46% grade I, 9% grade II). There was a gradual LAS decrease with increased DD degree (normal =  $35 \pm 6\%$ ; degree I =  $23 \pm 7\%$ ; degree II =  $18 \pm 6\%$ ;  $p < 0.001$ ). It was not possible to obtain a tricuspid reflux curve to measure TRV in 14 patients (24%); the other patients had a mean TRV of  $2.4 \pm 0.4$  m/s.

## Discussion

The findings of this study suggest that the LA reserve function (estimated by LAS) in patients with indeterminate diastolic function is similar to that of patients with DD and that LAS progressively decreases with DD severity.

**Table 1** - Main demographic and clinical characteristics of the study population.

Variable	n=58
Age, years	61±14
Male sex	43 (25)
Body mass index	26±37
Systolic blood pressure, mmHg	134 ± 24
Diastolic blood pressure, mmHg	79 ± 19
Heart rate, bpm	68 ± 11
Dyspnea	28 (16)
Arterial hypertension	50 (29)
Diabetes	22 (13)
Dyslipidemia	36 (21)
Smoking	12 (7)
Sedentary lifestyle	38 (22)
Previous myocardial infarction	7 (4)
Angina pectoris	7 (4)
Family history of coronary artery disease	21 (12)
ARB	31 (18)
ACEI	9 (5)
Calcium channel blocker	9 (5)
Beta-blocker	34 (20)
Diuretic	17 (10)
Statin	36 (21)
Acetylsalicylic acid	26 (15)

Results expressed as mean ± standard deviation or n (%). ARB, angiotensin receptor blocker; ACEI, angiotensin-converting enzyme inhibitor.

Several studies and clinical experiences indicate that the noninvasive LV FP estimation provided by echocardiography is useful in clinical decision-making, but some problems persist regarding sensitivity and positive predictive value, notably in patients with a preserved EF (>50%) and in some specific clinical conditions.<sup>1</sup> The ASE/EACVI guideline, based on a tripartite approach (E/e' ratio, LAVI, and TRV), increases the specificity of increased FP findings but fails to detect DD in approximately 8–15% of cases.<sup>5-7</sup> Much of the problem lies in the fact that some patients have no tricuspid regurgitation and that an appropriate TRV measurement is not always feasible in some who do. It may not be possible to obtain an adequate Doppler signal from the tricuspid regurgitation curve in up to

40% of patients.<sup>8</sup> In this situation, an essential portion of the algorithm becomes absent and, if the other two parameters (E/e' and LAVI) are conflicting, the diastolic function becomes indeterminate, making it impossible to determinate the FP.

In the past decade, pioneering studies on LA deformation using the speckle tracking technique proposed that a decreased reserve function estimated by LAS measurement would be a subclinical DD marker.<sup>3</sup> Within this scope, Singh et al. evidenced the relationship between DD severity and LAS. The authors demonstrated that LAS has an inverse correlation with DD severity and the New York Heart Association functional class.<sup>5</sup> The best diagnostic performance seems to be achieved with a cutoff value of <19%, which separates grade III DD from the other grades.<sup>5</sup> A subsequent invasive study by the same group showed that an LAS < 20% is more accurate than the ASE/EACVI guideline algorithm for predicting a high FP.<sup>9</sup> This study, despite using a different group stratification method and not considering invasive hemodynamic data, also found an LAS cutoff value of <20% as a predictor of high FP.

It is worth mentioning that the definition of normal LAS values remains open since the LA reserve function is influenced by several factors, such as age, LV systolic function, one- or two-dimension LA image acquisition, and software version used. A meta-analysis by Pathan et al. reported that the mean normal LAS value was 39% with a minimum expected value of 27.6%.<sup>10</sup> In contrast, the NORRE study reported a mean normal LAS value of 42% with a minimum expected value of 26%.<sup>11</sup> Consequently, the definitive LAS cutoff value to be used as a high FP marker has not yet been fully defined.

LA remodeling and dysfunction secondary to an increased LV pressure is associated with more clinical symptoms, lower exercise capacity, and adverse clinical outcomes. Morris et al. demonstrated that LAS was a predictor of hospitalization and mortality in HF patients with a preserved EF, highlighting the potential clinical application of echocardiographic determination of atrial reserve function.<sup>12</sup> This study showed that LA reserve function may be decreased in indeterminate

**Table 2** - Main echocardiographic characteristics of the studied population.

Variable	n = 58
Percentage of two-dimensional EF	62 ± 6
Percentage of three-dimensional EF*	61 ± 8
LVDD, mm	48 ± 5
LV mass index, g/m <sup>2</sup>	88 ± 26
LAD, mm	34 ± 5
LAVI, mL/m <sup>2</sup>	28 ± 7
E wave, cm/s	78 ± 17
A wave, cm/s	80 ± 24
E/A ratio	1.0 ± 0.4
Mean e', cm/s	7.6 ± 2.6
E/e' ratio	12 ± 3
TRV, m/s	2.4 ± 0.4
Percentage of LV GLS†	-18.9 ± 1.9
Percentage of LAS in the reserve phase	26.2 ± 8.1

Results expressed as mean ± standard deviation. \*n = 27; †n = 44; A, mitral flow velocity at atrial contraction; E, early diastolic mitral inflow velocity; e', early diastolic mitral annular velocity; EF, ejection fraction; GLS, global longitudinal strain; LAD, left atrium dimension; LAS, left atrial strain; LAVI, left atrial volume index; LV, left ventricle; LVDD, left ventricular diastolic dimension; TRV, tricuspid regurgitation velocity.

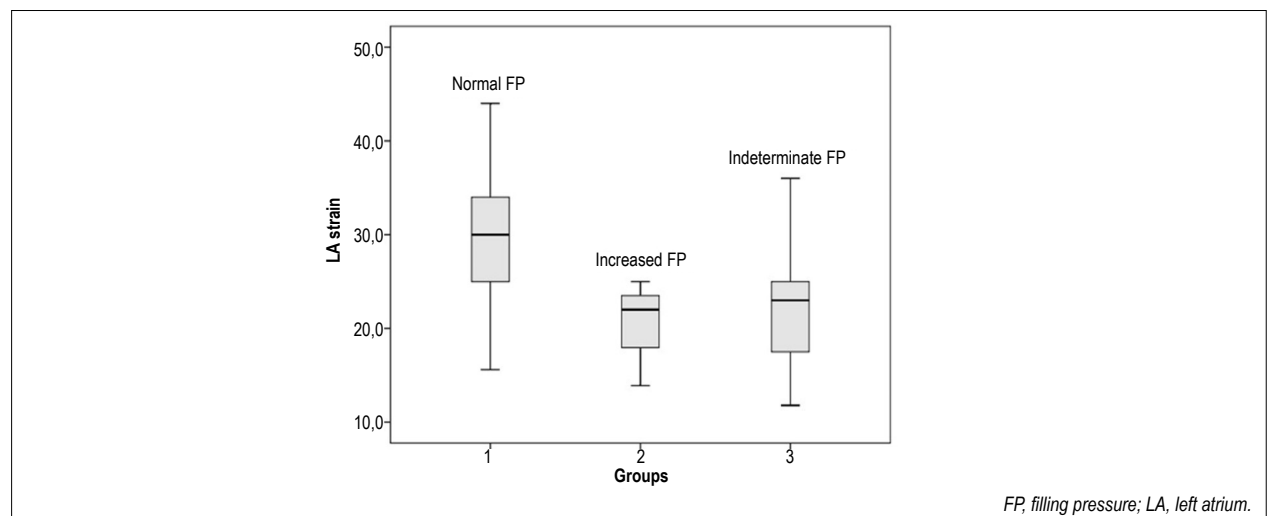


**Figure 2** – Intergroup comparison of the mean peak LA longitudinal strain.

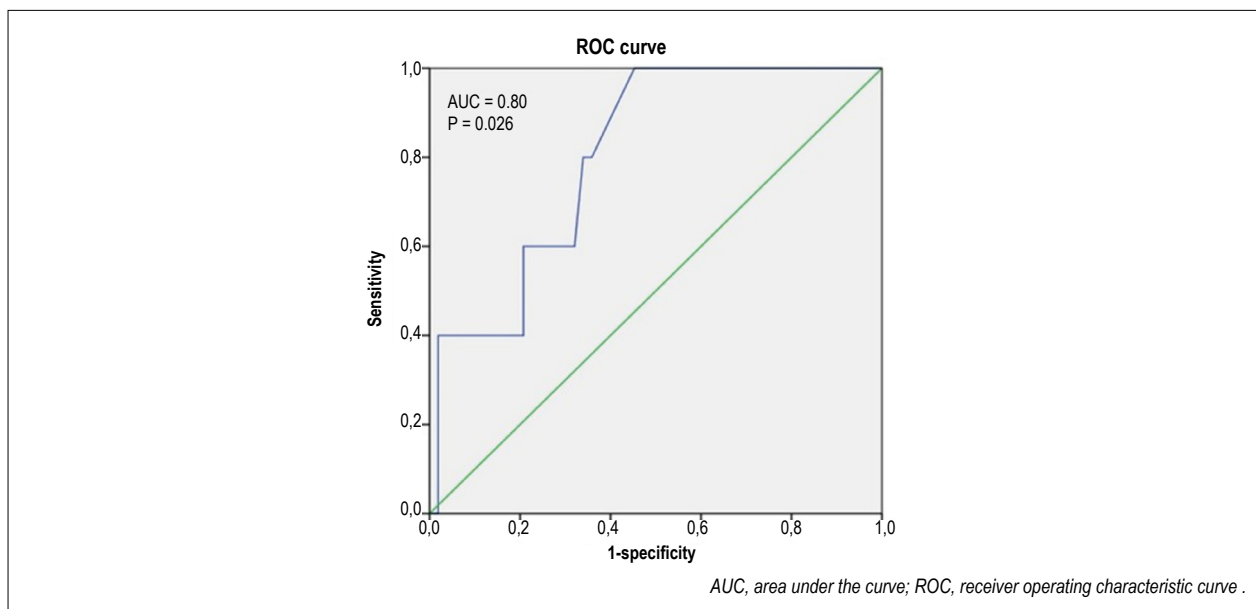


**Figure 3** – ROC of peak LA longitudinal strain used to detect high filling pressure.

diastolic function in a way similar to that found in patients with severe DD, which should make cardiologists establish more rigorous clinical follow-up for these patients.

This study has limitations that should be highlighted. First, it was a small study that included a select group of outpatients without arrhythmia, LV systolic dysfunction, heart valve disease, or pericardial disorders. Second, the presence of an increased FP was not confirmed through an invasive assessment. Third, the LAS cutoff values presented here cannot be generalized since different commercial brands of echocardiography machines present significantly varied estimates for the same patient. In addition, the semi-automatic software detection of myocardial deformation used in this study, originally designed for LV use, was adapted to assess the LA.

## Conclusion

These study findings suggest that the LA reserve function of patients with indeterminate diastolic function is similar to that of patients with severe DD. In practical terms, LAS shows great potential to improve the reclassification of indeterminate diastolic function cases obtained using

current algorithms. Larger-scale prospective studies are needed to validate normal LAS values in the general population and cutoff values indicative of increased LV diastolic pressure in populations with cardiovascular diseases before this technique becomes part of the clinical evaluation of DD. It seems reasonable to assume that LAS will be incorporated into future guidelines to decrease indeterminate diastolic function rates.

## Authors' contributions

Research creation and design: Barberato SH; Data acquisition: Barberato SH, Borsoi R; Data analysis and interpretation: Barberato SH, Borsoi R; Statistical analysis: Barberato SH; Obtaining financing: Barberato SH; Manuscript writing: Barberato SH; Critical revision of the manuscript for important intellectual content: Barberato SH, Borsoi R.

## Conflict of interest

The authors have declared that they have no conflict of interest.

## References

1. Fernandes-Silva MM, Barberato SH. O que o cardiologista espera do ecocardiograma na insuficiência cardíaca com fração de ejeção preservada? *Arq Bras Cardiol: Imagem Cardiovasc.* 2020;33(1):e0003.
2. Nagueh SF, Smiseth OA, Appleton CP, Byrd BF, Dokainish H, Edvardsen T, et al. Recommendations for the evaluation of left ventricular diastolic function by echocardiography: an update from the American Society of Echocardiography and the European Association of Cardiovascular Imaging. *J Am Soc Echocardiogr.* 2016;29(4):277-314.
3. Hortegal R, Abensur H. Como eu faço análise da função diastólica nos casos indeterminados pela Diretriz da American Society of Echocardiography 2016? *Arq Bras Cardiol: Imagem Cardiovasc.* 2020;33(3):ecom13.
4. Badano LP, Koliaas TJ, Muraru D, Abraham TP, Aurigemma G, Edvardsen T, D'Hooge J, Donal E, Fraser AG, Marwick T, Mertens L, Popescu BA, Sengupta PP, Lancellotti P, Thomas JD, Voigt JU; Industry representatives; Reviewers: This document was reviewed by members of the 2016–2018 EACVI Scientific Documents Committee. Standardization of left atrial, right ventricular, and right atrial deformation imaging using two-dimensional speckle tracking echocardiography: a consensus document of the EACVI/ASE/Industry Task Force to standardize deformation imaging. *Eur Heart J Cardiovasc Imaging.* 2018;19(6):591-600.
5. Singh A, Addetia K, Maffessanti F, Mor-Avi V, Lang RM. LA strain for categorization of LV diastolic dysfunction. *JACC Cardiovasc Imaging.* 2017;10(7):735-43.

6. Balaney B, Medvedofsky D, Mediratta A, Singh A, Ciszek B, Kruse E, et al. Invasive validation of the echocardiographic assessment of left ventricular filling pressures using the 2016 diastolic Guidelines: head-to-head comparison with the 2009 Guidelines. *J Am Soc Echocardiogr.* 2018;31(1):79-88.
7. Almeida JG, Fontes-Carvalho R, Sampaio F, Ribeiro J, Bettencourt P, Flachskampf FA, et al. Impact of the 2016 ASE/EACVI recommendations on the prevalence of diastolic dysfunction in the general population. *Eur Heart J Cardiovasc Imaging.* 2018;19(4):380-6.
8. Wang YC, Huang CH, Tu YK. Pulmonary hypertension and pulmonary artery acceleration time: a systematic review and meta-analysis. *J Am Soc Echocardiogr.* 2018;31(2):201-10.e3.
9. Singh A, Medvedofsky D, Mediratta A, Balaney B, Kruse E, Ciszek B, et al. Peak left atrial strain as a single measure for the non-invasive assessment of left ventricular filling pressures. *Int J Cardiovasc Imaging.* 2019;35(1):23-32.
10. Pathan F, D'Elia N, Nolan MT, Marwick TH, Negishi K. Normal ranges of left atrial strain by speckle-tracking echocardiography: a systematic review and meta-analysis. *J Am Soc Echocardiogr.* 2017;30(1):59-70.e8.
11. Sugimoto T, Robinet S, Dulgheru R, Bernard A, Ilardi F, Contu L, et al. Echocardiographic reference ranges for normal left atrial function parameters: results from the EACVI NORRE study. *Eur Heart J Cardiovasc Imaging.* 2018;19(6):630-8.
12. Morris DA, Belyavskiy E, Aravind-Kumar R, Kropf M, Frydas A, Braunauer K, et al. Potential Usefulness and Clinical Relevance of Adding Left Atrial Strain to Left Atrial Volume Index in the Detection of Left Ventricular Diastolic Dysfunction. *JACC Cardiovasc Imaging.* 2018;11(10):1405-15.

## Cardiac Amyloidosis: Infiltrative Cardiomyopathy with Restrictive Hemodynamic Behavior – Case Report

*Amiloidose Cardíaca: Cardiomiopatia Infiltrativa com Comportamento Hemodinâmico Restritivo – Relato de Caso*

José Leonardo Gomes Rocha Júnior<sup>1</sup>, Ivan Lucas Rocha Liberato<sup>1</sup>, Larissa Ferreira Lopes<sup>1</sup>, Letícia Maria Queiroz Rocha<sup>1</sup>, Christiane Bezerra Rocha Liberato<sup>2</sup>

Christus University Center,<sup>1</sup> Fortaleza, CE, Brazil; Walter Cantídio University Hospital, Federal University of Ceará,<sup>2</sup> Fortaleza, CE, Brazil.

### Abstract

Amyloidosis is a rare heterogeneous group of disorders that occur with the extracellular deposition of fibrillar protein aggregates in the tissues and organs. Here we report the case of a 76-year-old with a 2-month history of progressive dyspnea on minimal effort. In the investigation, a global cardiac increase was observed, and echocardiography showed infiltrative restrictive heart disease and a pericardial effusion. Cardiac magnetic resonance imaging findings were highly suggestive of cardiac amyloidosis. Thus, as reported here, cardiac involvement primarily manifests as restrictive cardiomyopathy, a chronic heart failure with a difficult-to-diagnose etiology in patients over 50 years of age and a very poor prognosis. Thus, although it remains a diagnostic challenge for clinicians, cardiac amyloidosis must always be considered in the absence of another cause of such findings.

### Introduction

Amyloidosis (AL) is a heterogeneous group of disorders that involve the extracellular deposition of fibrillar protein aggregates in the tissues and organs. A rare condition, it can manifest in an isolated or systemic way. Thus, these aggregates compromise target organ function and are responsible for clinical manifestations of the disease. From this perspective, in the cardiac context, protein deposits result in a series of disorders, such as heart failure (HF), arrhythmias, and angina syndromes. In addition, infiltration of the peripheral nerves induces symptomatic neuropathy, whereas deposits in the central nervous system can trigger dementia or, in the vascular context, cerebral hemorrhage.

Here we report a clinical case of a patient with infiltrative cardiomyopathy with restrictive hemodynamic behavior and characteristic echocardiography findings for which anatomopathological evaluation findings of the fibrillar protein aggregates were suggestive of AL.

### Case Report

A 76-year-old man from Fortaleza, CE, Brazil, presented with a main complaint of dyspnea on minimal effort

associated with fever and a productive cough with a greenish mucus secretion that had started in March 2019. He had been admitted to a referral university hospital 2 months after the onset of symptoms with no improvement. He also complained of oscillatory postural vertigo that had started 6 months prior and recently progressed to severe ambulation and a reduced quality of life. The patient had a previous pathological history of systemic arterial hypertension, diabetic neuropathy, and tonic-clonic seizure episodes. On physical examination, he appeared in good general condition and was acyanotic, anicteric, afebrile, hydrated, and pale (+ +/4+) with a systemic blood pressure of 110/60 mmHg, heart rate of 90 bpm, respiratory rate of 18/min, axillary temperature of 34.6°C, and macroglossia. Cardiac auscultation showed a regular double heart rhythm with normal sounds and no murmurs as well as the presence of a mild pericardial friction rub. Electrocardiography (ECG) showed low diffuse voltage with a first-degree atrioventricular block. Echocardiography (ECHO) showed significant ventricular concentric hypertrophy, biatrial enlargement, preserved systolic function (ejection fraction, 64%), grade II diastolic dysfunction (increased left atrial volume, 39 mL/m<sup>2</sup>; mitral flow E/A ratio, 0.64; mitral flow E-wave velocity, 79 cm/s; and mean mitral and tissue Doppler E/E', 29.39), a moderate pericardial effusion (PE), (Figure 1) and a reduced left ventricular global longitudinal strain of -8.2 (Figure 2). Chest magnetic resonance imaging (MRI) showed mediastinal lymphadenopathy and left ventricular myocardial thickening with circumferential subendocardial delayed enhancement and a pattern suggestive of cardiac AL. A cranial MRI showed areas of demyelination and left cerebellar hemisphere infarcts. In addition, his Mini-Mental State Examination score was 25 and gamma globulin, alpha-1, and alpha-2 peaks were found on protein electrophoresis. The patient underwent electroneuromyography, the findings of which were positive and showed nerve involvement, and transthyretin testing, a specific test for AL that evaluates peripheral neuromuscular involvement, findings of which were negative. The patient clinically progressed with stable vital signs, was oriented, was conscious, and was waiting for a medical opinion to better understand the cause.

### Keywords

Amyloidosis; Restrictive cardiomyopathy; Echocardiography.

Mailing Address: José Leonardo Gomes Rocha Júnior •

E-mail: leonardogomesrochajunior@gmail.com

Manuscript received 10/23/2020; revised 12/16/2020; accepted 1/27/2021

DOI: 10.47593/2675-312X/20213402eabc162

### Discussion

Cardiac AL is characterized by the extracellular deposition of insoluble fibrillar amyloid  $\beta$ -protein in the heart. It can be part of a systemic disease, which is more common, or a localized phenomenon.<sup>1</sup> Its clinical presentation varies according to the affected organs and the importance of their involvement. Less than 5% of patients with light-chain



## Case Report

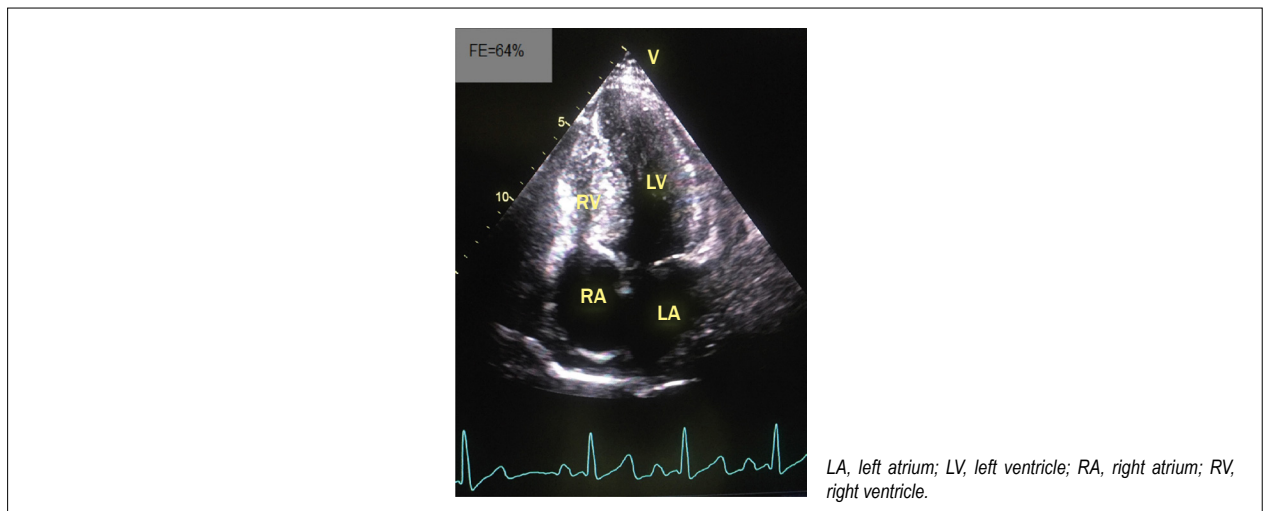


**Figure 1** – Echocardiogram showing significant ventricular concentric hypertrophy, biatrial enlargement, preserved systolic function, and a moderate pericardial effusion.

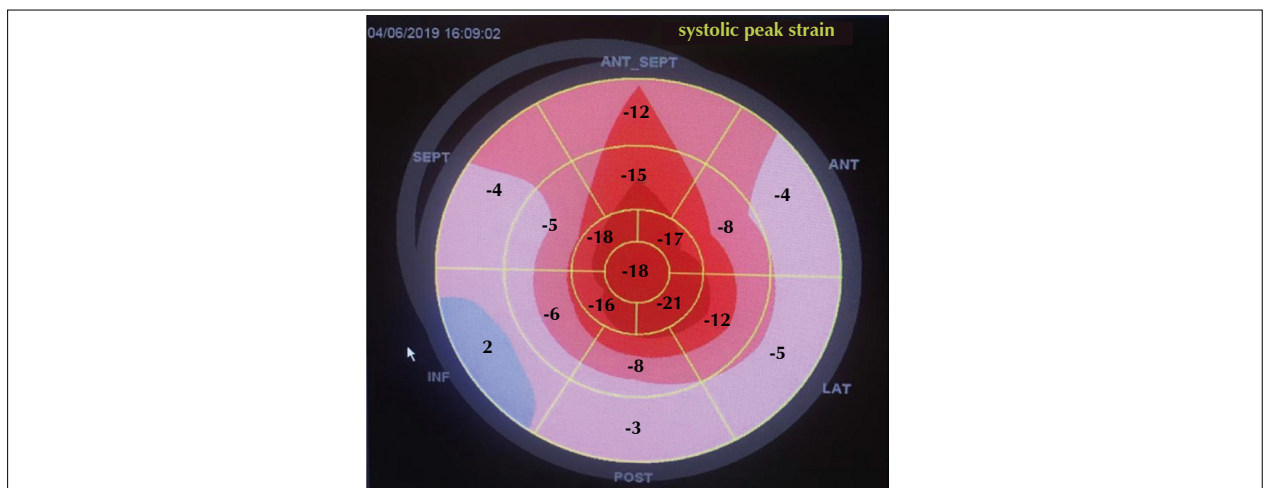


**Figure 2** – Reduced left ventricular global longitudinal strain of -8.2 with involvement of the basal and median regions of the heart and apical sparing.

AL involving the heart have clinically isolated heart disease. Non-cardiac symptom complaints should be investigated because their presence is a clue to the systemic nature of the disease. Each patient should be carefully questioned about dizziness and syncope with emphasis placed on the positional nature of any of these symptoms since there are several potential syncope mechanisms in AL. As in the reported case, macroglossia, which is characterized by tongue stiffness and enlargement and often associated with dental indentation, is seen in about 10–20% of patients and can result in dysphonia or dysgeusia. Neurological symptoms include carpal tunnel syndrome and peripheral and autonomic neuropathy.<sup>2</sup>

The cardiac form is heterogeneous, with amyloid deposition in the myocardium, interatrial septum, cardiac valves, papillary muscles, and coronary arteries. Cardiac involvement can lead to diastolic dysfunction or, in the later course of the disease, systolic dysfunction and HF symptoms with conduction disorders, low cardiac output, autonomic dysfunction, PE, and

arrhythmias such as atrial fibrillation, ventricular tachycardia, or ventricular fibrillation.<sup>3</sup> Its main cardiac presentation is restrictive cardiomyopathy, an intractable chronic HF of unknown etiology in patients over 50 years of age.

At least 30 different proteins have been identified to date,<sup>4</sup> with the most common being AL, serum amyloid A protein, and transthyretin AL (ATTR). Cardiac AL is more commonly caused by the ATTR and AL forms. Thus, despite their heterogeneous structure and function, these proteins deposit in the amyloid form in several organs in a localized or systemic manner, which may cause multiorgan dysfunction.

As a pathology with a nonspecific clinical presentation, cardiac AL is usually diagnosed late after being frequently ignored or confused with other pathologies. From this perspective, AL complementary exams play an important role in the characterization of the case and the patient's respective prognosis. Some noninvasive tests may provide



## Case Report

the ventricular circumference. Thus, MRI can identify the presence of myocardial and interatrial septum thickening, diastolic dysfunction signs, and the typical subendocardial delayed enhancement pattern in the left ventricle, which may affect all of the cardiac chambers. Amyloid tissue changes the pattern of delayed myocardial enhancement after gadolinium use.<sup>8</sup> Such changes were observed in this case. (Figure 5)

Scintigraphy detects cardiac transthyretin accumulation. It is an extremely useful method for distinguishing between AL and ATTR since there is selective cardiac technetium uptake in this disorder but not in AL. If scintigraphy detects transthyretin accumulation, the investigation can be complemented with genetic transthyretin testing to distinguish ATTR (mutant transthyretin) from senile amyloidosis (wild-type transthyretin).

The definitive diagnosis is made by endomyocardial biopsy, which allows the histological characterization of the amyloid substance considering specific Congo red or immunohistochemical staining under polarized light microscopy.

Systemic AL treatment includes the support of organic dysfunction and the treatment of associated clinical conditions, particularly inflammatory processes, to avoid the formation of new amyloid fibril precursors and provide a specific treatment to remove existing amyloid deposits. The main objectives are treating the underlying disease and relieving the symptoms, and the treatment must be coordinated by a multidisciplinary team.

In recent years, the first-line options for controlling amyloid deposits have been chemotherapy and immunomodulation, especially melphalan, dimethyl sulfoxide, colchicine, and corticosteroids.<sup>3</sup>

Cardiac involvement support includes blood volume management, a fundamental decompensation factor, with sodium restriction and the careful administration of diuretics; and ventricular arrhythmia management, usually with amiodarone and the careful use of some drugs, including digoxin, due to their specific binding to amyloid fibrils and high toxicity despite normal serum levels. Other general supportive measures include the use of gabapentin to manage neuropathic pain and the control of possible comorbidities and complications.<sup>6</sup>

Cardiac AL remains a clinical challenge. Patients with AL and congestive HF have a worse prognosis and a mean survival of 6–9 months. AL awareness and understanding is important for cardiologists and clinicians since an early diagnosis is associated with increased patient survival rates.

Cardiac AL results in a wide range of changes in which cardiac involvement imposes a worse prognosis and the development of an infiltrative cardiomyopathy with restrictive hemodynamic behavior. In cases of rare pathology, the diagnosis requires a high index of suspicion based on clinical and complementary noninvasive exams, especially transthoracic ECHO and cardiac MRI. The final diagnosis always requires histological confirmation. The intervention focuses on treating the underlying disease and relieving the patient's symptoms. This scenario emphasizes the importance of investigating cardiac AL among HF diagnostic possibilities with unfavorable chronic progression and an unknown etiology, especially in patients over 50 years of age.

Therefore, cardiac AL requires an early diagnosis due to the possibility of an unfavorable clinical progression with an important degree of cardiac restriction and congestive HF. At this point, patient prognosis is poor with a low chance of recovery.<sup>1</sup> Furthermore, it is important to note that AL usually involves other organs and systems, and its diagnosis is also important to treating other areas early, such as the nervous system as in the case reported here, which involve neurological clinical signs and changes on exams such as electroneuromyography.

### Authors' contributions

Manuscript writing: Lopes LF; data collection: Liberato ILR; critical review of the manuscript for important intellectual content: Rocha Júnior LG; manuscript reading and reviewing: Rocha LMQ; and study supervision: Liberato CBR.

### Conflict of interest

The authors have declared that they have no conflict of interest.

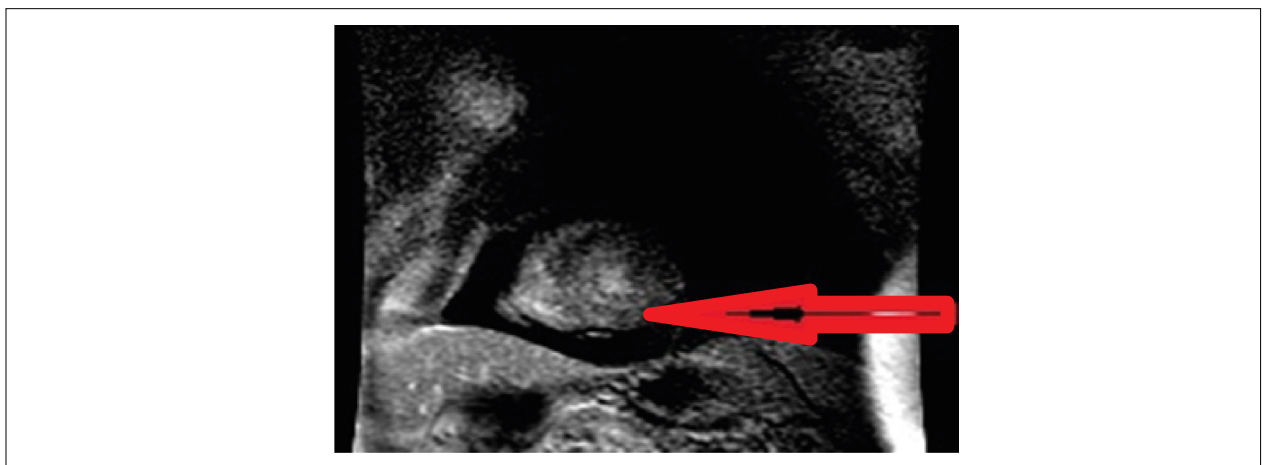


**Figure 5** – Cross-sectional chest magnetic resonance image showing circumferential subendocardial delayed enhancement.



## References

1. Mendes RG, Evora PR, Mendes JA, Haddad J, Carvalho A. Comprometimento cardíaco na amiloidose sistêmica. Diagnóstico in vivo. *Arq Bras Cardiol*, 1998;70(2):119-23.
2. Falk RH. Diagnosis and management of the cardiac amyloidoses. *Circulation*. 2005;112(13):2047-60. doi: 10.1161/CIRCULATIONAHA.104.489187
3. Di Bella G, Pizzino F, Minutoli F, Zito C, Donato R, Dattilo G, et al. The mosaic of the cardiac amyloidosis diagnosis: role of imaging in subtypes and stages of the disease. *Eur Heart J Cardiovasc Imaging*. 2014;15(12):1307-15. doi: 10.1093/ehjci/jeu158
4. Seldin DC, Sanchorawala V. Adapting to AL amyloidosis. *Haematologica*. 2006;91(12):1591-5
5. Selvanayagam JB, Hawkins PN, Paul B, Myerson SG, Neubauer S. Evaluation and management of the cardiac amyloidosis. *J Am Coll Cardiol*. 2007 Nov 27;50(22):2101-10. doi: 10.1016/j.jacc.2007.08.028. Epub 2007 Nov 13. Erratum in: *J Am Coll Cardiol*. 2011 Mar 29;57(13):1501.
6. Vieira TA, Negreiros SB, Sousa DW, Garbero RF, Capanema CO. Amiloidose cardíaca: protótipo de miocardiopatia restritiva e disfunção diastólica – relato de caso. *Arq Bras Cardiol: Imagem Cardiovasc*. 2017;30(1):13-7.
7. Al-Zahrani GB, Bellavia D, Pellikka PA, Dispenzieri A, Hayman SR, Oh JK, et al. Doppler myocardial imaging compared to standard two-dimensional and Doppler echocardiography for assessment of diastolic function in patients with systemic amyloidosis. *J Am Soc Echocardiogr*. 2009 Mar;22(3):290-8. doi: 10.1016/j.echo.2008.11.013
8. Lakdawala Neal K. Miocardiopatia e miocardite. In: Kasper D. *Medicina interna de Harisson*. 19. ed. Porto Alegre: Amgh; 2017. Cap. 287. p. 1566-1568.
9. Selvanayagam JB, Hawkins PN, Paul B, Myerson SG, Neubauer S. Evaluation and management of the cardiac amyloidosis. *J Am Coll Cardiol*. 2007;50(22):2101-10. doi: 10.1016/j.jacc.2007.08.028. Erratum in: *J Am Coll Cardiol*. 2011;57(13):1501.

## Amplatzer™ Prosthesis Embolization After Percutaneous Atrial Septal Defect Closure: A Case Report

*Embolização de Prótese de Amplatzer™ após Fechamento Percutâneo de Comunicação Interatrial: Relato de Caso*

Raul Serra Valério<sup>1</sup>, Alfredo Augusto Eyer Rodrigues<sup>1,2</sup>, Artur José da Silva Raoul<sup>1</sup>, Marly Maria Uellendahl<sup>1,2</sup>, Carlos Eduardo Suaide Silva<sup>1</sup>, Luciana Braz Peixoto<sup>1</sup>

<sup>1</sup>Dasa, São Paulo, SP, Brazil; <sup>2</sup>Federal University of São Paulo, São Paulo, SP, Brazil.

### Introduction

Atrial septal defect (ASD) is the most common congenital heart disease in adults; in specific cases, it has indications for treatment. The percutaneous approach has been highlighted as a less invasive method to close this defect, specifically in cases of ostium secundum ASD; however, it can have complications as described in the following report.

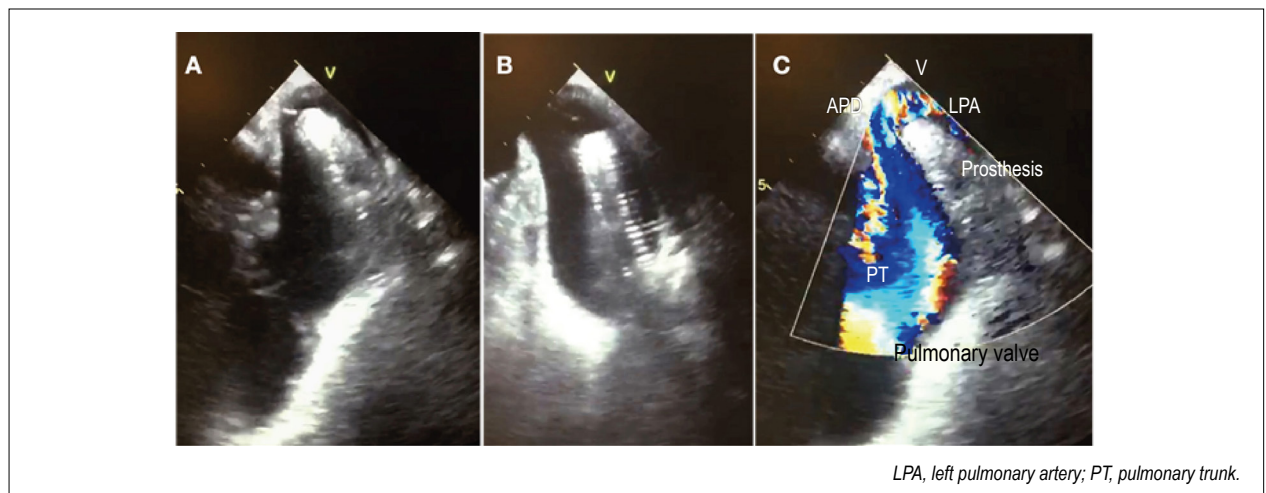
### Clinical case

A 44-year-old man with a history of undergoing percutaneous ASD closure using an Amplatzer™ prosthesis 2 years prior underwent transesophageal echocardiography (TEE). He remained symptomatic after the procedure but did not undergo complementary imaging tests during this period.

TEE revealed right chamber dilation, a large ostium secundum ASD measuring 26 mm, and transeptal flow from

the left to the right atria. The Amplatzer™ prosthesis moved to the pulmonary artery trunk just after the pulmonary valve close to the bifurcation, where it was firmly adhered by one of the edges to the lateral wall of the vessel. Color Doppler showed turbulent flow in the pulmonary trunk (Figure 1, Video 1).

The patient underwent computed tomography angiography, which confirmed the presence of an ASD measuring 44 mm × 28 mm, right chamber dilation, and the pulmonary artery trunk showing an image compatible with the Amplatzer™ prosthesis in the pulmonary artery near the bifurcation of right and left branches with no signs of filling failure in the pulmonary branches (Figure 2). The patient underwent conventional surgical correction consisting of a median sternotomy, ASD closure, and prosthesis removal from the pulmonary trunk (Figure 3). The patient's condition progressed with decreased pulmonary pressure, decreased sizes of the right chambers, and significant symptom improvement.



LPA, left pulmonary artery; PT, pulmonary trunk.

**Figure 1** – Transesophageal echocardiography images showing an Amplatzer™ prosthesis displaced to the pulmonary artery trunk (A and B). Color Doppler image showing turbulent flow in the pulmonary artery trunk (C).

### Keywords

Heart septal defects, atrial; Septal occluder device.

**Mailing Address:** Marly M. Uellendahl •

Rua Joaquim Nabuco, 1560, Brooklyn Paulista

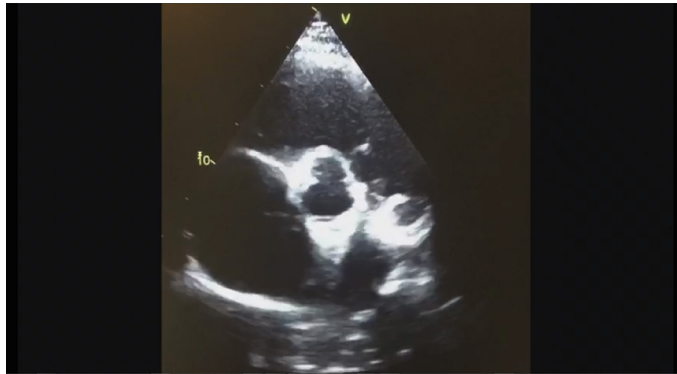
CEP: 04621-005, SP, Brazil. E-mail: mauellendahl@gmail.com

Manuscript received 7/31/2020; revised 8/1/2020; accepted 11/27/2020

**DOI:** 10.47593/2675-312X/20213402eabc135



## Case Report



Video 1 – Echocardiography showing occluder prosthesis displacement.

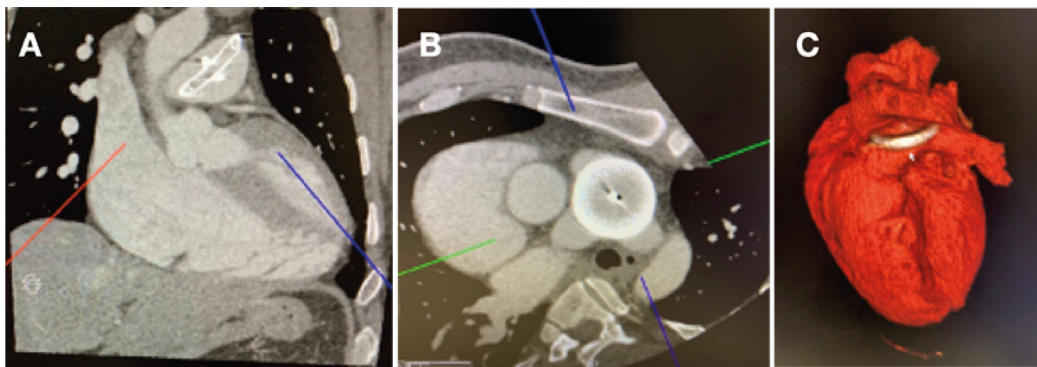


Figure 2 – Tomography images of planar (A and B) and three-dimensional (C) reconstruction showing an Amplatzer™ prosthesis in the pulmonary artery trunk.

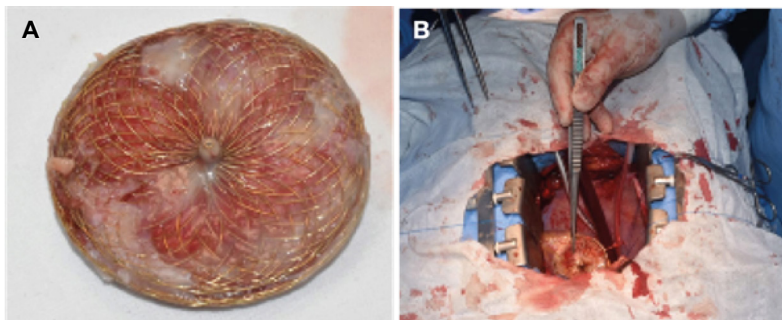


Figure 3 – Image of the Amplatzer™ prosthesis after open surgical extraction (A); and the Amplatzer™ prosthesis being removed from the pulmonary artery trunk (B).

## Discussion

The incidence of ASD in the literature is 3.78 per 10,000 births, corresponding to 5–9% of all cases of congenital heart malformation<sup>1,2</sup>. However, ASD is the most prevalent congenital heart disease in adults (reportedly involving up to 25% of cases), predominant in women, and classified into four types (ostium secundum [50–70%], ostium primum [30%], venous sinus [5–10%], and coronary sinus [3% – extremely rare]). Only ostium secundum ASD is considered an atrial defect itself<sup>2,3</sup>.

The percutaneous closure of ASD using the Amplatzer™ device is currently a therapeutic option fully established in the treatment of ostium secundum ASD in patients who meet the anatomical criteria<sup>2,3</sup>. The increased number of percutaneous prosthesis implants has increased possible complications. The main complication is device embolism during implantation with the risk of displacement, embolization, and incorrect placement of 0.5–1%<sup>1,2,4,5</sup>. Almost all cases of prosthesis embolization require surgical intervention<sup>3,5</sup>. It was not

possible to identify when the device migrated in the reported case, but there are reports of migration immediately after and up to 10 years after the implantation. The great adherence of the prosthesis to the pulmonary trunk and the absence of signs on the ASD edges indicate migration soon after the implantation in addition to the patient's report that his symptoms never resolved.

Percutaneous ASD treatment with the Amplatzer™ prosthesis may be the best option for most adult ASD cases requiring treatment (with signs of hemodynamic repercussion) since it presents a low rate of complications. However, prosthesis embolization is a severe complication with a high mortality rate that often requires surgical intervention. The cause of prosthesis displacement is ambiguous, but insufficient edges for device fixation can be a factor; thus, it is important to correctly select appropriate candidates for the

procedure. Since the authors did not know this patient prior to the procedure, it was impossible to specify the cause of the embolization in this case. Fortunately, this severe complication was successfully resolved after surgery.

### Authors' contributions

Research creation and design: Valerio, RS; Peixoto LB; Uellendahl, MM. Manuscript writing: Valerio, RS; Peixoto LB; Uellendahl, MM; Critical revision of the manuscript for important intellectual content: Rodrigues, AAE; Peixoto LB; Uellendahl, MM; Silva, CES; Raoul, AJS.

### Conflict of interest

The authors have declared that they have no conflict of interest.

### References

1. Chessa M, Carminati M, Butera C, Bini RM, Drago M, Rosti L, et al. Early and late complications associated with transcatheter occlusion of secundum atrial septal defect. *J Am Coll Cardiol*. 2002;39(6):1061-5. doi: 10.1016/s0735-1097(02)01711-4
2. Cardoso CO, Rossi Filho RI, Machado PR, François LM, Horowitz ES, Sarmiento-Leite R. Efetividade da prótese de Amplatzer® para fechamento percutâneo. *Arq Bras Cardiol*. 2007;88(4):384-9. doi: <https://doi.org/10.1590/S0066-782X2007000400003>
3. Martins GF, Jessen B, Cavalcanti CR. Embolização da prótese de amplatzer® após fechamento percutâneo de comunicação interatrial. *Rev Bras Cardiol*. 2012[citado 2021 Mar 8];25(6):498-500. Disponível em: <http://www.onlineijcs.org/english/sumario/25/pdf/v25n6a09.pdf>
4. Nath RK, Pandit N. Asymptomatic late embolization of Amplatzer septal occluder device. *Indian Heart J*. 2017;69(3):338-40. doi: <http://dx.doi.org/10.1016/j.ihj.2016.12.013>
5. Son JW, Park JS. Subacute, silent embolization of amplatzer atrial septal defect closure device to the pulmonary artery. *J Cardiovasc Ultrasound*. 2012;20(4):201-4. doi: <http://dx.doi.org/10.4250/jcu.2012.20.4.201>

# Left Ventricular Pseudoaneurysm in a Diabetic Patient without Clinical Acute Coronary Syndrome

*Pseudoaneurisma Ventricular Esquerdo em Paciente Diabético sem Clínica de Síndrome Coronariana Aguda*

Alice Mirane Malta Carrijo<sup>1</sup>, Marcela Gomes de Souza<sup>1</sup>, Marina Vitória Silva Costa<sup>1</sup>, João Lucas O'Connell<sup>1</sup>

<sup>1</sup>Federal University of Uberlândia, Uberlândia, MG, Brazil

## Introduction

Left ventricular (LV) pseudoaneurysm consists of a free wall rupture contained by the adjacent pericardium.<sup>1</sup> It is a severe pathology with high morbidity and mortality and usually a complication of acute myocardial infarction (AMI).<sup>2</sup> Its clinical status may be nonspecific; in some situations, the patient is asymptomatic, which may hinder the diagnosis.<sup>1-3</sup> Surgical correction is the treatment of choice due to the high risk of rupture and cardiac tamponade.<sup>3,4</sup>

This is a case report of an asymptomatic diabetes mellitus (DM) patient with a previous history of kidney transplantation and immunosuppression who had an incidental diagnosis of LV pseudoaneurysm.

## Case report

A Brazilian 55-year-old man with hypertension and hypothyroidism had a 25-year history of DM (on insulin therapy for the past 5 years) and chronic stage IV renal failure and had undergone a renal transplant using immunosuppressants 3 years prior. He was admitted with diabetic foot and underwent antibiotic therapy and amputation of the third right toe. The patient denied other symptoms. During the hospitalization, he underwent echocardiography (transthoracic and, due to the changes found, transesophageal), which evidenced left cavity diameters at the upper limit of normal, preserved left ventricular function (left atrium, 40 mm; LV, 56 mm; ejection fraction, 56%), and significant hypokinesia in the middle and basal segments of the lower wall. Inferolateral wall akinesia was also identified associated with myocardial discontinuity and a saccular bulge with a thrombus inside, which communicated with the LV (flow detected on Doppler) and was quite suggestive of LV pseudoaneurysm. The pseudoaneurysm measured 1.7 cm at the neck and had an internal anteroposterior diameter of 3 cm, laterolateral diameter of 3.7 cm, and longitudinal diameter of 4 cm (Figure 1).

Cine computed tomography angiography revealed 30% proximal and 70% middle third stenoses in the right posterior ventricular (RPV) branch of the right coronary artery (Figure 2) but no other significant stenosis. Left

ventriculography was not performed due to risks related to the already established diagnosis of ventricular pseudoaneurysm associated with the thrombi.

The patient underwent LV reconstruction surgery with closure of the free wall rupture and implantation of bovine pericardium patch. No complications occurred. Myocardial revascularization was not performed due to distal bed inadequacy in the RPV branch. Intraoperative transesophageal echocardiography and a Doppler examination showed correction of the ventricular discontinuity. The patient remained asymptomatic in the postoperative period and was discharged from the hospital 5 days after the surgery.

## Discussion

LV pseudoaneurysm forms when a cardiac wall rupture is blocked by adherent pericardium or scar tissue without containing endocardium or myocardium.<sup>1</sup> Due to the inflammatory and prothrombotic condition, a hematoma looking like an aneurysm forms.<sup>5</sup> This is usually a mechanical complication after classic AMI<sup>2</sup> that occurs within 5–7 days after the event when the infarcted necrotic tissue is friable, making the ventricular wall significantly fragile.<sup>6</sup>

Due to greater ventricular wall thinning in its lower portion, infarcts in this region versus the anterior wall are associated with a greater chance of pseudoaneurysm.<sup>7</sup> Some important risk factors for false aneurysm include: female sex; older age; hypertension; first AMI; transmural AMI; absence of thrombolysis, late thrombolysis; chemical thrombolysis (versus mechanical); absence of collateral circulation; and the use of corticoids, immunosuppressants, or other drugs.<sup>2</sup> The mean age at presentation is 60 years, and most patients are Caucasian.<sup>1</sup> Conditions other than AMI (cardiac surgery, chest trauma, tumor invasion, and infection) may also result in LV pseudoaneurysm.<sup>1,5,8</sup>

LV pseudoaneurysm develops in less than 0.1% of AMI<sup>8,9</sup> patients; due to its greater tendency to rupture (30–45% of untreated patients),<sup>8</sup> cardiac tamponade, shock, and death,<sup>1,3</sup> it is considered an urgent condition that requires immediate treatment.<sup>4</sup> In contrast, a true aneurysm results from cardiac wall weakening involves maintained layer integrity (endocardium, myocardium, epicardium, and pericardium) and does not require an urgent or even interventionist approach.<sup>2,7</sup>

Dyskinetic movement of the heart can result in heart failure, and the infarcted area can cause arrhythmias and form clots that can embolize.<sup>7</sup> A false LV aneurysm usually has symptoms such as chest pain, dyspnea, and hypotension.<sup>9</sup> However, more than 10% of cases may be asymptomatic and incidentally

## Keywords

Aneurysm, false; Diabetes mellitus; Echocardiography.

**Mailing Address:** João Lucas O'Connell •

Rua da Carioca, 2.005, casa 852. Morada da Colina. CEP: 38411-151. Uberlândia, MG, Brazil. E-mail: oconnelljl@me.com

Manuscript received 8/3/2020; revised 9/3/2020; accepted 10/10/2020

DOI: 10.47593/2675-312X/20213402eabc136



## Case Report

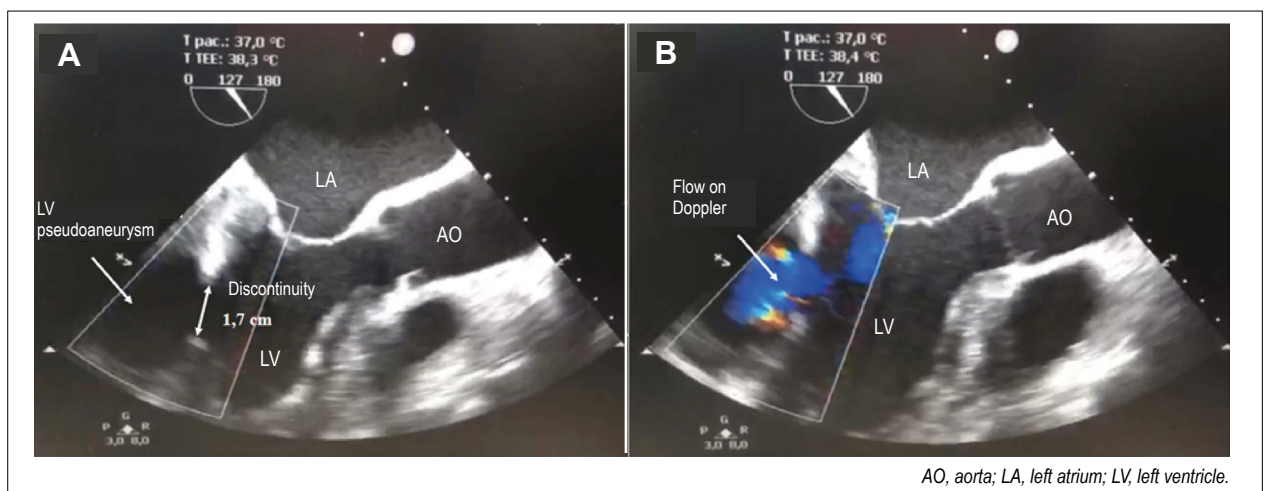


**Figure 1** – Transesophageal echocardiogram revealing a longitudinal median esophageal cut. (A) Left ventricle inferolateral wall discontinuity measuring 1.7 cm in this projection. (B) Color Doppler image in the same projection showing flow (in blue) toward the pseudoaneurysm.

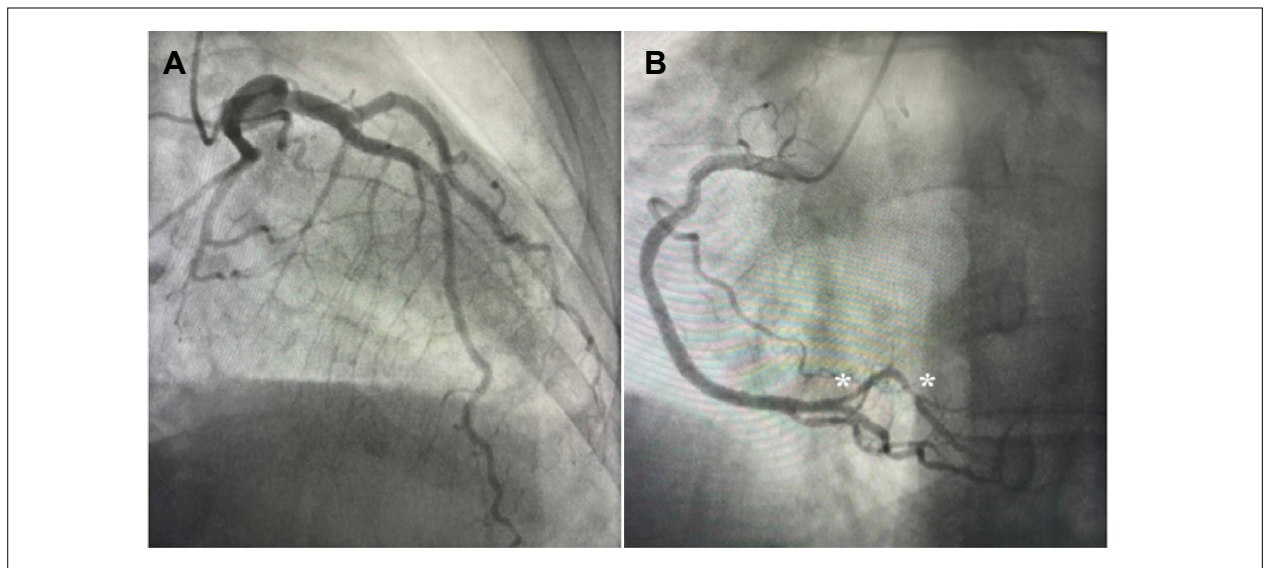


**Figure 2** – Coronary computed tomography angiogram. (A) Left view shows no significant obstructive coronary artery disease. (B) Right view shows significant stenosis in the middle-distal segment of the right posterior ventricular branch.

diagnosed.<sup>1,4,9</sup> In such cases, the patients are diagnosed in the chronic phase since pseudoaneurysm can progress for years without rupturing. Nevertheless, a significant proportion of patients will not have their diagnosis established in the acute phase due to early and fatal rupture.<sup>10</sup>

An incidental detection on angiography or transthoracic echocardiography is common due to the greater availability and routine use of this exam during the initial evaluation of patients with chest pain, murmur, and heart failure.<sup>4</sup> LV angiography is the method of choice since it can show the narrow orifice that leads to a sacular structure in addition to the absence of coronary arteries around it. Left ventriculography has a diagnostic acuity of 85% despite the real risk of embolizing any thrombotic material present. On the other hand, transthoracic

echocardiography can show the endocardial discontinuity, the connection of the LV turbulent systolic flow to the aneurysmal sac, and a ratio between the size of the orifice and the diameter of the pseudoaneurysm greater than 0.5.<sup>7</sup>

Computed tomography and cardiac magnetic resonance imaging (CMRI) can also be used for diagnosis. In practice, these methods can further detail the characteristics of the discontinuity. For instance, CMRI can show the absence of endocardium and myocardium near the aneurysm in addition to effectively assessing myocardial function, contractility, tissue perfusion, and turbulent blood flow in the cardiac chambers through a false aneurysm.<sup>1,2,5,9</sup>

DM patients, as described in this case report, are at significant risk of developing coronary artery disease and have

a higher incidence of silent AMI.<sup>12</sup> Renal failure and the use of immunosuppressive drugs after kidney transplantation are risk factors for the development of ischemic heart disease and the occurrence of ventricular rupture after infarction.<sup>13</sup>

Surgery is the most appropriate treatment for pseudoaneurysm due to the possibility of its removal and the restoration of LV morphology.<sup>14</sup> Due to its high tendency to rupture (30–45%) and the risk of sudden death, surgical treatment should be recommended and performed as early as possible.<sup>2</sup> The mortality rate of cases treated surgically is lower than of cases treated clinically (23% versus 48%).<sup>7</sup>

The medical team considered the patient's clinical condition and the pseudoaneurysm's morphological characteristics and chose surgical correction. After the surgery and discontinuity correction, the patient became asymptomatic and stable and was discharged from the hospital after 5 days.

LV pseudoaneurysm is a rare condition that usually occurs after AMI and has a high mortality rate when not accurately diagnosed and treated. It requires immediate treatment due to the possibility of rupture. Knowledge of all diagnostic methods and treatment

strategies for LV pseudoaneurysm is extremely important to ensuring its appropriate management and decreasing its high morbidity and mortality rates. The present report also reinforces the importance of a good preoperative evaluation that considers all risk factors for the development of ischemic heart disease and stabilizes the patient before major surgeries.

### Authors' contributions

Research conception and design: Carrijo AMM, Souza MG, and Costa MVS; data collection: Carrijo AMM, Souza MG, and Costa MVS; data analysis and interpretation: Carrijo AMM, Souza MG, Costa MVS, and O'Connell JL; manuscript writing: Carrijo AMM, Souza MG, Costa MVS, and O'Connell JL; and critical review of the manuscript for important intellectual content: O'Connell JL.

### Conflict of interest

The authors have declared that they have no conflict of interest.

### References

1. Frances C, Romero A, Grady D. Left ventricular pseudoaneurysm. *J Am Coll Cardiol.* 1998;32(3):557-61. doi: 10.1016/s0735-1097(98)00290-3
2. Bhardwaj R, Sondhi S, Mehta A. Unruptured giant left ventricular pseudoaneurysm after silent myocardial infarction. *BMJ Case Rep.* 2018;2018:bcr2018225812. doi: 10.1136/bcr-2018-225812
3. Meng X, Yang YK, Yang KQ, Zhang Y, Lu PP, Fan P, et al. Clinical characteristics and outcomes of left ventricular pseudoaneurysm: A retrospective study in a single-center of China. *Medicine (Baltimore).* 2017;96(18):e6793. doi: 10.1097/MD.0000000000006793
4. Hulten EA, Blankstein R. Pseudoaneurysms of the heart. *Circulation.* 2012;125(15):1920-5. doi: 10.1161/CIRCULATIONAHA.111.043984
5. Garcia-Guimaraes M, Velasco-Garcia-de-Sierra C, Estevez-Cid F, Perez-Cebey L, Bouzas-Mosquera A, Mendez-Eirin E, et al. Current role of cardiac imaging to guide surgical correction of a giant left ventricular pseudoaneurysm. *Int J Cardiol.* 2015;198:152-3. doi: 10.1016/j.ijcard.2015.06.129
6. Bonow RO, Mann D, Zipes D, Libby P, Braunwald E. Braunwald's heart disease: a textbook of cardiovascular medicine. 9th ed. Philadelphia: Elsevier; 2012.
7. Bisoyi S, Dash AK, Nayak D, Sahoo S, Mohapatra R. Left ventricular pseudoaneurysm versus aneurysm a diagnosis dilemma. *Ann Card Anaesth.* 2016;19(1):169-72. doi: 10.4103/0971-9784.173042.
8. Hoey DR, Kravitz J, Vanderbeek PB, Kelly JJ. Left ventricular pseudoaneurysm causing myocardial infarction and cerebrovascular accident. *J Emerg Med.* 2005;28(4):431-5. doi: 10.1016/j.jemermed.2004.12.013.
9. Alapati L, Chitwood WR, Cahill J, Mehra S, Movahed A. Left ventricular pseudoaneurysm: A case report and review of the literature. *World J Clin Cases.* 2014;2(4):90-3. doi: 10.12998/wjcc.v2.i4.90.
10. Jacob JL, Buzelli C, Machado NC, Garzon PG, Garzon SA. Pseudoaneurysm of left ventricle. *Arq Bras Cardiol.* 2007;89(1):e1-2. doi: 10.1590/s0066-782x2007001300012.
11. Oliveira SM, Dias P, Pinho T, Gavina C, Almeida PB, Madureira AJ, et al. Giant left ventricular pseudoaneurysm: the diagnostic contribution of different non-invasive imaging modalities. *Rev Port Cardiol.* 2012;31(6):439-44. doi: 10.1016/j.repc.2012.04.009.
12. Draman MS, Thabit H, Kiernan TJ, O'Neill J, Sreenan S, McDermott JH. A silent myocardial infarction in the diabetes outpatient clinic: case report and review of the literature. *Endocrinol Diabetes Metab Case Rep.* 2013;2013:130058. doi: 10.1530/EDM-13-0058.
13. Chakkeria HA, Sharif A, Kaplan B. Negative Cardiovascular Consequences of Small Molecule Immunosuppressants. *Clin Pharmacol Ther.* 2017;102(2):269-276. doi: 10.1002/cpt.738.
14. Brown KN, Singh R. Transcatheter management of left ventricular pseudoaneurysms. *Treasure Island.* 2019;18.

# Mucopolysaccharidoses IV and VI: Aspects in Two-dimensional Speckle-tracking Strain Echocardiogram Imaging in a Case Series

*Mucopolissacaridoses IV e VI: Aspectos ao Ecocardiograma Bidimensional com Strain pelo Speckle Tracking em uma Série de Casos*

João Vitor Tiveron Teodoro<sup>1</sup>, Lavínia Ayumi Borges Ribeiro<sup>1</sup>, José Marques Ferreira Neto<sup>1</sup>, Vinícius Marques Ferreira<sup>1</sup>, Carlos Henrique Paiva Grangeiro<sup>1,2</sup>, Adriana de Nazaré Miziara Oliveira<sup>1</sup>

<sup>1</sup>Triângulo Mineiro Federal University, Uberaba, MG, Brazil; <sup>2</sup>Hospital Complex of the Federal University of Ceará, Fortaleza, CE, Brazil.

## Introduction

Mucopolysaccharidosis (MPS) belongs to the group of lysosomal storage diseases associated with the partial or total deficiency of 11 different lysosomal hydrolases responsible for glycosaminoglycan (GAG) degradation<sup>1</sup>. GAG accumulation may affect the valves, myocardium, and coronary vessels. The forms that accumulate dermatan sulfate (MPS I, II, VI, and VII) are associated with valvular thickening (L > R). MPS is one of the most common causes of mitral annulus thickening in children. Cardiac involvement also includes hypertrophy, tendinous cord shortening, and papillary muscle thickening<sup>2</sup>. Echocardiography is an essential technique used to assess cardiac involvement in MPS. The study of myocardial strain using two-dimensional speckle-tracking echocardiography (2D-STE) provides a more sensitive evaluation of myocardial fiber strain that can reveal early and subclinical myocardial involvement regardless of left ventricular ejection fraction (LVEF) changes<sup>3,4</sup>.

This case series reviews relevant echocardiographic aspects of cardiac involvement complemented by 2D-STE in three patients with MPS during outpatient follow-up and taking enzyme replacement therapy (ERT).

## Case reports

### Patient 1

A 25-year-old woman previously received the biochemical diagnosis of Morquio syndrome (MPS IVA) at 5 years of age due to her short stature and craniofacial dysmorphism. Her parents were consanguineous. At that time, she had a height of 111.5 cm, a weight of 23.6 kg, a body mass index of 18.6 kg/m<sup>2</sup>, generalized joint laxity, valgus deformity in the knees, corneal opacity, horizontal nystagmus, tactile and painful glove hypoesthesia, and a mild mesocardial systolic murmur. Transthoracic echocardiography (TTE) revealed a thickened mitral valve and prolapse of the competent posterior cusp.

## Keywords

Echocardiography; Echocardiography, Doppler; Mucopolysaccharidosis IV; Mucopolysaccharidosis VI; Rare diseases.

Mailing Address: João Vitor Tiveron Teodoro •

E-mail: jvitoriveron@gmail.com

Manuscript received 10/29/2020; revised 12/14/2020; accepted 1/20/2021

DOI: 10.47593/2675-312X/20213402eabc159

There was also left atrial enlargement, signs of diastolic dysfunction with increased filling pressures (grade II), and aortic valve thickening without dysfunction. A small atrial septal defect (ASD) was observed in the middle third of the septum. The use of 2D-STE showed reduced shortening in the anterior wall and a normal global longitudinal strain (GLS). The patient had been treated with elosulfase alfa (Vimizim®) 2 mg/kg weekly for 6 years (Figure 1).

### Patient 2

A 16-year-old female patient previously received the biochemical diagnosis of Maroteaux-Lamy syndrome (MPS VI) at 7 years of age due to craniofacial dysmorphism. At that time, the patient had a height of 110 cm, a weight of 27.4 kg, a body mass index of 22.6 kg/m<sup>2</sup>, macrocephaly, infiltrated facies, exophthalmia, gingival hypertrophy, and joint restriction. TTE revealed left atrial enlargement, mild mitral reflux, mitral stenosis (valve area: 1.18 cm<sup>2</sup>), a thickened tricuspid valve, a thickened aortic valve with mild insufficiency, and concentric left ventricular (LV) remodeling (relative thickness of 0.6, mass of 83 g/m<sup>2</sup>) (Figure 2). The use of 2D-STE revealed reduced longitudinal shortening in the lower and inferolateral basal wall and anterior middle and anteroseptal segment but a normal GLS. The patient had received ERT consisting of galsulfase (Naglazyme®) 1 mg/kg weekly for 8 years.

### Patient 3

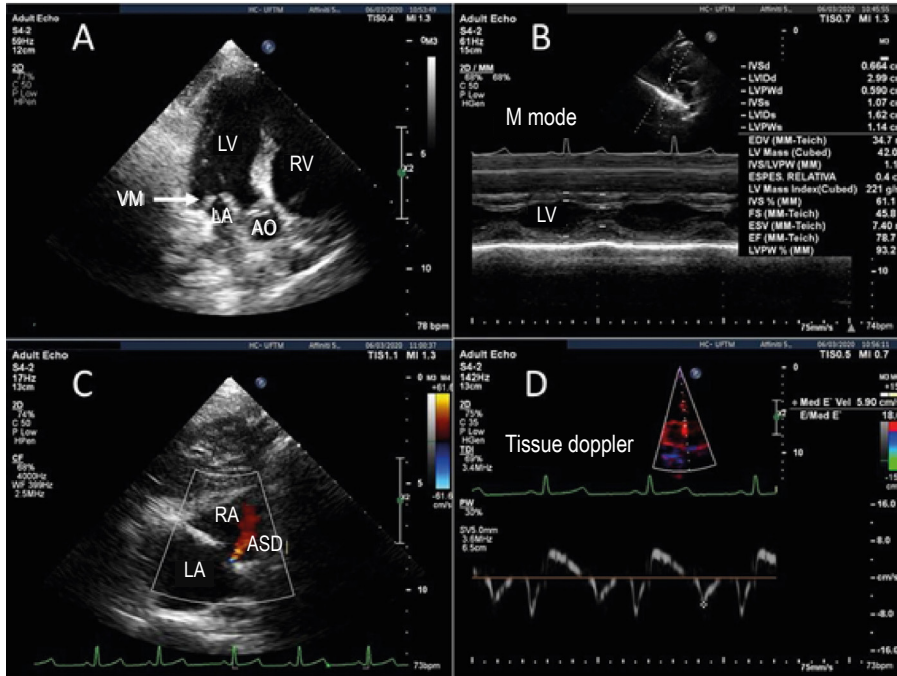
A 13-year-old male patient previously received the biochemical diagnosis of Maroteaux-Lamy syndrome (MPS VI) at 2 years of age due to craniofacial dysmorphism. At that time, the patient had a height of 126 cm, a weight of 26.6 kg, a body mass index of 16.73 kg/m<sup>2</sup>, macrocephaly, and joint stiffness. TTE revealed a thickened mitral valve, a reduced mitral valve opening, a mean gradient of 5 mmHg and maximum gradient of 11 mmHg, an estimated valvar area of 2.27 cm<sup>2</sup>, mild reflux (mild double mitral valve lesion), and a thickened aortic valve without dysfunction (Figure 3). The use of 2D-STE showed reduced longitudinal shortening in the anterior wall and a preserved GLS. The patient had received ERT consisting of galsulfase (Naglazyme®) 1 mg/kg weekly for 11 years.

All patients were evaluated by the same echocardiographer. Good quality videos were made in three echocardiographic windows (four-, three-, and two- chamber). The exams were performed using Philips Affiniti 50 equipment. The 2D-STE GLS analysis was performed offline using QLAB software (Figure 4).



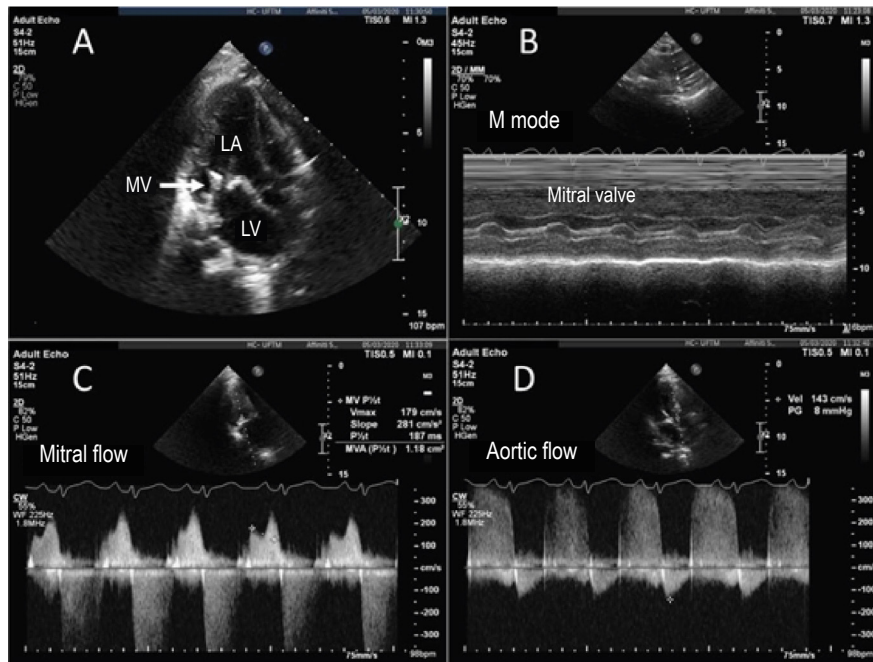


## Case Report



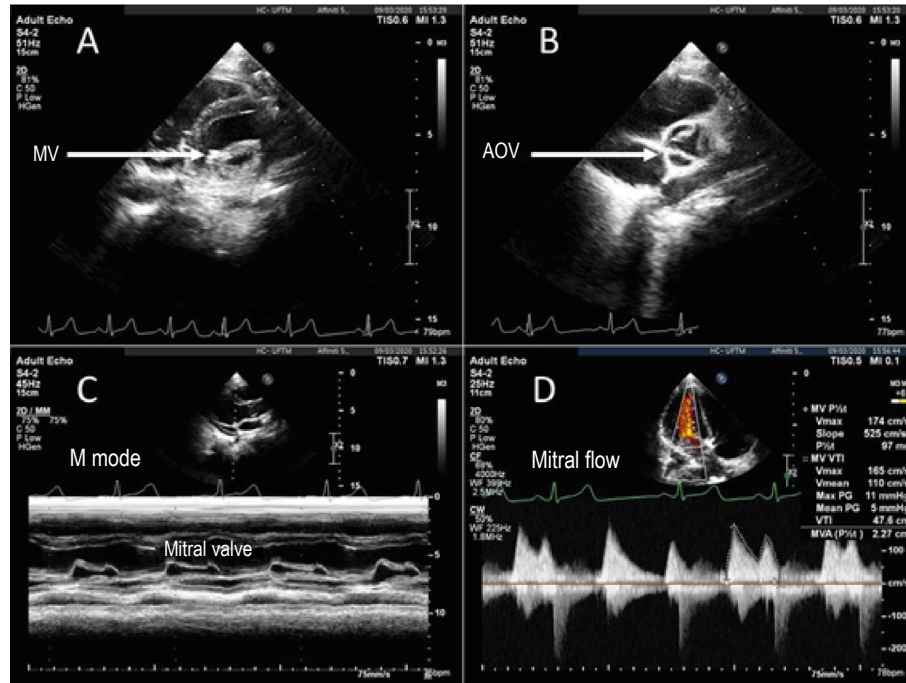
AO, aorta; ASD, atrial septal defect LA, left atrium; LV, left ventricle; MV, mitral valve; RA, right atrium; RV, right ventricle.

**Figure 1** – Echocardiogram of patient 1. (A) Five-chamber apical view showing mitral and aortic valve thickening. (B) M mode demonstrating preserved left ventricular systolic function. (C) Atrial septal defect with no repercussion. (D) Tissue Doppler showing increased left ventricular filling pressures with a decreased E-wave.



LA, left atrium; LV, left ventricle; MV, mitral valve.

**Figure 2** – Echocardiogram of patient 2. (A) Tree-chamber apical view showing a thickened mitral valve. (B) M-mode showing a reduced mitral valve opening. (C) Continuous Doppler showing mitral valve stenosis and reflux. (D) Continuous Doppler showing aortic insufficiency.



AOV, aortic valve; MV, mitral valve.

**Figure 3** – Echocardiogram of patient 3. (A) Transverse parasternal view showing thickening and a reduced mitral valve opening. (B) Transverse parasternal view of base vessels showing a thickened aortic valve. (C) M-mode showing thickening and a reduced mitral valve opening. (D) Continuous Doppler showing mitral valve insufficiency and an increased mean gradient.

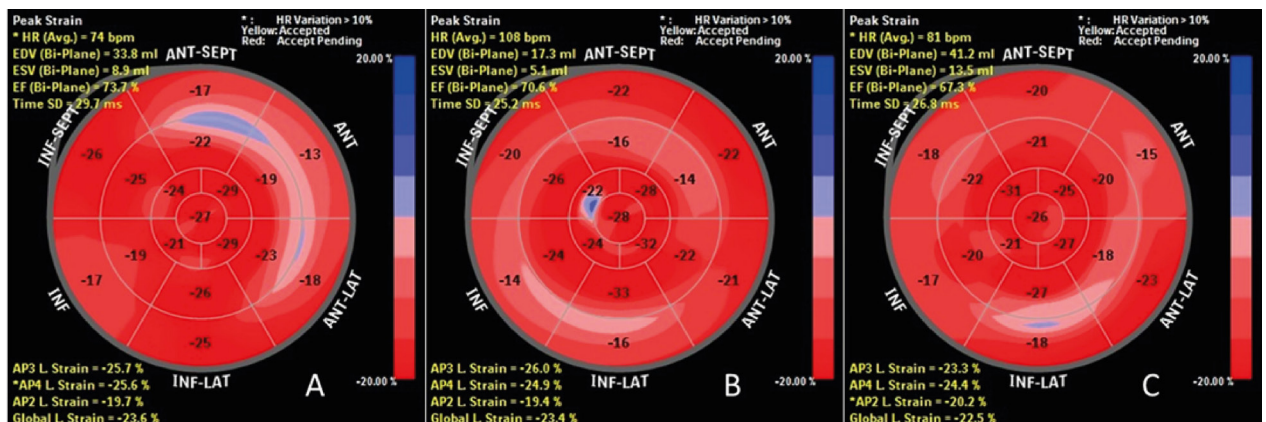


**Figure 4** – The 2D-STE longitudinal strain bullseye. (A) Patient 1: Reduced shortening of the anterior wall without repercussion on the global longitudinal strain. (B) Patient 2: Reduced longitudinal shortening of the lower and inferolateral basal wall of the anterior middle and anteroseptal segment without repercussion on the global longitudinal strain. (C) Patient 3: Reduction anterior and inferior wall strain without repercussion on the global longitudinal strain.

## Discussion

The global MPS incidence is 1 per 25 live births<sup>3</sup>, making it a rare disease. The specific prevalence of MPS IV (Morquio syndrome) is 0.15–1.3 cases per 100,000 inhabitants, whereas MPS VI (Marateaux-Lamy syndrome), although rarer, represents around 20% of all MPP cases in Brazil<sup>5</sup>. Cardiac involvement in PSS is progressive and among the main causes of early morbidity and mortality. The

main causes of death are heart failure, severe arrhythmia leading to sudden death, and coronary occlusion<sup>4</sup>. The use of 2D-STE has become important for MPS patients due to the possibility of early cardiac involvement detection and more accurate follow-up<sup>3</sup>.

The most common echocardiography findings of these analyzed patients were mitral and aortic valve thickening with different degrees of valve dysfunction. Other studies reported

this characteristic in all MPS VI patients except in cases with slower progression<sup>6</sup> and almost half of MPS IV patients<sup>4</sup>.

LV involvement was observed in patient 1, who presented signs of grade II diastolic dysfunction, and patient 2, who presented slightly increased myocardial thickness, which may be related to increased ventricular mass and/or decreased compliance due to intra- and intercellular storage. There are reports of hypertrophy regression after about 1 year of ERT (if started promptly).

The patients analyzed in this study showed no significant LV GLS changes, which primarily reflects subendocardial fiber strain<sup>7</sup> with normal overall values for their age groups<sup>3,7</sup>. However, some studies reported circumferential and radial GLS changes in MPS patients involving the middle and subepicardial layer fibers, respectively<sup>7</sup>. Reports on Fabry disease, another multisystemic storage disorder, demonstrated myocardial strain changes in the three directions evaluated using 2D-STE, i.e., longitudinal, circumferential, and radial<sup>7</sup>. This report also showed regional changes in a heterogeneous pattern that occurred more frequently in the anterior and inferolateral basal wall segments. Although this case series included a small number of patients that precludes any higher statistical inferences in the analysis of rare diseases, it provides important data for future research.

Although the use of 2D-STE in clinical practice is not universal, several studies have established its accuracy and reliability. One aspect that interferes with its potential routine use is the possibility of GLS variability, and, although it

presented good intra- and interobserver reproducibility and a small learning curve, it involves factors that may limit the accuracy of our findings, such as inter-device variability, which can reach  $\pm 5\%$ , and image quality<sup>8</sup>.

Finally, 2D-STE is a useful and important tool in the early detection of myocardial diseases, particularly in patients with storage diseases who can benefit from an early diagnosis and the introduction of specific treatment in addition to the use of cardioprotective therapeutic interventions. However, further studies on the prognostic and progressive control aspects of the use of 2D-STE are necessary.

### Authors' contributions

Research conception and design: Oliveira ANMO and Grangeiro CHP; data collection: Teodoro JVTT, Ribeiro LAB, Oliveira ANMO, and Grangeiro CHP; data analysis and interpretation: Teodoro JVTT, Ribeiro LAB, Ferreira Neto JM, Ferreira VM, Oliveira ANMO, and Grangeiro CHP; manuscript writing: Teodoro JVTT, Ribeiro LAB, Ferreira Neto JM, Ferreira VM, Oliveira ANMO, and Grangeiro CHP; critical review of the manuscript for important intellectual content: Teodoro JVTT, Ribeiro LAB, Ferreira Neto JM, Ferreira VM, Oliveira ANMO, and Grangeiro CHP.

### Conflict of interest

The authors have declared that they have no conflict of interest.

### References

1. Zhou J, Lin J, Leung WT, Wang L. A basic understanding of mucopolysaccharidosis: Incidence, clinical features, diagnosis, and management. *Intractable Rare Dis Res.* 2020;9(1):1-9. doi: 10.5582/irdr.2020.01011
2. Nair V, Belanger EC, Veinot JP. Lysosomal storage disorders affecting the heart: a review. *Cardiovasc Pathol.* 2019;39:12-24. doi: 10.1016/j.carpath.2018.11.002
3. Andrade MFA, Guimarães ICB, Acosta AX, Leão EKEA, Moreira MIG, Mendes CMC. Left ventricular assessment in patients with mucopolysaccharidosis using conventional echocardiography and myocardial deformation by two-dimensional speckle-tracking method. *J Pediatr (Rio J).* 2019;95(4):475-81. doi: 10.1016/j.jped.2018.05.006
4. Braunlin EA, Harmatz PR, Scarpa M, Furlanetto B, Kampmann C, Loehr JP, et al. Cardiac disease in patients with mucopolysaccharidosis: presentation, diagnosis and management. *J Inher Metab Dis.* 2011;34(6):1183-97. doi: 10.1007/s10545-011-9359-8
5. Khan SA, Peracha H, Ballhausen D, Wiesbauer A, Rohrbach M, Gautschi M, et al. Epidemiology of mucopolysaccharidoses. *Mol Genet Metab.* 2017;121(3):227-40. doi: 10.1016/j.ymgme.2017.05.016
6. Boffi L, Russo P, Limongelli G. Early diagnosis and management of cardiac manifestations in mucopolysaccharidoses: a practical guide for paediatric and adult cardiologists. *Ital J Pediatr.* 2018;44(Suppl 2):122. doi: 10.1186/s13052-018-0560-3
7. Borgia F, Pezzullo E, Lomoriello VS, Sorrentino R, Lo Iudice F, Cocozza S, et al. Myocardial deformation in pediatric patients with mucopolysaccharidoses: A two-dimensional speckle tracking echocardiography study. *Echocardiography.* 2017;34(2):240-9.
8. Mirea O, Corici OM, Berceanu M, Donoiu I, Militaru C, Istratoaie O. Variability of longitudinal strain measurements: levelling the playing field. *Acta Cardiologica.* 2019;74(3):188-97.

## Left Atrial Appendage Pseudo-Thrombus

### *Pseudotrombo em Apêndice Atrial Esquerdo*

Marcio Augusto Silva<sup>1</sup>, Marcelo Pazolini<sup>1</sup>, José Guilherme Cazelli<sup>1</sup>, Daniel Escobar Bueno Peixoto<sup>1</sup>, Rafael Soares Rua<sup>1</sup>, Rodolpho Jacques de Melo Farinazzo<sup>1</sup>

Unimed Hospital of Vitória,<sup>1</sup> Vitória, ES, Brazil.

A 65-year-old man was admitted with a suspected cerebrovascular accident (CVA). Brain magnetic resonance imaging (MRI) revealed an intracranial hemorrhage (hemorrhagic CVA) in the thalamus region and findings suggestive of old cerebral infarctions. The patient had systemic arterial hypertension, dyslipidemia, carotid artery disease (complete occlusion of the right internal carotid artery and 50% occlusion of the left internal carotid artery), and severe obstructive coronary artery disease with a history of previous left ventricular (LV) anterior wall myocardial infarction (MI). He underwent surgical myocardial revascularization in 1998 (bypass of the right [RC], diagonal [DG], and circumflex [CX] coronary arteries in addition to left internal mammary artery bypass of the anterior descending artery), coronary RC angioplasty in 2004, and CX angioplasty in 2014.

After the MI, severe LV systolic dysfunction (ejection fraction of 24%) developed. The patient received an implantable cardioverter defibrillator (ICD; Intica 5 DR-T, Biotronik) 1 year prior to the current presentation. He had been clinically followed up on optimized heart failure (HF)

drug therapy and dual antiplatelet aggregation therapy (DAPT) with acetylsalicylic acid (ASA) and clopidogrel. ICD follow-up was performed every 6 months and continuously by remote telemetry (Biotronik Home Monitoring®).

During the current hospitalization, the patient underwent transesophageal echocardiography (TEE), which revealed echo density in the left atrial appendage (LAA) suggestive of a thrombus (Figure 1). ICD data collected since implantation showed no atrial fibrillation (AF) or rapid atrial rhythm. Dynamic TEE imaging (Video 1) showed a streaking image in the LAA suggestive of an artefact.

Therefore, considering the absence of AF, the imaging findings, and the important impact that a thrombus in the LAA would have on the patient's treatment (recent hemorrhagic CVA), the patient underwent computed tomography coronary angiography (CT-angio), which revealed no evidence of an LAA thrombus but showed a coronary artery bypass graft from the aorta to the diagonal branch of the left coronary artery in a segment closely related to the LAA that was considered the cause of the suspected artefact (Figure 2, Video 2).

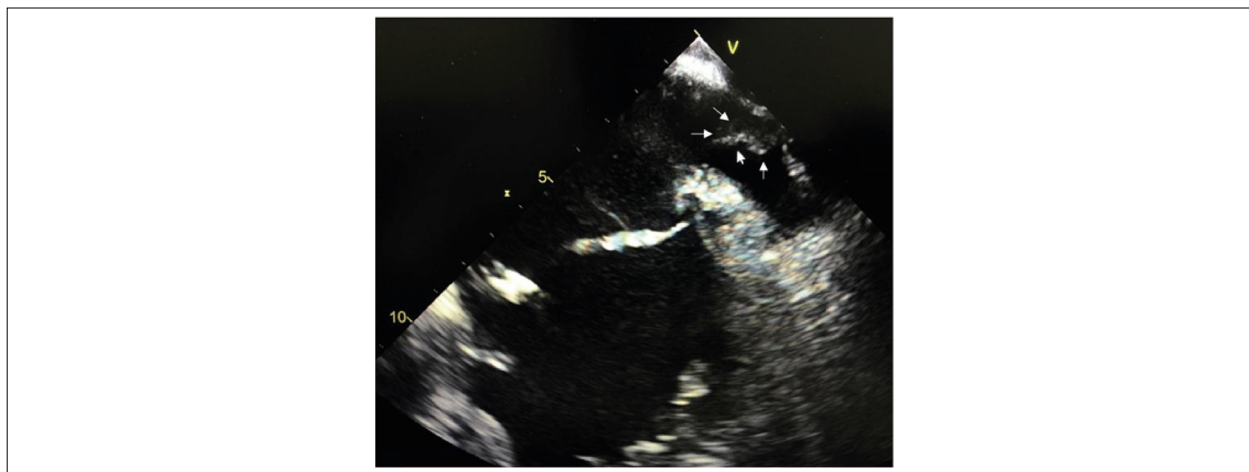


Figure 1 – Transesophageal echocardiogram In the mid-esophageal plane demonstrating an echo dense structure in the proximal segment of the left atrial appendage.

### Keywords

Atrial appendage; Computed tomography; Echocardiography.

Mailing Address: Márcio Augusto Silva •

Rua Pedro Luiz Zanandrea 85, Mata da Praia, Vitória, ES, CEP 29065-610

E-mail: masilva.cardio@gmail.com

Manuscript received 11/20/2020; revised 11/25/2020; accepted 12/2/2020

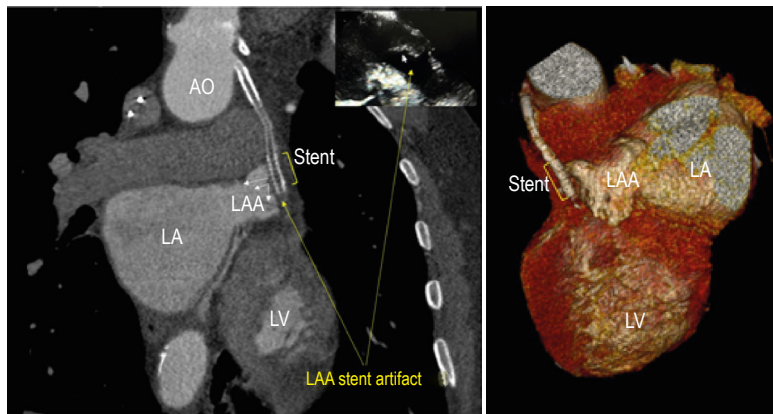
DOI: 10.47593/2675-312X/20213402eabc168



## Relato de Caso

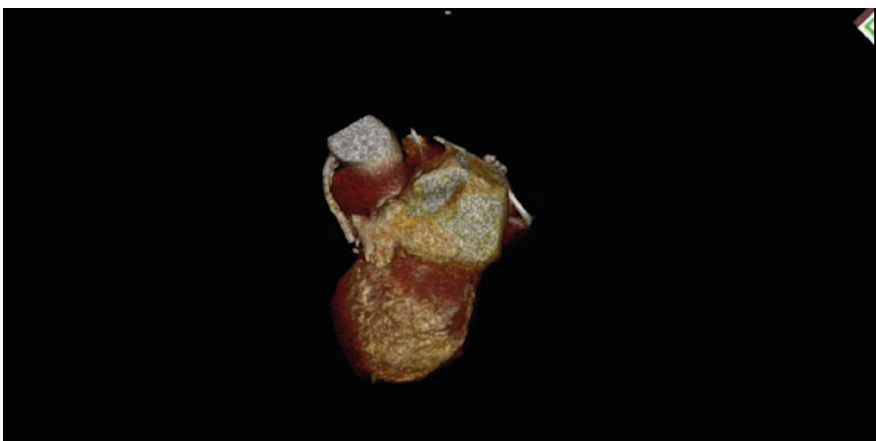


**Video 1** – Transesophageal echocardiogram's dynamic view in the mid-esophageal plane demonstrating (arrow) an echo dense structure in the proximal segment of the left atrial appendage.



AAE: apêndice atrial esquerdo; AE: átrio esquerdo; VE: ventrículo esquerdo.

**Figure 2** – Computed tomography angiogram (curved multiplanar reconstruction) showing stent thrombosis of an aortic bypass to the diagonal branch in close contact with the outer border of the left atrial appendage.



**Video 2** – Computed Tomographic Angiogram's dynamic view showing close contact of the aortic bypass to the diagonal branch with the outer border of the left atrial appendage.

## Discussion

TEE is considered the gold standard test to detect LAA thrombi.<sup>1,2</sup> With the incorporation of heart CT-angio into clinical practice, the diagnosis of a “false” thrombus, called pseudo-thrombus, in the LAA has become more frequent and is explained by contrast filling failure due to reduced flow velocity in the LAA trabeculae.<sup>3</sup> The recent use of specific CT-angio protocols to evaluate thrombi and late imaging capture has significantly improved its sensitivity and specificity, which reaches near 100% in some series,<sup>4,5</sup> thus becoming a less invasive option than TEE. It has been widely used in preoperative catheter ablation to treat AF or LAA percutaneous occlusions.

In this case, it is noteworthy that the diagnosis of pseudo-thrombus by TEE corresponded to an extracardiac metallic structure (stent) artefact closely related to the LAA but

only identified on the cardiac CT-angio and relevant in the patient’s treatment.

## Authors’ contributions

Research concept and design: Silva MA; data collection: Silva MA, Cazelli JG, Peixoto DEB, Rua RS, and Farinazzo RJM; data analysis and interpretation: Silva MA, Pazolini M, Cazelli JG, Peixoto DEB, Rua RS, and Farinazzo RJM; manuscript writing: Pazolini M and Cazelli JG; critical review of the manuscript: Pazolini M and Cazelli JG.

## Conflict of interest

The authors have declared that they have no conflict of interest.

## References

1. Manning WJ, Weintraub RM, Waksmonski CA, Haering JM, Rooney PS, Maslow AD, et al. Accuracy of transesophageal echocardiography for identifying left atrial thrombi. A prospective, intraoperative study. *Ann Intern Med.* 1995;123(11):817-22. doi: 10.7326/0003-4819-123-11-199512010-00001
2. Zabalgoitia M, Halperin JL, Pearce LA, Blackshear JL, Asinger RW, Hart RG. Transesophageal echocardiographic correlates of clinical risk of thromboembolism in nonvalvular atrial fibrillation. *Stroke Prevention in Atrial Fibrillation III Investigators. J Am Coll Cardiol.* 1998;31(7):1622-6. doi: 10.1016/s0735-1097(98)00146-6
3. Zimmerman S. Pseudothrombus in the left atrial appendage. In: Zimmerman S, Fishman E (eds.). *Pearls and pitfalls in cardiovascular imaging: pseudolesions, artifacts, and other difficult diagnoses.* Cambridge: Cambridge University Press; 2015. p. 20-21.
4. Romero J, Husain SA, Kelesidis I, Sanz J, Medina HM, Garcia MJ. Detection of left atrial appendage thrombus by cardiac computed tomography in patients with atrial fibrillation: a meta-analysis. *Circ Cardiovasc Imaging.* 2013;6(2):185-94. doi: 10.1161/CIRCIMAGING.112.000153
5. Lazoura O, Ismail TF, Pavitt C, Lindsay A, Sriharan M, Rubens M, et al. A low-dose, dual-phase cardiovascular CT protocol to assess left atrial appendage anatomy and exclude thrombus prior to left atrial intervention. *Int J Cardiovasc Imaging.* 2016;32(2):347-54. doi: 10.1007/s10554-015-0776-x.

## Use of Color Doppler of Carotids in the Diagnosis of a Patient with Direct Carotid-Cavernous Fistula

*Uso do Doppler Colorido das Carótidas no Diagnóstico de um Paciente com Fístula Carotídeocavernosa Direta*

Mauro de Deus Passos<sup>1,2</sup>, Isabella Godoy-Gomes<sup>3</sup>, Mariana de Gregório Faria<sup>1</sup>

<sup>1</sup>Sobradinho Regional Hospital, Brasília, DF, Brazil; <sup>2</sup>Santa Maria Regional Hospital, Brasília, DF, Brazil; <sup>3</sup>Formosa Regional Hospital, Formosa, GO, Brazil.

### Abstract

An 18-year-old patient developed a direct carotid fistula after a mild craniocerebral trauma. The patient presented with tinnitus and exophthalmia, both pulsatile and on the left. A carotid Doppler study revealed high blood flow velocities and reduced resistance rates in the left internal and common carotid arteries compatible with a direct carotid fistula. Computed tomography angiography of the brain confirmed the carotid fistula. The patient was successfully referred for endovascular embolization treatment. This case demonstrates that carotid Doppler may play an important role in the diagnosis of direct carotid fistulae and the follow-up of patients undergoing endovascular therapy.

### Introduction

A carotid-cavernous fistula (CCF) is an abnormal communication between arteries and veins inside the cavernous sinus<sup>1</sup> (Figure 1). According to Barrow D (1985)<sup>2</sup>, these fistulas are classified into types A to D: type A, a direct high flow deviation between the internal carotid artery (ICA) and the cavernous sinus; type B, a dural shunt between the meningeal branches of the ICA and the cavernous sinus; type C, a shunt between the meningeal branches of the external carotid artery (ECA) and the cavernous sinus; and type D, a shunt between the meningeal branches of the ICA, ECA, and cavernous sinus.<sup>2</sup>

The most common cause of direct CCF is trauma, followed by less frequent causes such as rupture of an ICA aneurysm inside the cavernous sinus, Ehlers-Danlos syndrome type IV,<sup>3,4</sup> or iatrogenic interventions<sup>5-11</sup> including transarterial endovascular intervention, internal carotid endarterectomy, percutaneous trigeminal neuralgia treatment, transphenoidal resection of a hypophysis tumor, and maxillofacial surgery. Indirect CCF (Barrow types B, C, and D) are also called dural fistulae and usually present with low flow rates (Figure 2).

The largest arterial supply for indirect fistulae comes from branches of the internal maxillary, middle meningeal, accessory pharyngeal, and ascending pharyngeal ECA as

well as from cavernous segments of the ICA.<sup>12</sup> Indirect CCF tend to occur more frequently in postmenopausal women. The cause of these lesions remains uncertain, but pediatric cases of dural fistulae described in the literature evidence a possible congenital origin.<sup>13-15</sup> Some factors that may predispose patients to the development of dural CCF include hypertension, diabetes, pregnancy, trauma, exertion, atherosclerosis, cavernous sinus thrombosis, sinusitis, and collagen vascular disease. Trauma is less commonly associated with indirect CCF.<sup>2,14,16</sup>

Treatment modalities include transarterial or transvenous conservative, surgical, and endovascular management.<sup>17</sup> Direct and indirect CCF have different mechanisms; thus, they present with different symptoms and severity levels.<sup>18</sup>

Recent advances in endovascular technology have resulted in different CCF treatment options. As a result, the endovascular approach has become the main CCF treatment. Treatment choice varies according to type, exact anatomy, arterial defect size, and operator and institutional preferences.

In direct CCF, the aim of treatment is to occlude the rupture between the ICA and the cavernous sinus and preserve the unobstructed artery. These objectives can be achieved using transarterial obliteration of the fistula with a detachable balloon, transarterial or transvenous obliteration of the ipsilateral cavernous sinus with coils or other embolic material, or implantation of a covered stent through the fistula.<sup>1</sup> Chi et al. studied 172 patients with direct CCF caused by trauma. They reported a medium-sized fistula predominance of 35.5% and large-sized fistula predominance of 51.7% in addition to a fistula occlusion success rate of 94% using endovascular embolization and 70% using carotid artery preservation.<sup>19</sup>

In cases of indirect CCF, the objective is to stop fistulous communications and decrease the cavernous sinus pressure. This can be achieved by occluding the arterial branches supplying the fistula (transarterial embolization) or, more commonly, by occluding the cavernous sinus in which the fistulous communications occur (transvenous embolization).<sup>1</sup>

### Case report

An 18-year-old patient presented with the complaint of pulsatile tinnitus in the left ear. The patient mentioned that the symptoms had started after a recent car accident involving mild craniocerebral trauma. A physical examination detected discrete left eye proptosis. Carotid ultrasonography (Figures 3 and 4) showed healthy walls, high blood flow velocities, and decreased resistance index (RI) rates in the left common and internal carotid arteries. These findings were compatible with a diagnosis of a direct CCF. The velocities were normal on the right side.

### Keywords

Brain injury, traumatic; Carotid-cavernous sinus fistula; Doppler ultrasonography.

Mailing Address: Mauro de Deus Passos •

E-mail: mauropassos@cardiol.br

Manuscript received 12/21/2020; revised 2/2/2021; accepted 3/5/2021

DOI: 10.47593/2675-312X/20213402eabc178



## Case Report

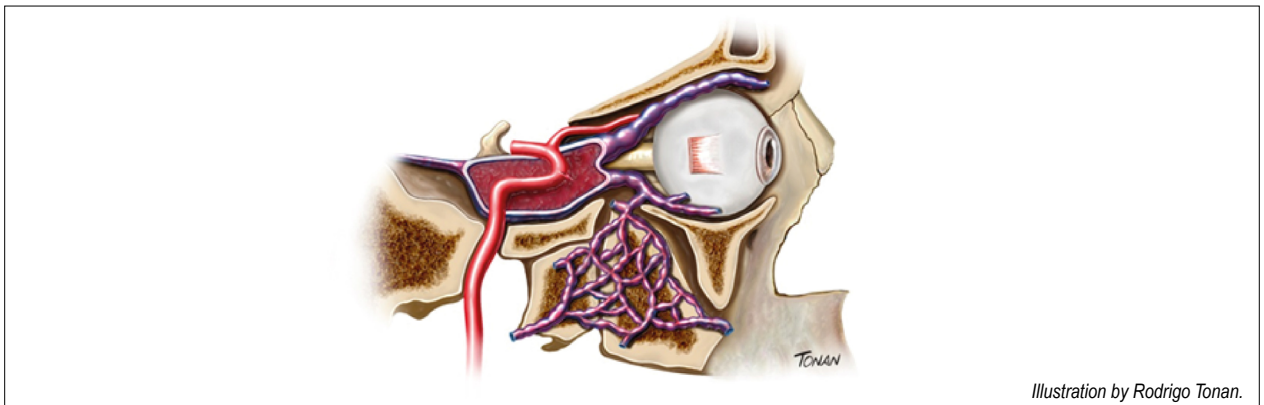
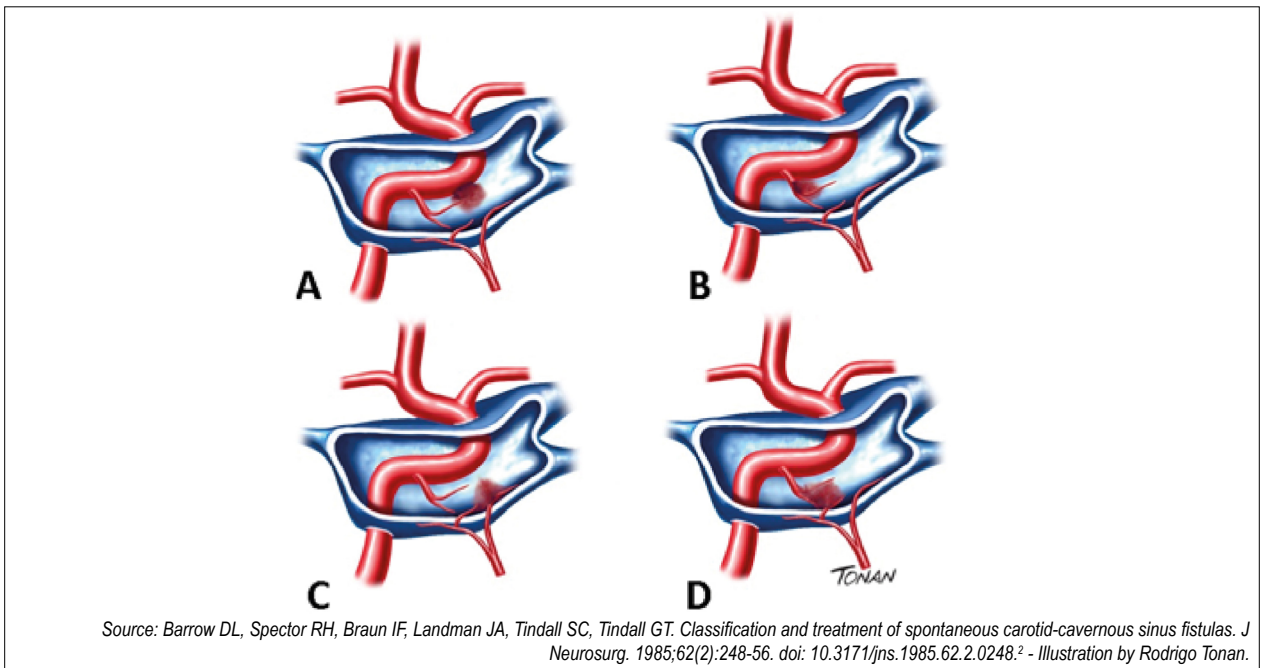


**Figure 1** – Direct carotid-cavernous (Barrow type A) fistula.



Source: Barrow DL, Spector RH, Braun IF, Landman JA, Tindall SC, Tindall GT. Classification and treatment of spontaneous carotid-cavernous sinus fistulas. *J Neurosurg.* 1985;62(2):248-56. doi: 10.3171/jns.1985.62.2.0248.<sup>2</sup> - Illustration by Rodrigo Tonan.

**Figure 2** – Barrow classification of carotid-cavernous fistulae. Type A fistulae are characterized by a direct connection between the internal carotid artery and the cavernous sinus. Type B fistulae involve meningeal branches of the internal carotid artery. Type C fistulae involve external carotid branches. Type D fistulae include meningeal branches of the internal and external carotid arteries.

The patient underwent 256-channel cerebral computed tomography angiography (Figure 5), which showed the presence of CCF on the left, tumefaction of the respective cavernous sinus, and a large ipsilateral ophthalmic vein. He was successfully referred for endovascular embolization treatment.

### Discussion

Carotid color Doppler is rarely reported in the literature as a diagnostic modality for CCF. Direct fistulae are characterized by a direct connection between the ICA and the cavernous sinus. Thus, direct CCF usually have a high flow that translates on a spectral Doppler study as high velocity. The reported patient showed typical direct CCF findings.

Lin et al. analyzed 2,600 consecutive carotid Doppler examinations performed from October 1987 to June 1992 and reported 14 CCF cases. Special emphasis was given to the RI and flow volume. Of the 11 patients with a direct CCF, the most common abnormal hemodynamic parameters included high systolic and diastolic peak velocities, increased flow volume, and decreased RI.<sup>20</sup>

Dural CCF (Barrow types B, C, and D) often presents as recurrent arteriovenous communication after complete treatment.<sup>21</sup> Tsai et al. compared carotid Doppler with cerebral angiography and reported that the ECA RI parameter (cutoff point of 0.72 on the right and of 0.71 on the left) resulted in better sensitivity (74%), specificity (89%), better positive



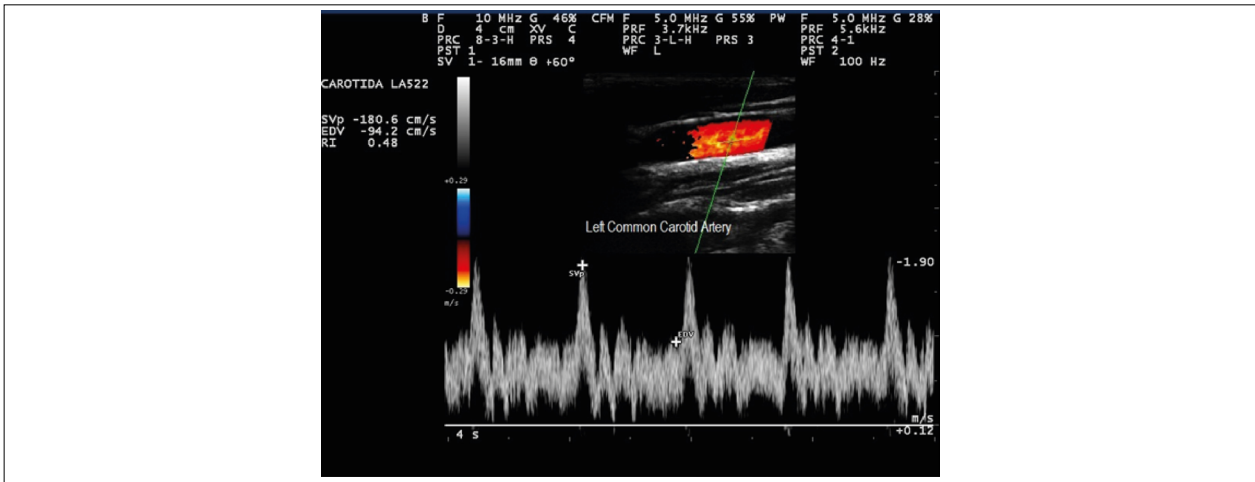


Figure 3 – Spectral Doppler (pulsed wave) of the left common carotid artery showing high velocities and spectrum oscillation (serrated).

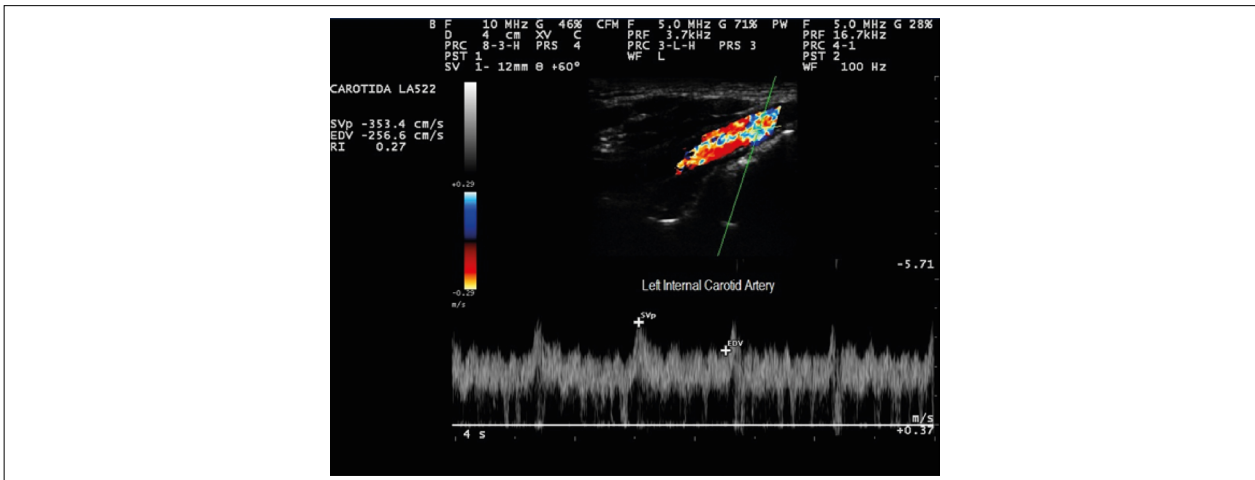


Figure 4 – Spectral Doppler (pulsed wave) of the left internal carotid artery showing high velocities and spectrum oscillation (serrated).

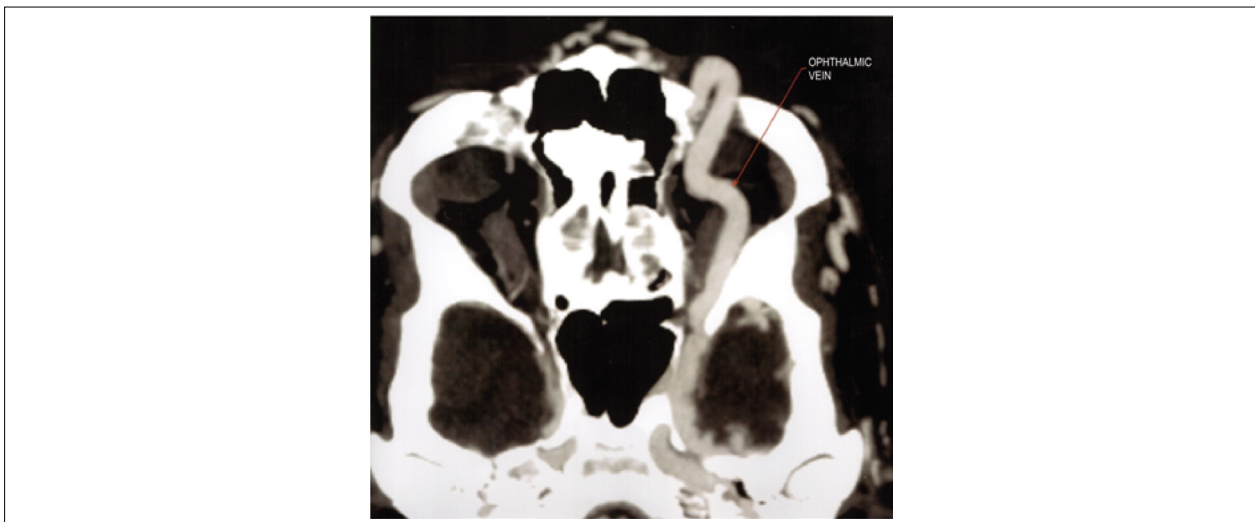


Figure 5 – Image of 256-channel computed tomography angiography showing cavernous sinus tumefaction and a large ipsilateral ophthalmic vein.

predictive value (79%), better negative predictive value (86%), and higher accuracy (84%) for predicting dural CCF.<sup>22</sup> Thus, carotid Doppler can be used as an initial screening tool for diagnosing patients with symptoms related to dural CCF. In another study, the same authors reported that ECA carotid Doppler RI was correlated with treatment efficacy and sensitive to dural CCF clinical progression; therefore, they proposed that patients with a dural CCF should undergo carotid Doppler before and immediately after endovascular therapy to enable the evaluation of treatment efficacy and determination of the patient's hemodynamic status before follow-up.<sup>22</sup>

## References

1. Henderson AD, Miller NR. Carotid-cavernous fistula: current concepts in aetiology, investigation, and management. *Eye (Lond)*. 2018;32(2):164-72. doi: 10.1038/eye.2017.240
2. Barrow DL, Spector RH, Braun IF, Landman JA, Tindall SC, Tindall GT. Classification and treatment of spontaneous carotid-cavernous sinus fistulas. *J Neurosurg*. 1985;62(2):248-56. doi: 10.3171/jns.1985.62.2.0248
3. Schievink WI, Piepgras DG, Earnest F 4th, Gordon H. Spontaneous carotid-cavernous fistulae in Ehlers-Danlos syndrome Type IV. Case report. *J Neurosurg*. 1991;74(6):991-8. doi: 10.3171/jns.1991.74.6.0991
4. Masson-Roy J, Savard M, Mackey A. Carotid Cavernous Fistula in a Patient with Type IV Ehlers-Danlos Syndrome. *Can J Neurol Sci*. 2017;44(4):427-8. doi: 10.1017/cjn.2016.456
5. Ono K, Oishi H, Tanoue S, Hasegawa H, Yoshida K, Yamamoto M, et al. Direct carotid-cavernous fistulas occurring during neurointerventional procedures. *Interv Neuroradiol*. 2016;22(1):91-6. doi: 10.1177/1591019915617321
6. Barr JD, Mathis JM, Horton JA. Iatrogenic carotid-cavernous fistula occurring after embolization of a cavernous sinus meningioma. *AJNR Am J Neuroradiol*. 1995;16(3):483-5. PMID: 7793369
7. Kuether TA, O'Neill OR, Nesbit GM, Barnwell SL. Direct carotid cavernous fistula after trigeminal balloon microcompression gangliolysis: case report. *Neurosurgery*. 1996;39(4):853-5; discussion 855-6. doi: 10.1097/00006123-199610000-00042
8. Dolenc VV, Lipovsek M, Slokan S. Traumatic aneurysm and carotid-cavernous fistula following transsphenoidal approach to a pituitary adenoma: treatment by transcranial operation. *Br J Neurosurg*. 1999;13(2):185-8. doi: 10.1080/02688699943961
9. Song IC, Bromberg BE. Carotid-cavernous sinus fistula occurring after a rhinoplasty. Case report. *Plast Reconstr Surg*. 1975;55(1):92-6. doi: 10.1097/00006534-197501000-00019
10. Lister JR, Sybert GW. Traumatic false aneurysm and carotid-cavernous fistula: a complication of sphenoidotomy. *Neurosurgery*. 1979;5(4):473-5. doi: 10.1227/00006123-197910000-00012
11. Pedersen RA, Troost BT, Schramm VL. Carotid-cavernous sinus fistula after external ethmoid-sphenoid surgery. Clinical course and management. *Arch Otolaryngol*. 1981;107(5):307-9. doi: 10.1001/archotol.1981.00790410045012
12. Meyers PM, Halbach VV, Dowd CF, Lempert TE, Malek AM, Phatouros CC, et al. Dural carotid cavernous fistula: definitive endovascular management and long-term follow-up. *Am J Ophthalmol*. 2002;134(1):85-92. doi: 10.1016/s0002-9394(02)01515-5
13. Ringer AJ, Salud L, Tomsick TA. Carotid cavernous fistulas: anatomy, classification, and treatment. *Neurosurg Clin N Am*. 2005;16(2):279-95, viii. doi: 10.1016/j.nec.2004.08.004
14. Gemmete JJ, Ansari SA, Gandhi DM. Endovascular techniques for treatment of carotid-cavernous fistula. *J Neuroophthalmol*. 2009;29(1):62-71. doi: 10.1097/WNO.0b013e3181989fc0
15. Pang D, Kerber C, Biglan AW, Ahn HS. External carotid-cavernous fistula in infancy: case report and review of the literature. *Neurosurgery*. 1981;8(2):212-8. doi: 10.1227/00006123-198102000-00011
16. Tjoumakaris SI, Jabbour PM, Rosenwasser RH. Neuroendovascular management of carotid cavernous fistulae. *Neurosurg Clin N Am*. 2009;20(4):447-52. doi: 10.1016/j.nec.2009.07.013
17. Korkmaz B, Kocak B, Tureci E, Islak C, Kocer N, Kizilkilic O. Endovascular treatment of carotid cavernous sinus fistula: A systematic review. *World J Radiol*. 2013;5(4):143-55. doi: 10.4329/wjr.v5.i4.143
18. Sanal B, Nas OF, Korkmaz M, Erdogan C, Hakyemez B. Endovascular Treatment in Traumatic and Spontaneous Carotid Cavernous Fistulas: with Different Embolization Agents and via Various Vascular Routes. *J Vasc Interv Neurol*. 2018;10(2):18-24. PMID: 30746005
19. Chi CT, Nguyen D, Duc VT, Chau HH, Son VT. Direct traumatic carotid cavernous fistula: angiographic classification and treatment strategies. Study of 172 cases. *Interv Neuroradiol*. 2014;20(4):461-75. doi: 10.15274/INR-2014-10020
20. Lin HJ, Yip PK, Liu HM, Hwang BS, Chen RC. Noninvasive hemodynamic classification of carotid-cavernous sinus fistulas by duplex carotid sonography. *J Ultrasound Med*. 1994;13(2):105-13. doi: 10.7863/jum.1994.13.2.105
21. Kim MS, Han DH, Kwon OK, Oh CW, Han MH. Clinical characteristics of dural arteriovenous fistula. *J Clin Neurosci*. 2002;9(2):147-55. doi: 10.1054/jocn.2001.1029
22. Tsai LK, Jeng JS, Wang HJ, Yip PK, Liu HM. Diagnosis of intracranial dural arteriovenous fistulas by carotid duplex sonography. *J Ultrasound Med*. 2004;23(6):785-91. doi: 10.7863/jum.2004.23.6.785.

## Authors' contributions

Research conception and design: Passos MD and Faria MG; data collection: Passos MD, Godoy-Gomes I, and Faria MG; data analysis and interpretation: Passos MD, Godoy-Gomes I, and Faria MG; manuscript writing: Passos MD, Godoy-Gomes I and Faria MG.

## Conflict of interest

The authors have declared that they have no conflict of interest.

## Large Lymphoma Involving the Aortic Arch and its Branches: Demonstration by Echocardiography and Contribution to the Assessment of Hemodynamic Repercussions

*Grande Linfoma Envolvendo o Arco Aórtico e seus Ramos: Demonstração pela Ecocardiografia e Contribuição na Avaliação de Repercussão Hemodinâmica*

Israel Nilton de Almeida Feitosa<sup>1</sup>, Máisa Carneiro Wanderley<sup>1</sup>

<sup>1</sup>Federal University of Campina Grande, Campina Grande, PB, Brazil.

An 18-year-old man reported cervical adenomegaly that had progressively increased for about one year. The tumor was visible, was non-mobile, had a fibroelastic consistency, was painless on palpation, and showed no signs of inflammation. He was diagnosed with classical Hodgkin's lymphoma by a lesion biopsy with anatomopathological and immunohistochemical tests (CD15-, CD30-, and PAX-5-antibody-positive). Transthoracic echocardiography showed a large mass with a heterogeneous texture involving the pulmonary artery, the aortic arch (and its main branches), and the proximal descending aorta. Pulse and continuous wave color Doppler showed no evidence of flow impairment in the proximal descending aorta or the proximal segments of the brachiocephalic trunk, left common carotid artery, and left subclavian artery. Contrast chest tomography corroborated the echocardiographic findings, showing an extensive solid mediastinal tumor looking resembling a lymph node conglomerate occupying

the anterior and middle compartments of the mediastinum and involving the vascular structures. There were no signs of compression or invasion.

### Authors' contributions

Research conception and design: Feitosa INA; data collection: Feitosa INA, Wanderley MC; data analysis and interpretation: Feitosa INA, Wanderley MC; manuscript writing: Feitosa INA; critical review of the manuscript for important intellectual content: Feitosa INA and Wanderley MC; and collection of echocardiographic images: Feitosa INA.

### Conflict of interest

The authors have declared that they have no conflict of interest.



**Figura 1** – Chest X-ray in posteroanterior incidence demonstrating enlargement of the upper part of the mediastinum.

### Keywords:

Echocardiography; Lymphoma; Thoracic aorta .

Mailing Address: Israel Nilton de Almeida Feitosa •

E-mail: inafeitosa@hotmail.com

Manuscript received 8/11/2020; revised 1/27/2021; accepted 2/26/2021

DOI: 10.47593/2675-312X/20213402eabc138



## Images

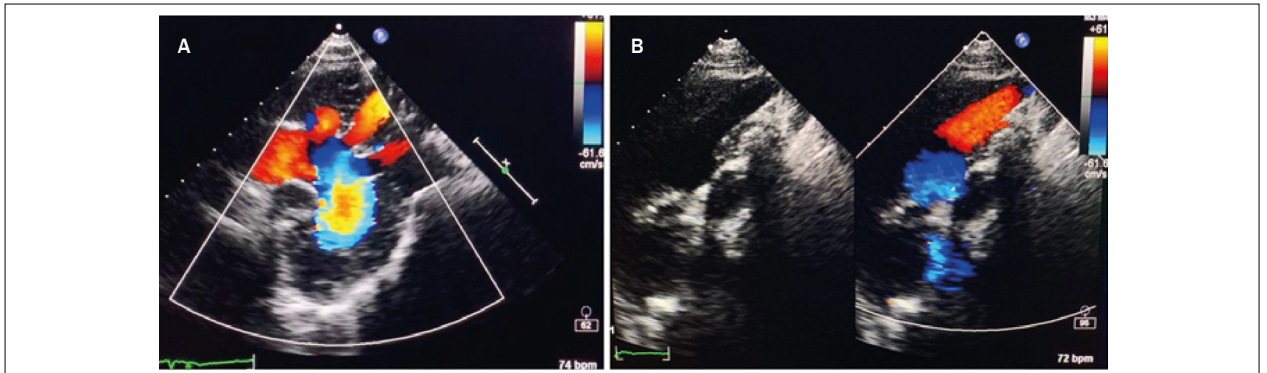


**Figura 2** – A - Transthoracic echocardiography (suprasternal notch view) showing color Doppler flow of the aortic arch (and its main branches) and proximal descending aorta; B - Two-dimensional image and color Doppler flow of the brachycephalic trunk.

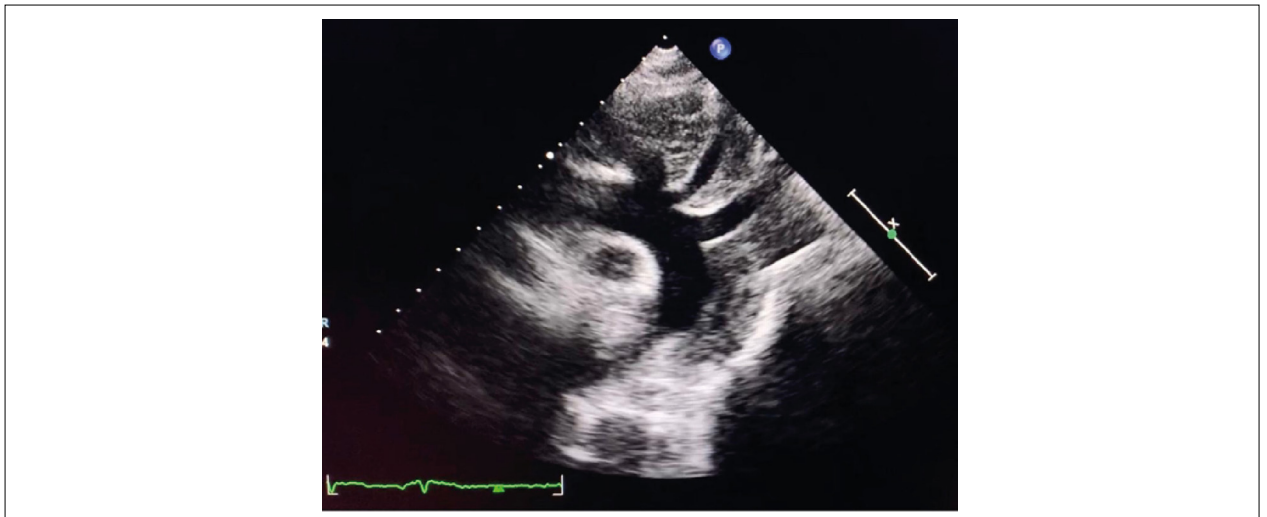


**Figura 3** – Transthoracic echocardiography (suprasternal notch view) showing a mass of heterogeneous echogenicity involving the aortic arch (and its main branches) and the proximal descending aorta.

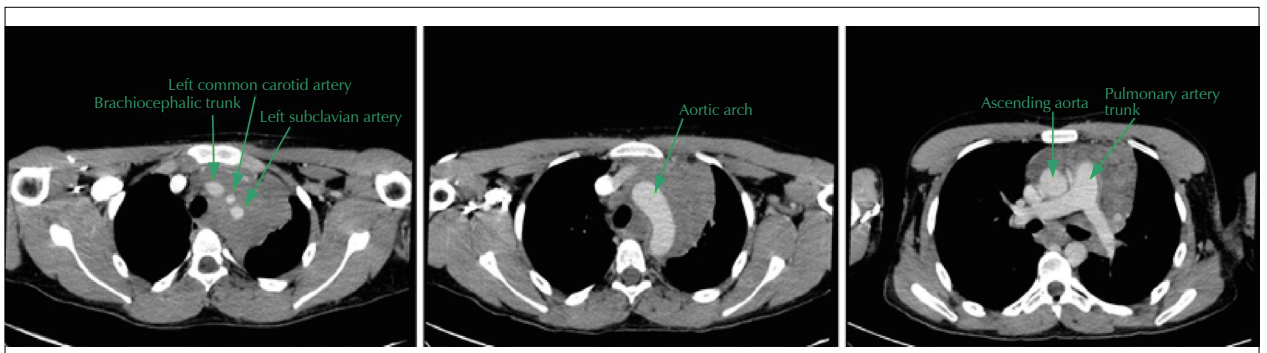


**Figura 4** – Contrast-enhanced chest computed tomography revealing extensive solid mediastinal tumor involving pulmonary artery, aortic arch (and main branches) and proximal descending aorta. There is no evidence of compression or invasion.

## Ebstein's anomaly, noncompaction cardiomyopathy, and mitral valve stenosis

### *Anomalia de Ebstein, não Compactação Miocárdica e Estenose Valvar Mitral*

Anderson da Costa Armstrong<sup>1,2</sup>, Gustavo Volpe<sup>1</sup>, Tiago Augusto Magalhães<sup>1,3,4</sup>, Dinani Armstrong<sup>2</sup>, Marcelo Nacif<sup>1,3</sup>

<sup>1</sup>Johns Hopkins University, Baltimore, MD, USA; <sup>2</sup>Federal University of Vale do São Francisco, Petrolina, PE, Brazil; <sup>3</sup>Complexo Hospital das Clínicas, Federal University of Paraná, Curitiba, PR, Brazil; <sup>4</sup>Hospital do Coração, São Paulo, SP, Brazil.

A 29-year-old woman who was previously diagnosed with Ebstein's anomaly was referred for magnetic resonance imaging of the heart due to progressively worsening dyspnea on exertion.

Cardiac magnetic resonance images (Siemens Essenza 1.5T) showed right atrial dilation and low insertion of the tricuspid valve septal leaflet. The patient also presented with increased left ventricular trabeculation characteristic of noncompaction cardiomyopathy and signs of posterior mitral leaflet restriction secondary to probable rheumatic valvular disease.

### Authors' contributions

All authors contributed equally to the design, data collection and description of the case.

### Conflict of interest

The authors have declared that they have no conflict of interest.

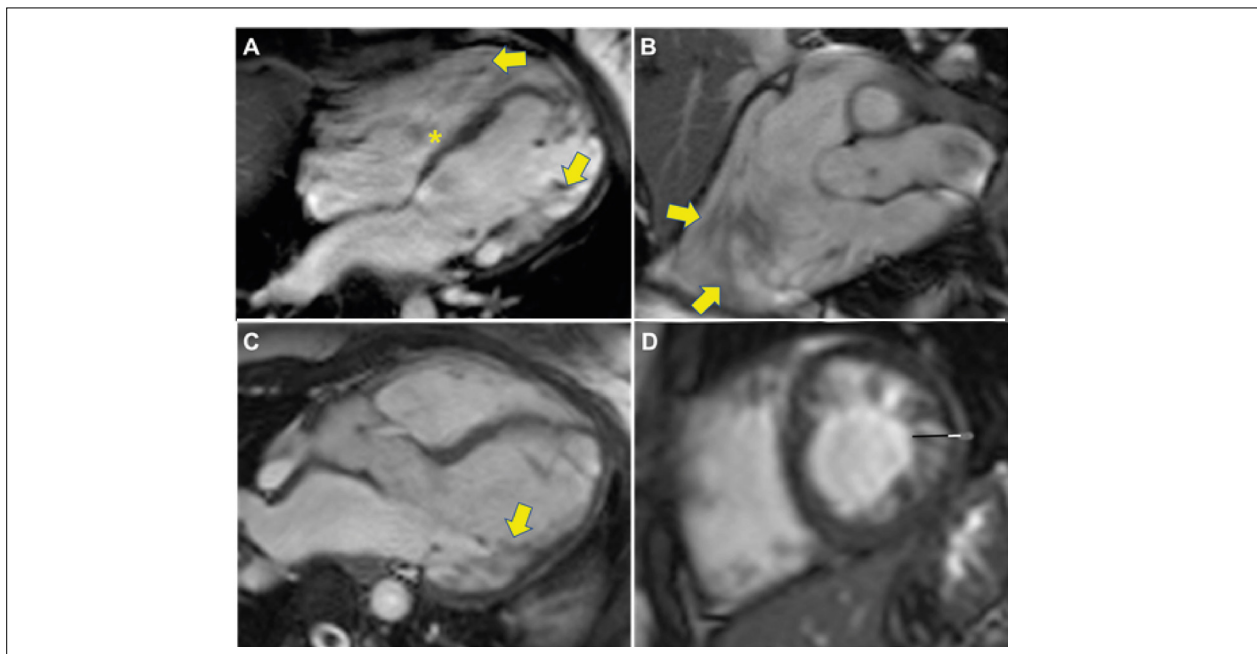


**Figure 1** – Cardiac magnetic resonance. (A) Low tricuspid insertion, right ventricular atrialization (asterisk), and biventricular noncompaction (arrows). (B) Increased trabeculation of the right ventricle (arrows). (C) Three-chamber view: papillary muscle malformation (arrow) and ventricular remodeling. (D) Short axis: compacted and noncompact myocardial thickness (estimated thickness ratio, 2.9 – white and black arrows).

### Keywords

Ebstein's anomaly; Magnetic resonance imaging; Mitral valve stenosis.

Mailing Address: Tiago Augusto Magalhães •

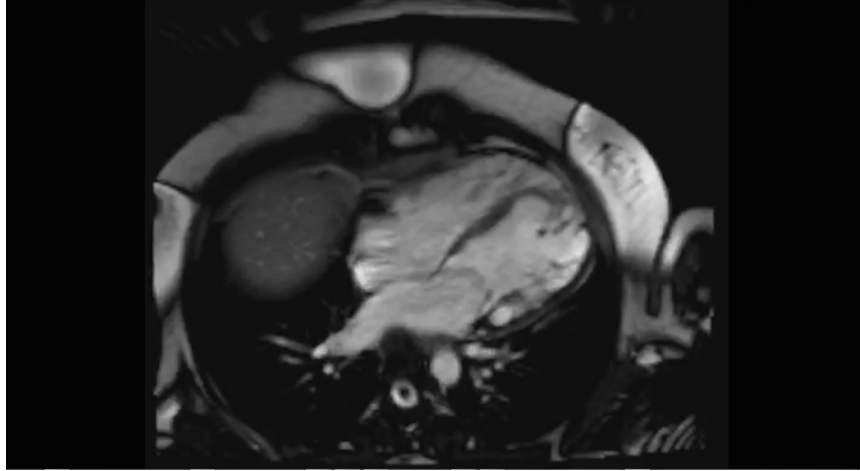
E-mail: tiaugusto@gmail.com

Manuscript received 10/15/2020; revised 11/27/2020; accepted 12/10/2020

DOI: 10.47593/2675-312X/20213402eabc158



## Images



**Video 1** – Cine magnetic resonance imaging (four-chamber) showing noncompaction cardiomyopathy. There was also low insertion of the tricuspid valve with right ventricular atrialization associated with valvular regurgitation jet. The mitral valve showed decreased leaflet mobility, especially in the posterior leaflet.

## Spontaneous Pneumomediastinum

### *Pneumomediastino Espontâneo*

Luísa Gonçalves<sup>1</sup>, Inês Pires<sup>1</sup>, João Santos<sup>1</sup>, Joana Correia<sup>1</sup>, Davide Moreira<sup>1</sup>

<sup>1</sup>Cardiology department, Centro Hospitalar Tondela-Viseu, Viseu, Portugal.

### Case

A 31-year-old male athlete presented with acute chest pain that was aggravated with swallowing after completing a marathon. Physical examination findings and his vital signs were normal. Electrocardiography revealed sinus rhythm, an incomplete right bundle block, and a negative T wave in V1-V2. A blood analysis showed normal D-dimer values and a slightly elevated troponin-I level (maximum at 72 hours: 0.52 ng/mL; normal, <0.07 ng/mL) with fluctuations. Chest X-ray, echocardiography, and coronary angiography findings were normal. Cardiac computed tomography (CT) revealed small gas collections on the superior and middle mediastinum compatible with spontaneous pneumomediastinum (SP). (Figures 1 and 2) SP is rare, usually benign, and often underdiagnosed. Intense physical exercise

is a recognized cause. Cardiac CT assesses the extension, causative factors, and pathologies and discloses the diagnosis of SP when chest X-ray findings are normal.

### Authors' contributions

Research creation and design: Gonçalves L, Pires I, Santos J; Data acquisition: Gonçalves L, Santos J, Correia J; Data analysis and interpretation: Gonçalves L, Moreira D, Correia J; Manuscript writing: Gonçalves L Critical revision of the manuscript: Gonçalves L, Pires I, Moreira D.

### Conflict of interest

The authors have declared that they have no conflict of interest.

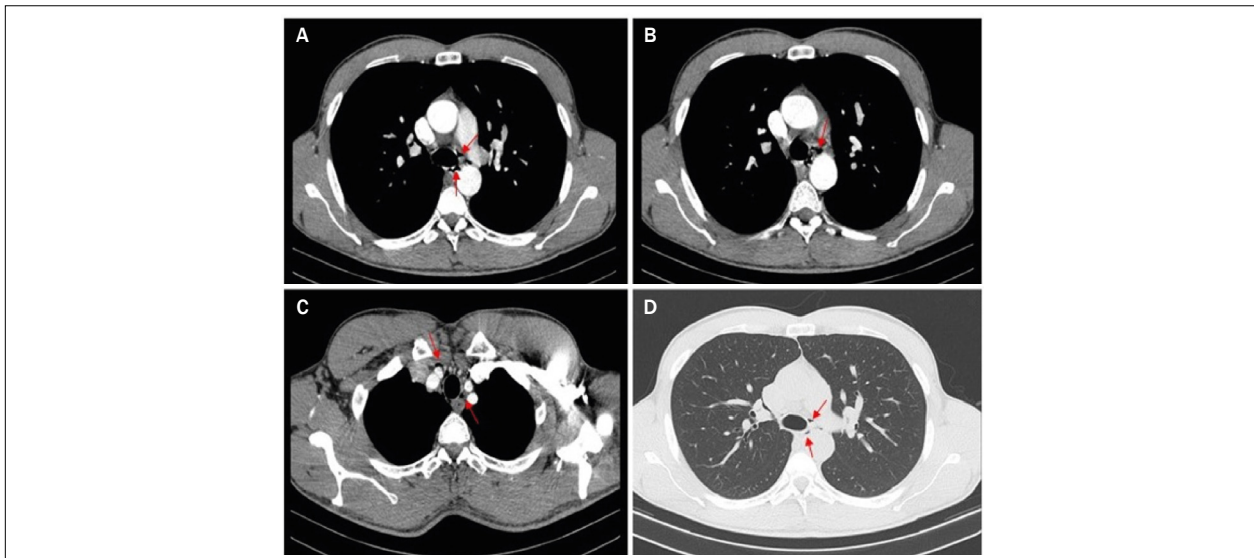


**Figure 1** – Contrast cardiac computed tomography image of the lung window (right inferior image) axial view revealed small amounts of gas on the superior and middle mediastinum (arrows).

### Keywords

Chest pain; Computed Tomography; Pneumomediastinum.

#### Mailing Address: Luísa Gonçalves •

Rei D. Duarte Avenue, Hospital de São Teotónio, Cardiology department, Viseu. Código postal: 3504-509. E-mail: malvar.luisa@gmail.com  
Manuscript received 11/30/2020; revised 12/7/2020; accepted 1/20/2021

DOI: 10.47593/2675-312X/20213402eabc170



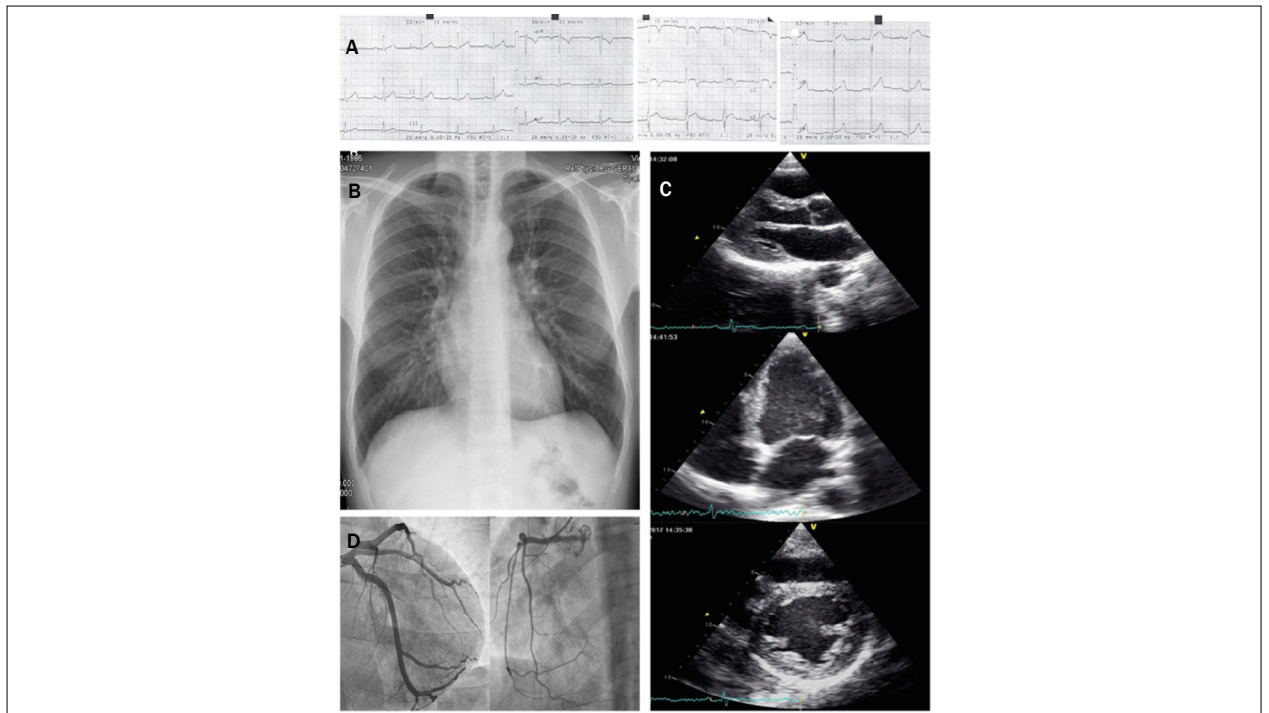


**Figure 2** – A – Standard 12-lead electrocardiogram obtained in the emergency department revealed normal sinus rhythm, an incomplete right bundle block, and T wave inversion on V1-V2. B – Chest X-ray posteroanterior view findings were normal. C – Transthoracic echocardiogram of the parasternal long-axis (superior), apical four chambers (medium), and parasternal short-axis (inferior) showed no alterations. D – Left and right coronary angiogram revealed no coronary heart disease.



## Cardioverter-Defibrillator Implantation Through Persistent Left Superior Vena Cava

*Implante de Cardioversor-Desfibrilador Através da Veia Cava Superior Esquerda Persistente*

*Luísa Gonçalves<sup>1</sup>, Inês Pires<sup>1</sup>, João Santos<sup>1</sup>, Joana Correia<sup>1</sup>, António Costa<sup>1</sup>*

<sup>1</sup>Cardiology Department, Centro Hospitalar Tondela-Viseu, Viseu, Portugal.

### Case

A 72-year-old woman with hypertension was admitted for sudden cardiac arrest secondary to idiopathic ventricular fibrillation. Cardiac magnetic resonance disclosed a persistent left superior vena cava (PLSVC) without other cardiovascular abnormalities for which an implantable cardioverter-defibrillator (ICD) was proposed with left access. Intraoperatively, cephalic vein cannulation placed the wire in the PLSVC that drained in the coronary sinus and subsequently the right atrium. A wide loop maneuver placed the lead tip facing the tricuspid valve, and right ventricle access was obtained with successful positioning of the ventricular lead. Device parameters were checked and considered suitable, and the procedure was finalized with active fixation, a fluoroscopy time of 1.35 minutes, and a radiation dose of 143.12  $\mu\text{Gy}/\text{cm}^2$ . Normal pacing parameters were present at the 3-year follow-up.

PLSVC is a congenital venous anomaly present in 0.5% of the general population that is usually asymptomatic and

incidental on invasive procedures or imaging. Although not a contraindication to ICD, lead placement is challenging because it has to negotiate two bends, one at the coronary sinus and the other in the tricuspid valve. Stylet shaping or wide loop techniques are reliable and present good outcomes not affecting pacing parameters on long-term follow-up.

### Authors' contributions

Research conception and design: Gonçalves L, Pires I, Santos J, Correia J; data collection: Gonçalves L, Santos J; data analysis and interpretation: Gonçalves L, Costa A; manuscript writing: Gonçalves L; critical review of the manuscript for important intellectual content: Gonçalves L, Pires I, Costa A.

### Conflict of interest

The authors have declared that they have no conflict of interest.

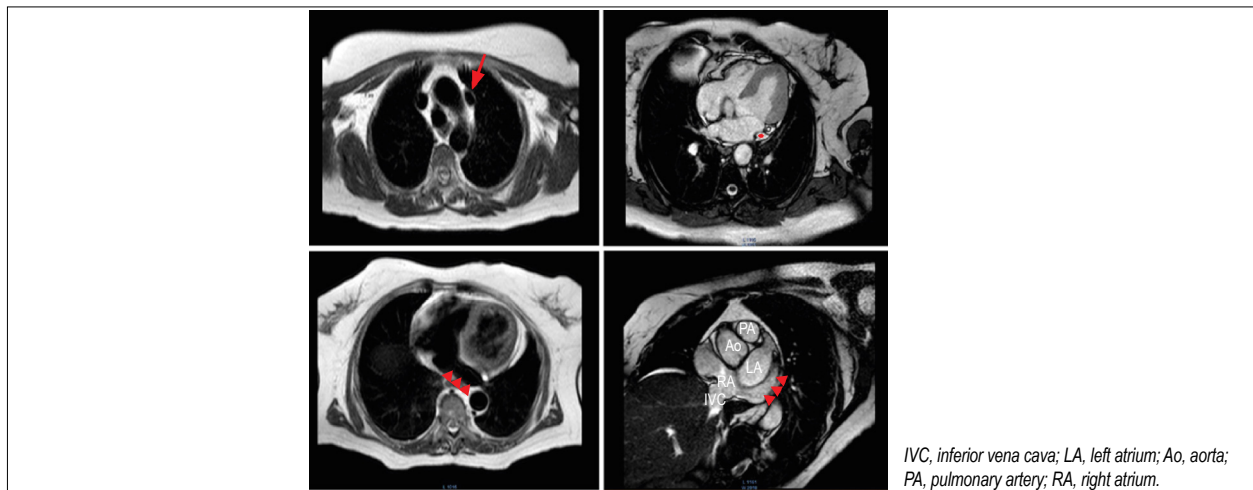


**Figure 1** – Cardiac magnetic resonance imaging showing persistent left superior vena cava (arrow) draining into a dilated coronary sinus (star and arrowheads) and subsequently the right atrium.

### Keywords

Ventricular Fibrillation; Cardioverter-Defibrillators, Implantable; Magnetic Resonance Imaging.

**Mailing Address:** Luísa Gonçalves •

Cardiologia, Centro Hospitalar Tondela-Viseu. Avenida Rei D. Duarte, Viseu, 3504-509. E-mail: malvar.luisa@gmail.com

Manuscript received 12/8/2020; revised 1/12/2021; accepted 1/27/2021.

**DOI:** 10.47593/2675-312X/20213402eabc172





**Figure 2** – X-ray of the thorax after cardioverter-defibrillator implantation showing the left paramediastinal path of the ventricular lead.

## Late Diagnosis of Anomalous Left Coronary Artery from Pulmonary Artery in Oligosymptomatic Women

*Diagnóstico Tardio de Origem Anômala da Artéria Coronária Esquerda a Partir da Artéria Pulmonar em Mulher Oligossintomática*

*Carolina de Souza Galvão<sup>1</sup>, Sterffeson Lamare Lucena de Abreu<sup>1</sup>, Magda Luciene de Sousa Carvalho<sup>1</sup>, José Eduardo da Cruz Sales<sup>1</sup>, Ana Bárbara Silva dos Santos Leite<sup>1</sup>*

*University Hospital, Federal University of Maranhão,<sup>1</sup> São Luis, MA, Brazil.*

A 33-year-old female patient presented with complaints of palpitations, precordialgia, and dyspnea on exertion. Echocardiography revealed that the left coronary artery originated from the pulmonary artery with reverse flow and dilation of the right coronary artery (Figure 1, Vídeo 1). Subsequent coronary angiography confirmed the diagnosis of anomalous left coronary artery from the pulmonary artery, also known as Bland-White-Garland syndrome (Figure 2), a rare and potentially fatal congenital pathology with an uncommon initial presentation in adults.

### Authors' contributions

Research concept and design: Galvão CSG and Abreu SLL; data collection: Galvão CSG, Abreu SLL, and Sales JEC; data analysis and interpretation: Galvão CSG, Abreu SLL, and Sales JEC; manuscript writing: Galvão CS and Abreu SLL.

### Conflict of interest

The authors have declared that they have no conflict of interest.

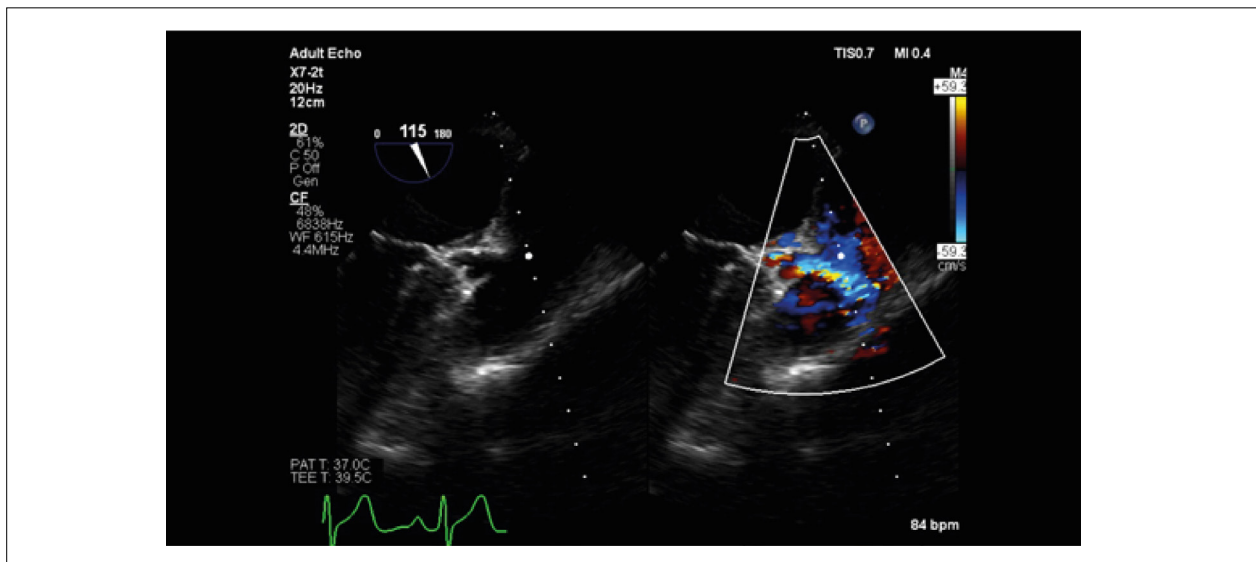


**Figure 1** – Transesophageal echocardiogram in the middle esophagus showing anomalous origin of the left coronary from the pulmonary artery and reverse flow from the left coronary to the pulmonary artery.

### Keywords

Bland-White-Garland Syndrome; Computed Tomography Angiography; Diagnosis; Echocardiography.

Mailing Address: Carolina de Souza Galvão •

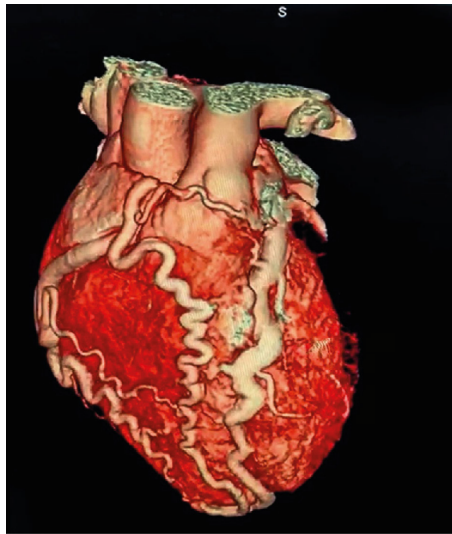
Email: carolgalvao5@hotmail.com

Manuscript received 12/23/2020; revised 1/15/2021; accepted 2/3/2021

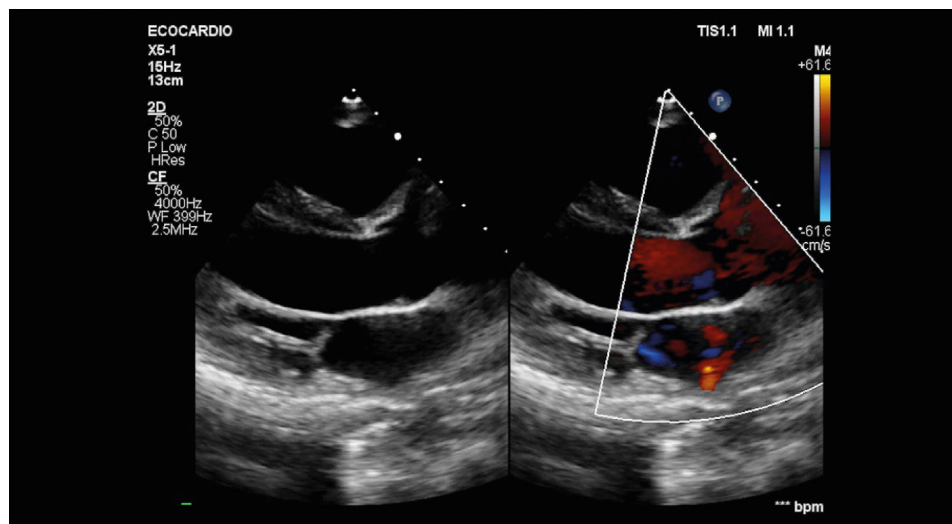
DOI: 10.47593/2675-312X/20213402eabc179



## Images



**Figure 2** – Coronary angiotomography showing diffuse ectasia of the coronary arteries, large network of intercoronary collateral circulation and anomaly of the origin of the left main coronary artery from the pulmonary artery.



**Video 1** – Echocardiogram, transthoracic and transesophageal sequence, showing preserved segmental contractility at rest, right coronary ectasia, acceleration of diffuse coronary flows and anomalous origin of the left coronary from the pulmonary trunk with retrograde flow from the coronary to a pulmonary artery.